

**CHARACTERISTIC STUDY OF ENERGY EFFICIENT
SOLID STATE LIGHTING AND ITS APPLICATION
IN INDOOR CULTIVATION**

CHIN LE YAN

MASTER OF ENGINEERING AND SCIENCE

**FACULTY OF ENGINEERING AND SCIENCE,
UNIVERSITI TUNKU ABDUL RAHMAN,**

NOV 2013

**CHARACTERISTIC STUDY OF ENERGY EFFICIENT SOLID STATE
LIGHTING AND ITS APPLICATION
IN INDOOR CULTIVATION**

By

CHIN LE YAN

A dissertation submitted to the Department of Electrical and Electronic

Engineering,

Faculty of Engineering and Science,

Universiti Tunku Abdul Rahman,

in partial fulfillment of the requirements for the degree of

Master of Engineering and Science

Nov 2013

ABSTRACT

CHARACTERISTIC STUDY OF ENERGY EFFICIENT SOLID STATE LIGHTING AND ITS APPLICATION IN INDOOR CULTIVATION

CHIN LE YAN

The world is facing energy and food shortage issues as population keep increasing. New and modern technologies are developed to explore higher agriculture productivity with a at lesser energy consumption. This has encouraged the study of energy efficient solid state lighting as a future important artificial lighting to be used for indoor cultivation. The novel energy efficient solid state lighting with the use of Aluminum Indium Gallium Phosphide (AlInGaP) and Indium Gallium Nitrate (InGaN) high power LEDs to produce high photosynthetic active radiation (PAR) light source which required for plant photosynthesis has been designed and constructed. Besides adopting high power LEDs to achieve energy efficiency, the solid state lighting has applied high efficient optical reflectors and LED drivers to generate optimum photosynthetic photon flux density (PPFD) and to increase electrical energy conversion. Due to the energy efficient solid state lighting only produces monochromatic wavelengths and easy to control, it can effectively and efficiently induce plant photosynthesis process and accelerate plant growth. The study has verified that the energy efficient solid state

lighting consumed lesser electrical energy when compared to conventional lighting such as fluorescent lamp. In addition, it could accelerate the growth rate of *Lactuca sativa* when compared to the plants cultivated under normal solar irradiance.

ACKNOWLEDGEMENT

First and foremost, I would like to take this opportunity to express my sincere appreciation and deepest gratitude to my supervisor, Prof. Chong Kok Keong and co-supervisor Dr. Tee Chong Siang for their full guidance, invaluable advice, understanding and considerations on my works.

I wish to express my gratitude to the Cameron Highland farmer, Mr. Hoo Chan Leang for his kind supply of young *Lactuca sativa* and providing a suitable place to conduct this research.

I would also wish to indicate special gratitude and deepest thankfulness to Yew Tiong Keat and Jessie Siaw Fei Lu for their great assistance and support during my research study.

To my beloved family and friends, appreciate for the encouragement and mentally support on my study.

APPROVAL SHEET

This dissertation entitled "**CHARACTERISTIC STUDY OF ENERGY EFFICIENT SOLID STATE LIGHTING AND ITS APPLICATION IN INDOOR CULTIVATION**" was prepared by CHIN LE YAN and submitted as partial fulfillment of the requirements for the degree of Master of Engineering and Science at Universiti Tunku Abdul Rahman.

Approved by:

(PROF. CHONG KOK KEONG)

Date:.....

Professor/Supervisor

Department of Electrical and Electronic Engineering

Faculty of Engineering and Science

Universiti Tunku Abdul Rahman

(DR. TEE CHONG SIANG)

Date:.....

Assistance Professor/Co-supervisor

Department of Biology Science

Faculty of Science

Universiti Tunku Abdul Rahman

FACULTY OF ENGINEERING AND SCIENCE
UNIVERSITI TUNKU ABDUL RAHMAN

Date: 15 Nov 2013

SUBMISSION SHEET

It is hereby certified that **CHIN LE YAN** (ID No: **09UEM08636**) has completed this dissertation entitled “**CHARACTERISTIC STUDY OF ENERGY EFFICIENT SOLID STATE LIGHTING AND ITS APPLICATION IN INDOOR CULTIVATION**” under the supervision of PROF. CHONG KOK KEONG (Supervisor) from the Department of Electrical and Electronic Engineering, Faculty of Engineering and Science, and DR. TEE CHONG SIANG (Co-Supervisor) from the Department of Biological Science, Faculty of Science. I understand that University will upload softcopy of my dissertation in pdf format into UTAR Institutional Repository, which may be made accessible to UTAR community and public.

I hereby give permission to my supervisors to write and prepare a manuscript of these research findings for publishing in any form, if I did not prepare it within six (6) months time from this date, provided, that my name is included as one of the authors for this article. Arrangement of names will depend on my supervisors.

Yours truly,



(CHIN LE YAN)

DECLARATION

I hereby declare that the dissertation is based on my original work except for quotations and citations which have been duly acknowledged. I also declare that it has not been previously or concurrently submitted for any other degree at UTAR or other institutions.

Name : CHIN LE YAN

Date : 15 Nov 2013

TABLE OF CONTENTS

	Page
ABSTRACT	ii
ACKNOWLEDGEMENT	iv
APPROVAL SHEET	v
SUBMISSION SHEET	vi
DECLARATION	vii
TABLE OF CONTENTS	viii
LIST OF TABLES	xi
LIST OF FIGURES	xii
LIST OF ABBREVIATIONS	xx
CHAPTER	
1.0 INTRODUCTION	1
1.1 Background	1
1.2 Research objectives	3
1.3 Dissertation overview	3
2.0 LITERATURE REVIEW	4
2.1 LED introduction	4
2.2 Lights and photosynthesis	10
2.3 LEDs and indoor plant cultivation	12

2.3.1	LED lighting in space agriculture	16
2.3.2	LED lighting in tissue culture	18
2.3.3	LED lighting in algaculture	23
2.4	Photosynthesis photoperiod and energy saving	26
2.5	LED drivers and design topology	28
2.6	LED and printed circuit board	33
3.0	METHODOLOGY	36
3.1	High power LED module	37
3.2	Alloy fixture LED lamp	44
3.3	LED driver	50
3.4	Luminous flux and PPF of solid state lighting	53
4.0	EXPERIMENTAL SETUP	58
5.0	RESULTS AND DISCUSSION	61
5.1	Physical observation of <i>Lactuca sativa</i> plants	61
5.2	Energy efficiency and growth rate analysis	73
6.0	CONCLUSION	80
	REFERENCES	82
	APPENDICES	88
A	Current state of the art in high brightness LEDs	88

B	Full spectrum lighting	90
C	Ceracon product specification	92
D	Dow Corning adhesive thermal management	93
E	Luxeon thermal design using Luxeon power light source	94
F	Heat transfer fundamentals	98
G	Luxeon Rebel technical datasheet	102
H	Diffraction Optics reflector product specification	111
I	Loctite adhesive product specification	112
J	LM3404 LED driver datasheet	113
K	Photopic luminous conversion table	120
L	Philips horticultural lighting	122
M	Study of high power light emitting diode (LED) lighting system in accelerating the growth rate of <i>Lactuca sativa</i> for indoor cultivation	127

LIST OF TABLES

Table	page
1. Spectral data for metal halide (MH), red LED plus blue fluorescent (660/BF), red LED (660), and red plus far-red LED (660/735) measured by Brown et al. (1995)	22
2. Optical characteristic of Luxeon Rebel LED	48
3. Measurement result of total leaf area index, plant fresh weight and leaf width of the ten randomly selected samples in experiment 1	69
4. Measurement result of total leaf area index, plant fresh weight and leaf width of the ten randomly selected samples in experiment 2	69
5. PAR energy efficiency, external power conversion efficiency and growth rate for different light sources: solar irradiance, high power LED based energy efficient solid state lighting and CWFL	78

LIST OF FIGURES

Figures	Page
2.1 Basic normal LED structure	5
2.2 Luminous efficacy of visible-spectrum LEDs and other light sources versus time	6
2.3 The pectrum of a white LED clearly shows blue light emitted by GaN based LED die with peak at 460nm and more broadband light emitted by Ce ³⁺ :YAG phosphor at 500-700nm	7
2.4 Early power LED mounted on MCPCB	8
2.5(a) Typical AlInGaP light output degradation loss	10
2.5(b) Typical InGaN light output degradation loss	10
2.6 The photosynthesis rate as a function of absorbed wavelength correlated well with the absorption frequencies of chlorophyll a	11
2.7 Relative photon output from radiation sources	13

2.8	Contour plot of the emitting surface of the LED lamp	14
2.9	The LED lamp head operating at full power emits light intensities equivalent to full sunlight yet remains cool to touch	14
2.10	LED pack consisted of hundreds of LED with different red and blue PPF control	15
2.11	LED array mounted on a fixture in KSC	17
2.12	Spectral radian flux distribution from some widely used light sources include a 100 W incandescent lamp, a 65 W White low pressure mercury (fluorescent) discharge lamp, a 90 W low pressure sodium (SOX) discharge lamp, a 400 W high pressure mercury (MBF) discharge lamp, a 400 W high pressure mercury metal halide (MBIF) discharge lamp and a 250 W high pressure sodium (SON) discharge lamp.	19
2.13	Spectral distribution of a Philips TBL growth light for horticulture	20
2.14	Spectral distribution of light from MH (A), red LED plus blue fluorescent (B), red LED (C) and red plus far-red LED (D)	22

2.15	Relative intensity on energy basis of artificial light from Tungsten-halogen lamp (Philips Halotone 300 W, 230 V, R7s), ‘Plant-growth’ fluorescent tube (Osram–Sylvania, Britegro 2023, 36 W) and a LED (Kingbright, L-53SRC-F). In all graphs the relative intensity of sunlight is presented as a reference.	24
2.16	Schematic diagram of the LEDSet	27
2.17	LEDSet control circuit design	27
2.18	LED driver with adaptive drive voltage for linear current regulators	29
2.19	Buck-boost LED driver	30
2.20	System diagram of LED-current sensing circuit	31
2.21	The BJT half bridge self-oscillating ZVS-CV LED driver circuit	32
2.22	Self-oscillating ZVS-CV LED driver drives 8 series power LEDs	32
2.23	Thermal conductivity of dielectric with varying filler sizes	35

and percentages of the boron nitride

3.1	Diagrams show the Luxeon Rebel pads functions	38
3.2	Correct way of manual handling of Luxeon Rebel emitter	39
3.3	Luxeon Rebel LED module in which a Luxeon Rebel emitter is mounted at the centre of a hexagonal shaped ceramic PCB. The positive and negative pads are printed on the surface for electrical connection.	40
3.4	An open-ended pyramidal reflector with two different slope angles of 25 and 52° supplied by Diffractive Optics. The reflector is mounted on each of the LED module using the high temperature grade thermal adhesive in order to produce collimated light with reasonably uniform illumination.	41
3.5	Lambertian radiation pattern of Luxeon Rebel royal-blue	42
3.6	Lambertian radiation pattern of Luxeon Rebel red	42
3.7	Typical 25° x 52° reflector radiation distribution pattern	43
3.8	Optical simulation result shows uniform light distribution reflected by Diffractive Optics reflector	43

3.9	A flow diagram indicating how the LED panel was constructed. The open-ended reflector is mounted to the LED module before They are fixed into an alloy fixture.	45
3.10	Relative light output vs. thermal pad temperature for red, red-orange & amber	48
3.11	Relative light output vs. thermal pad temperature for royal blue, blue, cyan & green	49
3.12	Pins function of LM3404	50
3.13	Circuit diagram shows a 24 V AC input LED driver based on LM3404IC that is capable of supplying constant output current of 700 mA and DC output voltage greater than 28.1 V in order to drive a maximum of eight Luxeon Rebel LEDs in series.	52
3.14(a)	Illuminance recorded at center	54
3.14(b)	Illuminance recorded at left edge	54
3.14(c)	Illuminance recorded at right edge	54

4.1	The two leaf stage <i>Lactuca sativa</i> seedlings were in pallet	58
4.2	The experimental setup in a dark room. The energy efficient solid state lighting is placed at 20 cm above the test specimen plants.	59
4.3(a)	Solar illumination in the morning	60
4.3(b)	Solar illumination in the afternoon	60
5.1	Images of grown <i>lactuca sativa</i> plantlets captured by CCD video camera for 11 days to monitor the progress of plant growth under the energy efficient solid state lighting system in the dark room: (a) Day 1, (b) Day 2, (c) Day 3, (d) Day 4, (e) Day 5, (f) Day 6, (g) Day 7, (h) Day 8, (i) Day 9, (j) Day 10 and (k) Day 11.	63-65
5.2	Images of grown <i>lactuca sativa</i> plantlets captured by CCD video camera for 8 days to monitor the progress of plant growth under the energy efficient solid state lighting system in the dark room: (a) Day 1, (b) Day 2, (c) Day 3, (d) Day 4, (e) Day 5, (f) Day 6, (g) Day 7, (h) Day 8.	66-67

5.3	The comparisons of <i>Lactuca sativa</i> plantlets growth under the solar irradiance and the energy efficient solid state lighting: (a) <i>Lactuca sativa</i> plants cultivated under the energy efficient solid state lighting in experiment 1, (b) <i>Lactuca sativa</i> plants cultivated under the solar irradiance in experiment 1, (c) <i>Lactuca sativa</i> cultivated under the energy efficient solid state lighting in left pallet and cultivated under the solar irradiance in right pallet in experiment 2.	68
5.4	The total leaf area index per plant were measured from 10 randomly selected plants to compare the <i>Lactuca sativa</i> plants cultivated under the solar irradiance and the energy efficient solid state lighting system, (a) experiment 1 and (b) experiment 2.	70
5.5	The fresh weight were measured from 10 randomly selected plants to compare the <i>Lactuca sativa</i> plants cultivated under the solar irradiance and the energy efficient solid state lighting system, (a) experiment 1 and (b) experiment 2.	71
5.6	The average values of both total leaf area index per plant and fresh weight were measured from 10 randomly selected plants to compare the <i>Lactuca sativa</i> plants cultivated under the solar irradiance and energy efficient solid state lighting system, (a) experiment 1 and (b) experiment 2.	72

- 5.7 The spectrum of energy efficient of high power LED based lighting system ranging from 200nm to 900nm acquired using AvaSpec-256-NIR1.7 spectrometer with the resolution of 0.6 nm. 75
- 5.8 The spectrum of Cool White Fluorescent Lamp (CWFL) ranging from 200nm to 900nm acquired using AvaSpec-256-NIR1.7 spectrometer with the resolution of 0.6 nm. 75
- 5.9 The spectrum of solar irradiance ranging from 200nm to 900nm acquired using AvaSpec-256-NIR1.7 spectrometer with the resolution of 0.6 nm. 76

LIST OF ABBREVIATIONS

A	Ampere
AC	Alternate Current
Al ₂ O ₃	Aluminum Oxide
AlInGaP	Aluminum Indium Gallium Phosphide
cm	Centimeter
CO ₂	Carbon Dioxide
CTE	Coefficient of Thermal Expansion
CWF	Cool White Fluorescent
DC	Direct Current
GaAs	Gallium Arsenide
GaAsP	Gallium Arsenide Phosphide
gram/Wh	gram per Watt hour
GaN	Gallium Nitrate
GaP	Gallium Phosphide
GaAlAs	Gallium Aluminum Arsenide
HPS	High Pressure Sodium
H ₂ O	water
Hz	Hertz
InGaAlP	Indium Gallium Aluminum Phosphide
InGaN	Indium Gallium Nitride

KSC	Kennedy Space Center
LED	Light Emitting Diode
mA	milli Ampere
ms	milli second
mW	milli Watt
MOSFET	Metal Oxide Semiconductor Field Effect Transistor
MCPCB	Metal-Core Printed Circuit Board
MHL	Metal Halide Lamp
PAR	Photosynthetically Active Radiation
PBR	Photobioreactor
PCB	Printed Circuit Board
PCM	Peak Current Mode
PPF	Photosynthetic Photon Flux
PPFD	Photosynthetic Photon Flux Density
PTC	Plant Tissue Culture
PWM	Pulse Width Modulation
SiC	Silicon Carbide
SMD	Surface Mount Device
SSL	Solid State Lamp
WPE	energy conversion efficiency
TFL	Tubular Fluorescent Lamp

ZVS-CV	Zero Voltage Switching Clamped-Voltage
W	Watt
Lm	Lumen
$^{\circ}\text{C}/\text{W}$	degree Celsius per Watt
$^{\circ}\text{C}$	degree Celsius
$^{\circ}$	degree
$\mu\text{molm}^{-2}\text{s}^{-1}$	micro mol per meter square per second
nos.	numbers
pcs	pieces
$\Delta\text{nm}/^{\circ}\text{C}$	delta nanometer per degree Celsius
Qe	irradiance energy
λ	photon wavelength
k Ω	kilo ohm
LM _{red}	Lumen output for red
LM _{blue}	Lumen output for blue
lx	Lux
RM _{red}	radiometric output for red
RM _{blue}	radiometric output for blue
RM _{tot}	total radiometric
PPF _{red}	Photosynthetic Photon Flux for red

PPF_{blue}

Photosynthetic Photon Flux for
blue

PPF_{tot}

Total Photosynthetic Photon Flux

μWcm^{-2}

micro Watt per centimeter square

W/m^2

Watt per meter square

CHAPTER 1.0

INTRODUCTION

1.1 Background

Today's food supply is becoming of paramount importance as the world population is increasing much faster than the food production. Many new lands have been developed from forest to agriculture land for the purpose of increasing the primary food supply. However, this development is not environmental friendly; instead it increases the global warming effect. To help reduce global warming effect and at the same time to increase the food supply productivity efficiently, a few modern scientific ways are implemented which includes growing vegetables and flowers in green houses and growing crops in the buildings. When comes to indoor plant cultivation, conventional lighting such as High Pressure Sodium lamp, Metal Halide lamp and Tissue Culture Fluorescent lamp are commonly used as artificial sunlight. The downside of these conventional artificial lamps is that they consume a lot of electric energy, radiate a lot of heat and high maintenance cost. On the contrary, with the advanced technology of Light Emitting Diode (LED), LED has become a prominent light source for intensive plant culture system and also an alternative source when the world is slowly depleting those conventional lamps which contain toxic mercury content. This has led to an arena to create and study the solid state lighting as a light source generator to replace the

conventional lamps. The advantages of solid state lighting include producing only monochromatic wavelengths that is suitable for plants photosynthesis, consuming lesser electric energy as well as radiating less heat in which will help decrease the global warming effect. Many relevant researches are conducted by using normal typical LED such as 5mm, Surface Mount Device (SMD) or some customized LED arrays to grow plants with continuous or pulse LED light source (Bula et al, 1991; Tennessen et al, 1994; Brown et al, 1995; Goins et al, 1997). Having said so, these LED lightings do required a substantial number of LED chips to produce sufficient light energy for plants photosynthesis because the lumen output per LED chip is relatively low. Thus normal LED solid state lighting requires a good thermal heat sink and to certain extends, a fan cooling system to dissipate large amount of heat generated from the large quantities numbers of LEDs. Indeed a new design on using the latest solid state LED namely the high power LED that has higher energy efficiency in producing higher lumen output at lesser quantities of LEDs to generate sufficient photosynthetic photon flux (PPF) for plants cultivation (Chin and Chong, 2012). In this research, a novel design of using high power LED solid state lighting is adopted and a low cost thermal dissipating method that uses passive cooling instead of active cooling to reduce solid state lighting operating temperature and the energy consumption.

1.2 Research objectives

There are three objectives on this work:

1. To design and construct a novel energy efficient solid state lighting to produce photosynthetic photon flux for plant photosynthesis,
2. To study the characteristics and features of energy efficient solid state lighting in indoor cultivation, and
3. To study the energy efficiency of energy efficient solid state lighting on cultivating *Lactuca Sativa*.

1.3 Dissertation overview

Chapter 2 gives the literature about evaluation on the LED light source for various plant cultivation, different method of driving the LED and the method of dissipate LED heat. In Chapter 3, the design and construction of the energy efficient solid state lighting are discussed in detail. While in Chapter 4, the experiment setup is described. Testing result and discussion are presented in Chapter 5 and finally overall conclusion of the study is stated in Chapter 6.

CHAPTER 2.0

LITERATURE REVIEW

2.1 LED introduction

LED also known as light emitting diode is a p-n junction diode that emits photons when forward bias. The LED history is traced to the beginning of last century where Round (1907) found the first electroluminescence light emitting from Silicon Carbide (SiC) in an experiment by chance. Later in 1950s, III-V compound materials were invented, thus laser and LED based on III-V compound materials stepped in the history and dominate the LED market till now. The early LED design consists of a die which is placed on a reflective cup that is connected to one of the lead frame which commonly designated for cathode, and a wire bond connecting the die surface to other lead frame as anode source. It ended by clear epoxy encapsulation into round shape as shown in Figure 2.1.

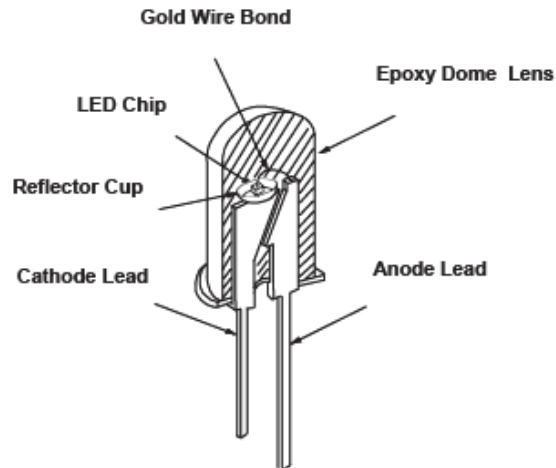


Figure 2.1: Basic normal LED structure

In the early LED development, the only available type of LED was made from Gallium Arsenide (GaAs) material with radiation wavelengths ranging from infrared to red. Advances in material science have then been made possible with the production of devices on ever-shorter wavelengths; in late 1960s, the first practical LED was invented by using Gallium Arsenide Phosphide (GaAsP) material to provide a 655 nm red light with low brightness levels of approximately 1-10 mcd at 20 mA driving current (Holonyak and Bevacqua 1962). As LED technology progressed through 1970s, additional colors and wavelengths became available from using Gallium Phosphide (GaP) material for green and red lights, GaAsP material for yellow and high efficient red light. In 1980s, a new material Gallium Aluminum Arsenide (GaAlAs) was developed to provide superior performance over previously available LEDs with an improvement in brightness and efficiency. This has led to the new development of Indium Gallium Aluminum Phosphide (InGaAlP) LED that can have different color output via adjusting the energy

band gap. Figure 2.2 shows the different materials and their luminous efficacy to produce different colors with timeline indication.

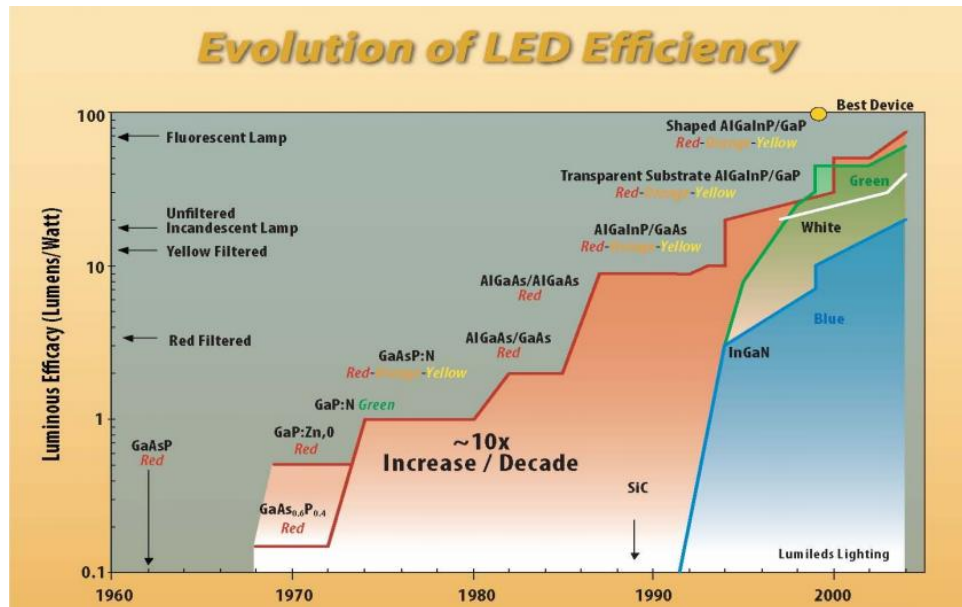


Figure 2.2: Luminous efficacy of visible-spectrum LEDs and other light sources versus time (Craford 2007)

After decades of research on new materials and process, LED technology has gone into never before possible where the solid state lighting illumination becomes reality concerned when Nakamura et al. (1991) invented the first high brightness Gallium Nitrate (GaN) LED. The brilliant blue light of GaN LED, when partially converted to yellow by a phosphor coating (YAG), is the key to white LED fabrication that produces a wide spectrum as shown in Figure 2.3.

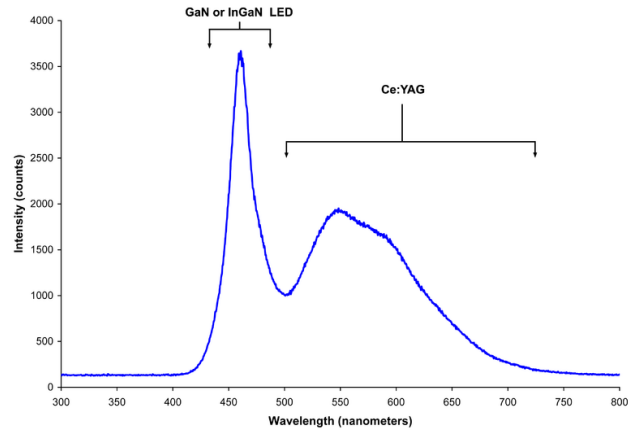


Figure 2.3: The spectrum of a white LED clearly shows blue light emitted by GaN based LED die with peak at 460nm and more broadband light emitted by Ce³⁺:YAG phosphor at 500-700nm (Nakamura et al., 1991)

In the mid to late 1990, Lumileds Lighting which the company was a 50-50 joint venture of Agilent Technologies and Philips Lighting has developed the early very high brightness LED producing more than ten lumens namely Luxeon 1-Watt Star (2002). Luxeon 1-Watt Star LED was rated for power dissipation of 1 watt and it consisted of an emitter, an anode, a cathode, a circular base and a lens integrated into a single unit. This LED was designed to be surface mounted on a metal-core printed circuit board (MCPCB) and required a heat-sink slug to help dissipating heat that was not electrically isolated. Figure 2.4 shows an early power LED mounted on the star shaped MCPCB made from Lumileds Lighting.



Figure 2.4: Early power LED mounted on MCPCB (High power LEDs 2010)

As material and process technologies keep improving, power LED luminous efficiency has become higher with increase of photon flux extraction to generate more luminous flux per watt and it is capable to engineer higher power dissipation; from this onwards it emerged the high power LED development. In today's Philips Lumileds LED technology for instance, their Luxeon Rebel family on white LED is able to produce more than 120 lumens of luminous flux per watt at 350 mA drive current compare to early power LED only produced 10 percent luminous flux per watt of Luxeon Rebel produces. This high power LED is able to be driven continuously for 1000 mA current which is 3 times higher power than early power LED which was only driven up to 350 mA current maximum for the purpose of producing much higher lumens output (Philips Lumileds DS64, 2012). Besides, the high power LED with a lower thermal resistance of $10^{\circ}\text{C}/\text{W}$ can withstand higher junction temperature (maximum temperature up to 150°C) (Philips Lumileds DS64, 2012) when comparing with the early power LED Luxeon 1-Watt Star (Luxeon 1-Watt Star, 2002). Indium Gallium Nitride (InGaN) and Aluminum Indium Gallium Phosphide (AlInGaP) materials are most widely used in

making high power LED for their high quantum efficiency. InGaN material is commonly being used to produce green, cyan, blue and white colors while AlInGaP material is used to produce red, red-orange and amber colors. This technology break through has led the world to start changing the conventional lighting into high power LED solid state lighting for it has very low catastrophic loss, on average of 70% lumen maintenance (L70) of initial light output remaining after 50,000 hours of operation time (Philips Lumileds DS65, 2011). This change has directly reduced a lot of lighting maintenance cost and contributes to a better green environment at much lesser waste and lower power consumption.

From high power LED energy conversion efficiency (WPE) aspect, only small portion of the electrical energy is converted into useful light while majority of the power energy is transformed into conduction heat (Kim et al., 2001). There will be more lights extraction at lower operating temperature, and it requires a good thermal management skill to dissipate the heat out of the high power LED in order to maintain good light output efficiency. Generally AlInGaP based high power LED's light output drops much higher percentage compare to InGaN based high power LED when reaching high junction temperature as shown in Figures 2.5(a) and 2.5(b) (Lumileds AB12, 2005). From the Figures 2.5(a) and 2.5(b), it is needed to put more attention on AlInGaP high power LED thermal handling than InGaN high power LED thermal handling in order to reduce the light output degradation due to high operating junction temperature.

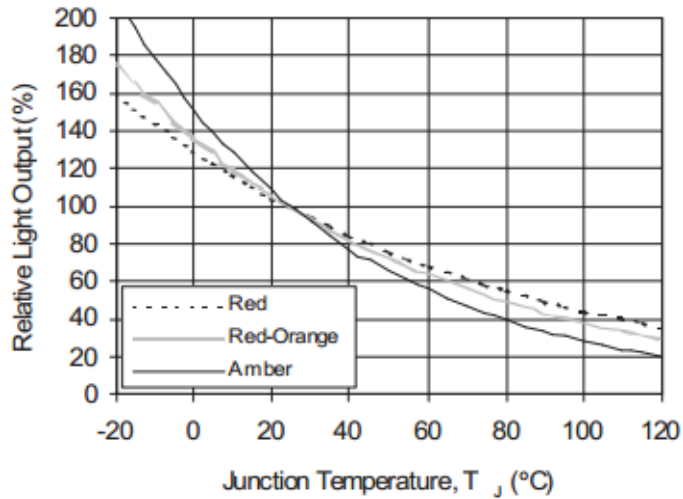


Figure 2.5(a): Typical AlInGaP light output degradation loss (Lumileds AB12 2005)

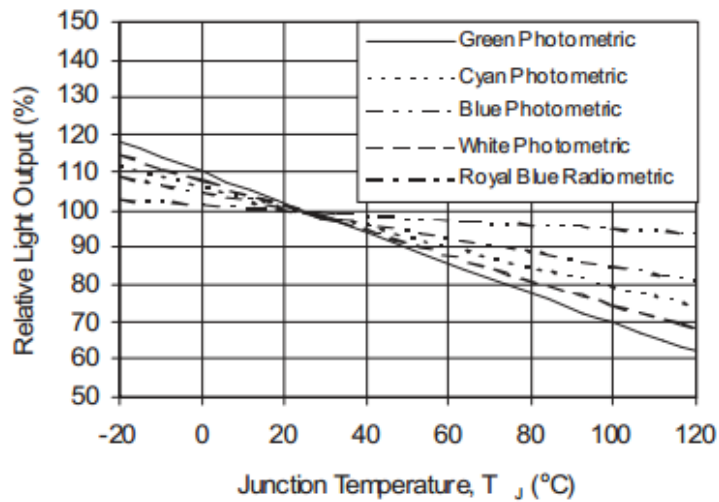
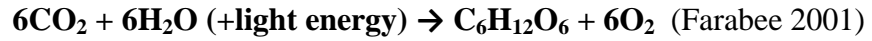


Figure 2.5(b): Typical InGaN light output degradation loss (Lumileds AB12 2005)

2.2 Lights and Photosynthesis

The chlorophyll molecules in the chloroplast initiate photosynthesis process by capturing light energy during light reaction state and converting it into chemical energy to help transforming water (H_2O) and carbon dioxide

(CO₂) into sugar in the dark reaction as the plants primary nutrient. The generalized equation for this chemical reaction involved in photosynthetic process is given as below:



Chlorophyll pigment absorbs its most light energy from the violet-blue and reddish wavelength bands while rejects green and yellow wavelength bands which are not important for photosynthesis. Among these wavelength bands chlorophyll pigment receives its peak energy at wavelengths around 680 nm and 420 nm and has the highest photosynthesis rate at these wavelength (Figure 2.6).

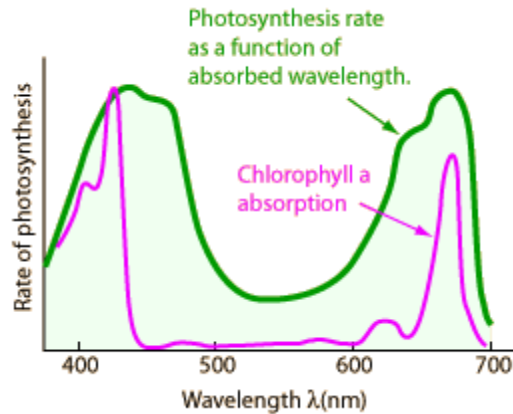


Figure 2.6: The photosynthesis rate as a function of absorbed wavelength correlated well with the absorption frequencies of chlorophyll a (Nave 2012).

Figure 2.6 clearly shows most of the plants highly response and absorb red and blue lights for photosynthesis, which means the plants are still able to grow

even without the full spectrum of light. As LED produces monochromatic light, it has enable researchers to eliminate other wavelengths found within the normal white light that produced by the conventional lamps for the plant growth. Thus, using LED lights would also reduce the amount of energy waste. The superimposed pattern of luminescence spectrum of red LED (650–665 nm) and blue LED (440–460 nm) corresponds well to light absorption spectrum of carotenoids and chlorophyll in the plants photosynthesis.

2.3 LEDs and indoor plant cultivation

Along with the LED technology advancement, LED light source has become a prominent light source for intensive indoor plant culture systems and photobiological researches. Bula et al. (1991) had proved that using the 72 pieces (nine x eight rows) Gallium-Aluminum-Arsenide chip that had a peak emission of 660 nm red LEDs supplemented with blue Tubular Fluorescent Lamp (TFL) was able to grow lettuce (*Lactuca sativa*). The growth rate was similar to that under Cool-White Fluorescent (CWF) plus incandescent lamps. The subsequent study carried out by Hoenecke et al., (1992) showed that hypocotyls and cotyledons of lettuce seedlings grown under 660 nm red LEDs were able to elongate, but that effect could be prevented by adding at least 15 $\mu\text{mol}/\text{m}^2/\text{s}$ of blue light from blue TFL. This had verified that blue light is required for lettuce seedling production under red LED cultivation.

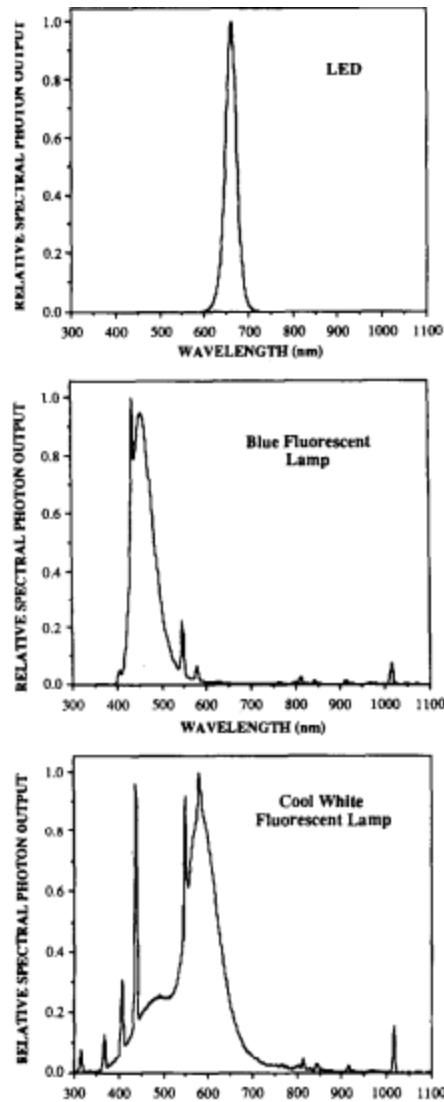


Figure 2.7: Relative photon output from radiation sources (Hoenecke et al., 1992)

Tennessee et al. (1994) had compared the response of photosynthesis to CO₂ was similar on leaves photosynthesis of kudzu (*Pueraria lobata*) enclosed in a leaf chamber illuminated by red LED and xenon arc lamp at the equal photosynthetic photon flux (PPF). The results showed that there was no statistical significant difference between using white light from the arc lamp and red light from red LED irradiance on the CO₂ absorption rate. In their research, the LED lamp was made from 250 red LED chips mounted on the

ceramic heat sink, backed by aluminium fins and cooling fan offered greater control of light intensity. Thus, it enables easy repetition of light treatments compare to natural lighting and use of neutral density filter.

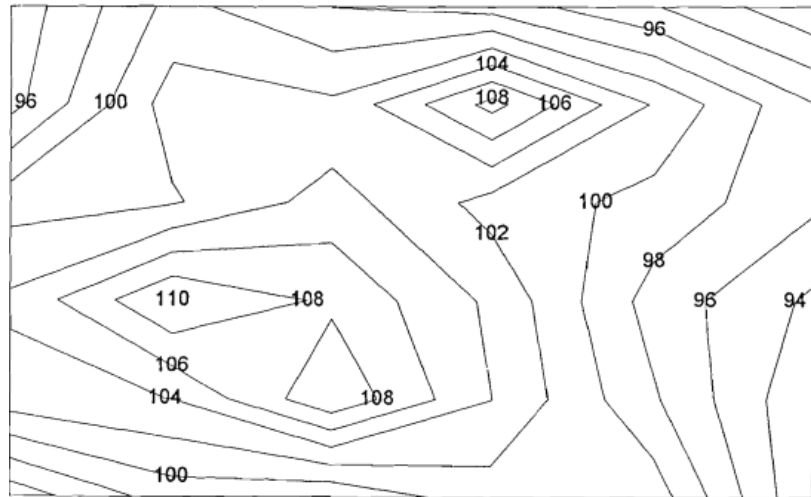


Figure 2.8: Contour plot of the emitting surface of the LED lamp (Tennessen et al., 1994)



Figure 2.9: The LED lamp head operating at full power emits light intensities equivalent to full sunlight yet remains cool to touch (Tennessen et al., 1994)

Okamoto et al. (1997) had used red and blue LED shown in Figure 2.10 to study the effects of different light quality and photosynthetic photon flux on the growth of lettuce (*Lactuca sativa*) plants. The investigation was conducted using three different light qualities (red, blue and red/blue) and two photosynthetic photon flux density (PPFD) levels (85 and 175 $\mu\text{mol}/\text{m}^2/\text{s}$) on the growth and morphogenesis of lettuce seedlings. The research found that irrespective of the two different PPFD levels, the plants grown under the red LEDs developed more leaves than the plants under the blue LEDs, but less leaves than the plants under red/blue light. The lettuce stem length decreased significantly with an increased in blue PPF and the whole plant dry weight was greater for the plants grown under the high PPFD level than the plants grown under the low PPFD level. The research also had identified that the photosynthesis process occurred under continuous or pulse lights irradiance.

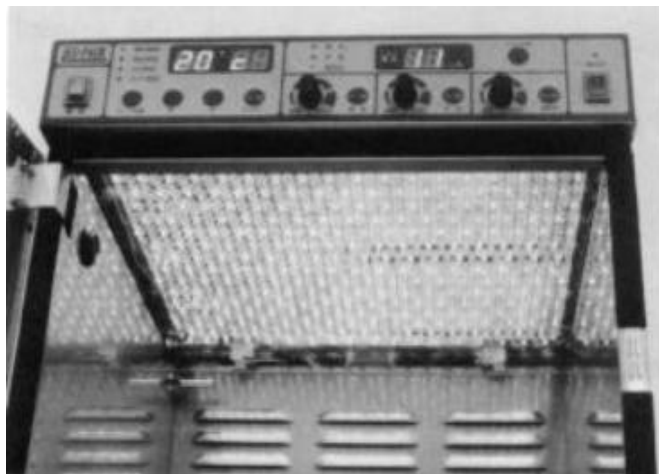


Figure 2.10: LED pack consisted of hundreds of LED with different red and blue PPFD control (Okamoto et al., 1997)

While Yanagi and Okamoto (1994) found that the dry mass production under the red LED light growth was slightly less than the spinach plants grown under the fluorescent lamp growth. Similarly, the spinach plant leaf area grown under the red LEDs was also smaller than that grown under the fluorescent lamp. Nevertheless, the research indicated an important possibility of using LED as an artificial light source for growing the plants.

2.3.1 LED lighting in space agriculture

United State has a good artificial lighting cultivation research on space agriculture study called NASA' Kennedy Space Center (KSC). The KSC has an objective of preparation for the development of plant-based regenerative life-support systems for future Moon and Mars bases. One of the researches from the very early stage in KSC was Goins et al. (1997). They conducted a research on growing the salad crops of radish (*Raphanus sativus*), onion (*Allium fistulosum*), lettuce (*Lactuca sativa*) and wheat (*Triticum aestivum*) by using cool white fluorescent lighting (CWF), blue fluorescent lighting (BF) and Aluminum Gallium Arsenide (AlGaAs) LED array. The AlGaAs LED consisted of 2600 pieces quantities of high intensity discrete LED with 660 nm dominant wavelength to generate 300 $\mu\text{mol}/\text{m}^2/\text{s}$ (Figure 2.11).

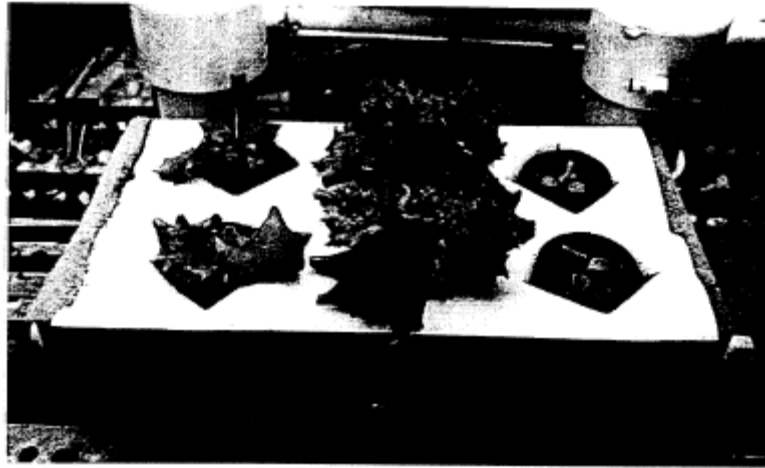


Figure 2.11: LED array mounted on a fixture in KSC (Goins et al., 1997)

Goins et al. (1997) reported that both the red light (660 nm) and blue light (450 nm) could induce photosynthesis process on the salad crops plants. However, there was no significant difference between plants grown under red LED light irradiance with 10% blue fluorescent light as compared to plants grown under the cool fluorescent lamp lighting irradiance in terms of shoot fresh mass and shoot dry mass. They also found when plants were grown under the red LED lamp irradiance without blue light supplement, the lettuce, radish and wheat plants all showed significant lower shoot fresh and lower dry weight compared with the plants grown under red LED irradiance with blue light supplement. Under the red LED irradiance with blue light supplement, it would increase the hypocotyls, cotyledons and stems, but overall leaves biomass yield was decreased. The research also found that with approximately of $350 \mu\text{molm}^{-2}\text{s}^{-1}$ of photosynthetic photon flux cultivation under 18 hours of light and 6 hours of dark photoperiod has enabled salad crop of lettuce (*Lactuca sativa*) to grow and harvest after 24 days of planting.

2.3.2 LED lighting in tissue culture

Plant tissue culture (PTC) is the growth of plants tissues or cells under a controlled environment which is free from microorganism contamination. PTC is usually carried out under a clean and controlled environment (filtered air, stable temperature and light) using different types of formulated growth media.

The plant propagating industries have long been using artificial light source for production of planting materials. Among the conventional lamps such as High Pressure Sodium lamp (HPS), Metal Halide lamp (MHL), tubular fluorescent lamp and incandescent lamp using for plant propagation; the most common and widely used is tubular fluorescent lamp. All these lamps produce a wide spectrum of wavelengths including visible lights (blue to red colors) and non-visible lights (ultra violet and infra red). Figures 2.12 and 2.13 show the spectral distribution from common used lamps and Philips Lighting horticulture TFL (Master TL-D reflex).

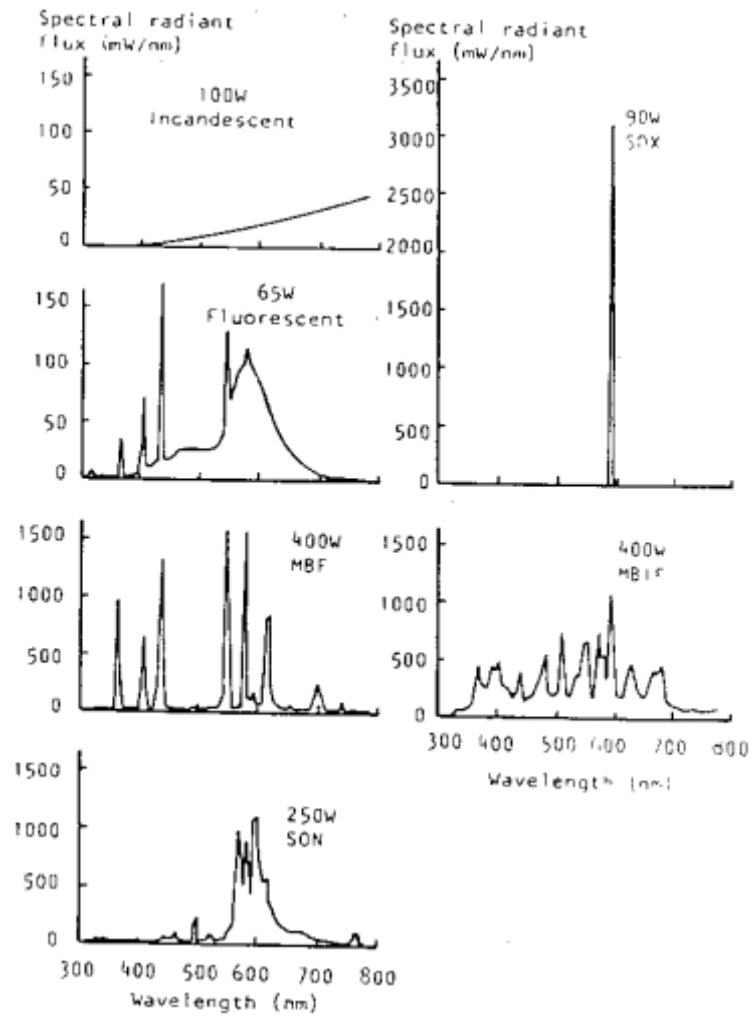


Figure 2.12: Spectral radiant flux distribution from some widely used light sources include a 100 W incandescent lamp, a 65 W White low pressure mercury (fluorescent) discharge lamp, a 90 W low pressure sodium (SOX) discharge lamp, a 400 W high pressure mercury (MBF) discharge lamp, a 400 W high pressure mercury metal halide (MBIF) discharge lamp and a 250 W high pressure sodium (SON) discharge lamp

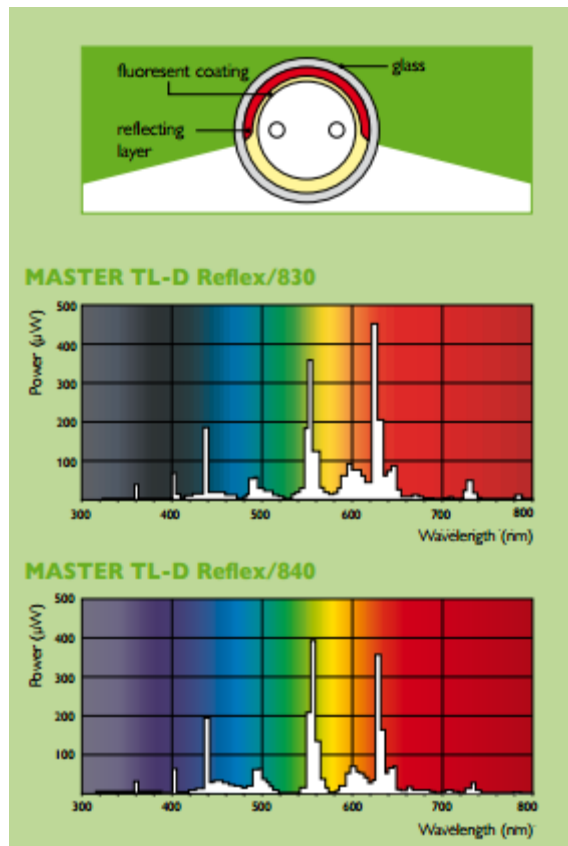


Figure 2.13: Spectral distribution of a Philips TBL growth light for horticulture

However in this wide spectrum it contains a lots of green light, which is reflected by the green leaves and led to low efficiency per quantum of light within the photosynthetically active radiation range. Besides, TFL consumes 65% of the total electricity in a tissue culture laboratory which is the highest non-labor cost. As a result, the concerned industries are seeking for a more efficient light source which has led to rapid development of the high brightness or high power LED lighting for tissue culture laboratories and plants growth in the controlled environment.

To study the efficiency of LED light on the plant growth, Nhut et al. (2000) cultured strawberry plantlets using the red and the blue LED lights with different ratio and different photosynthetic photon flux levels. Their results showed that by using the LED irradiance for strawberry plantlet micropropagation, the growth was optimum at 70 % red and 30 % blue LEDs ratio at the optimal light intensity of 60 $\mu\text{mol}/\text{m}^2/\text{s}$ of PPFD. The study also demonstrated that the LED light source used for the in vitro plantlet culture could improve the plant's growth rate during acclimatization.

Besides, Brown et al. (1995) also conducted the study on the growth and normal attribute host resistance of Hungarian Wax pepper (*Capsicum annuum L.*) plant using the red LED with supplemental blue or far red irradiance. The study reported that the pepper dry mass, number of leaves per plants, chlorophyll concentration and stomatal conductance reduced when growing the plants under red LED only compared to the plants grown under red LED supplemental with blue fluorescent lamps irradiance. While the application of far-red radiation to the plants it resulted in taller plants with greater stem mass than those plants grown under red LED irradiance alone. The study also showed that fewer leaves were developed under the red or far-red radiation than those plants grown under the lamps that also producing blue wavelength. Their study concluded that with the suitable amount of blue wavelength in combination with the red LED radiation might be suitable for plant tissue culture under tight controlled environment. Figure 2.14 and Table 1 below show the spectral distribution and spectral data of various lamps sources.

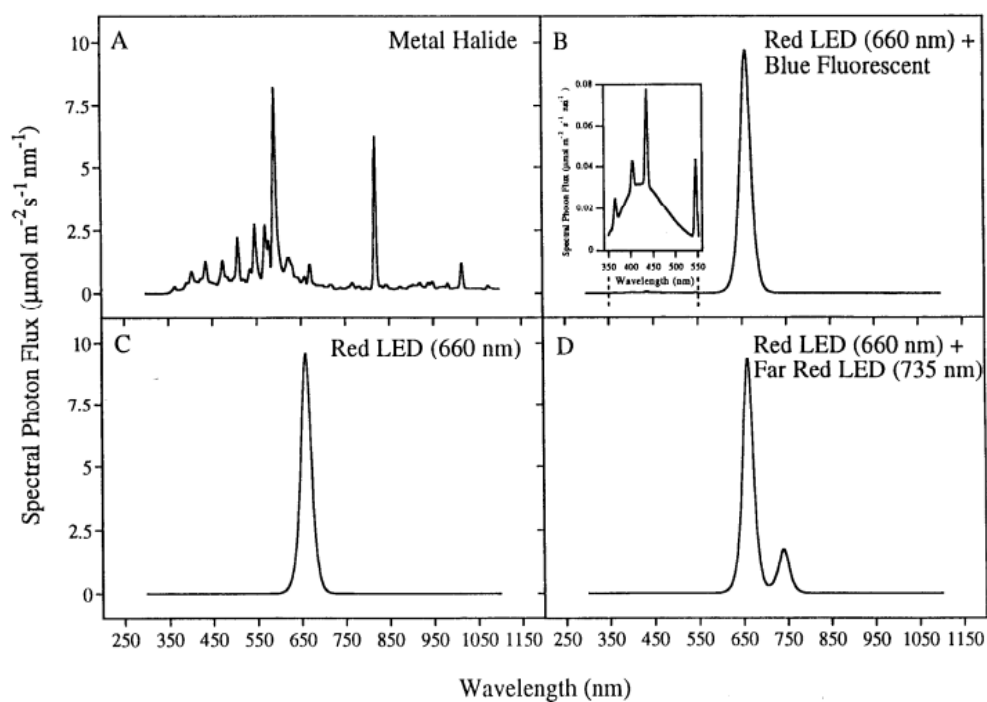


Figure 2.14: Spectral distribution of light from MH (A), red LED plus blue fluorescent (B), red LED (C) and red plus far-red LED (D) (Brown et al., 1995)

Table 1: Spectral data for metal halide (MH), red LED plus blue fluorescent (660/BF), red LED (660), and red plus far-red LED (660/735) measured by Brown et al. (1995)

Characteristic	Lamp			
	MH	660/BF	660	660/735
	<i>Irradiance (W·m⁻²)</i>			
Wavelength range (nm)				
400–700	69	57	54	53
300–800	77	58	54	63
800–3000	13	1	0	4
3000–50000	–8	50	38	35
	<i>Photon flux (μmol·m⁻²·s⁻¹)</i>			
300–400	11	1	0	0
400–500	63	3	0	0
500–600	180	1	0	0
600–700	75	310	296	293
700–800	25	3	2	59
400–700 (PPF)	318	314	296	293
300–800	354	318	298	352
Yield photon flux (YPF)	280	289	275	273
YPF : PPF	0.88	0.92	0.93	0.93
Phytochrome photostationary state (φ) ^z	0.82	0.88	0.88	0.84
R : FR ^y	3.0	103.0	148.0	5.0

2.3.3 LED lighting in algaculture

Algaculture is an alga farming industry that produces great source of valuable feedstock, color pigments, carbohydrates, bioplastics, pharmaceuticals, fuel and other fine chemicals. Algae indoor farming could be limited by problems such as polluted environment, contamination substances and inconsistent production yield. Growing algae in photobioreactor (PBR) incorporates with artificial lights in a closed and controlled system. It is required to supply nutrients to induce photosynthesis in making glucose for algae grow during the dark reaction. To effectively exploit the commercial potential of algae, a cheap, durable, reliable, and a low density but highly efficient light source is needed since algae only need small amount of sun light radiation for photosynthesis. This has led to the study of LED radiation as artificial sun light for alga culture which is most preferred with variable intensity and photoperiod control features.

IN another study, Matthijs et al. (1996) solely used red LED with peak emission 659 nm in 2 LEDs/cm² panel as cultivating light source in culturing the green alga (*Chlorella pyrenoidosa*). The research found that the continuous supply of LED light could promote maximum growth of alga and the intermittent flash LED light supplied with 5 μ s pulse on duration during 45 μ s pulse off duration of dark period would still sustain near maximum growth. The intermittent flash pulse method could reduce the overall light flux level but still able to sustain the alga growth comparable to the continuous LED light supplied method with the intention of reducing the photosynthetic photon

flux. As a result using the LED pulse or intermittent flash method allows energy saving and cause less heat waste generation if compared with the conventional fluorescent lamps.

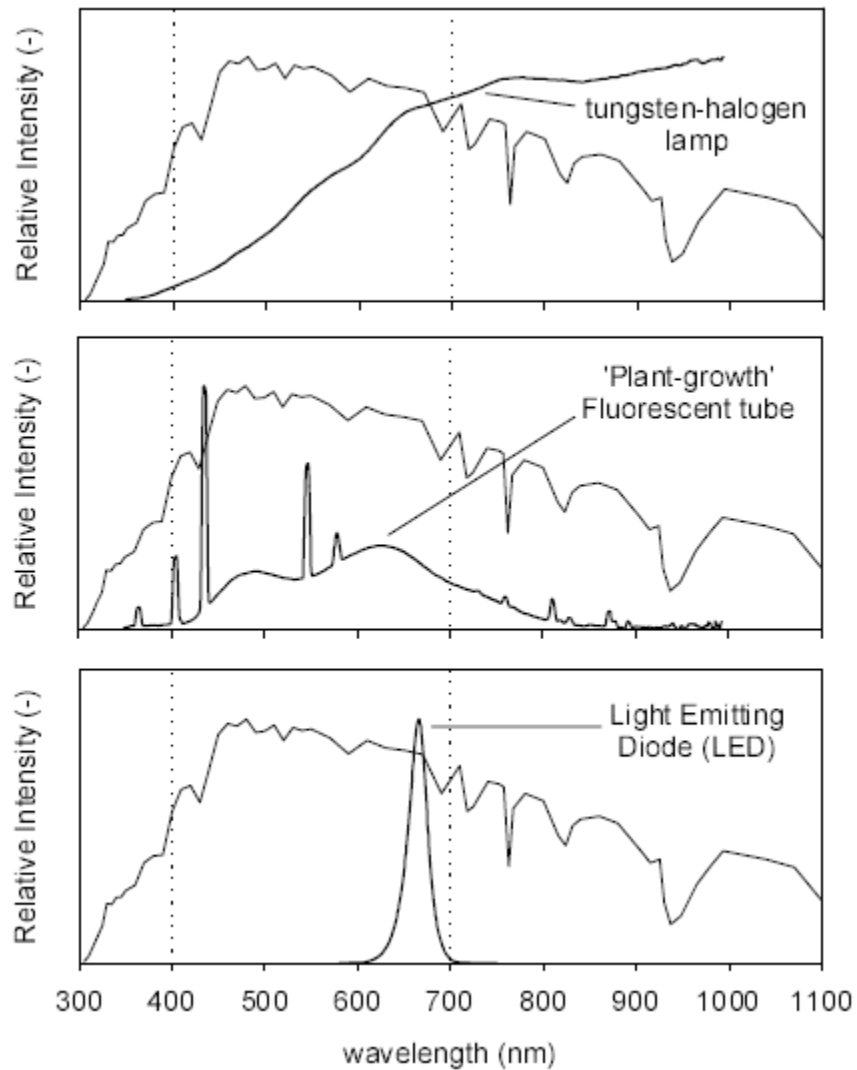


Figure 2.15: Relative intensity on energy basis of artificial light from Tungsten-halogen lamp (Philips Halotone 300 W, 230 V, R7s), 'Plant-growth' fluorescent tube (Osram-Sylvania, Britegro 2023, 36 W) and a LED (Kingbright, L-53SRC-F). In all graphs the relative intensity of sunlight is presented as a reference (Matthijs et al., 1996)

Due to the high potential of cultivating algae for commercialization, Lee and Palsson (1994) calculated a set of theoretical values on gas mass transfer requirements and lights intensity requirements for the LED based PBR to support high density alga cultivation. By using 680 nm red GaAlAs LED as the light source and on-line ultrafiltration to periodically supply fresh medium, it could achieve the highest cell concentration (more than 2×10^9 cell/mL) and the highest total cell volume fraction (more than 6.6% v/v). In addition, by modifying internal sparging (to improve overall light utilization), online ultrafiltration (to improve supply of fresh medium with removing the secondary metabolites), light intensity (to increase the light density) and shorter light path distance, the oxygen production rate in the final PBR could increase almost 5-fold, giving the maximal oxygen production rate of 10 mmol oxygen/L culture/h.

Besides, Nedbal et al. (1996) studied the fluctuation effects on various algae growth in the diluted cultures by using red LED arrays. Their results showed that the red LED arrays generated intermittent light in the small bioreactor could grow the algae as good as that grown under the continuous light condition. In certain intermittent light pattern testing, the growth of algae could be higher than those grown under the continuous light supply grown.

2.4 Photosynthesis photoperiod and energy saving

Photosynthesis process can be divided into three phases include primary photochemistry, electron shuttling and carbon metabolism. These three photosynthesis sub-processes can be uncoupled by providing pulses of PPF 400-700 nm wavelengths. At high frequency, these PPF 400-700 nm pulses treatment can be used to separate the light reaction from the dark reaction of photosynthetic electron transport and LED made from semiconductor can provide flexible pulsing pattern as short as nanoseconds to allow good energy saving.

Jao and Fang (2004) have investigated the effect of intermittent light on growing the potato in vitro. They used conventional TFL fluorescent lamp for continuous light source and LED lighting for adjustable frequency or duty cycle light source. The results showed that LED illumination at 720 Hz (1.4 ms) and 50% duty cycle with 16 hours light and 8 hours dark photoperiod provided maximum plant growth. The growth rate of potato plantlets under the continuous light of 24 hours/day was similar to those illuminated with 16 hours/day under intermittent light. In another similar testing where energy conservation was studied, changing intermittent light to 180 Hz (5.5 ms) and 50% duty cycle did not show significant difference on plant growth when compared to those illuminated by continuous light from TFL lighting. Instead the results showed 17% less energy consumption and have proved that the LED lighting could reduce electric energy.

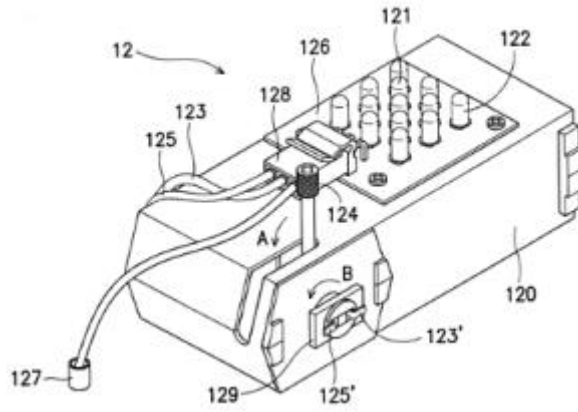


Figure 2.16: Schematic diagram of the LEDSet (Jao and Fang 2004)

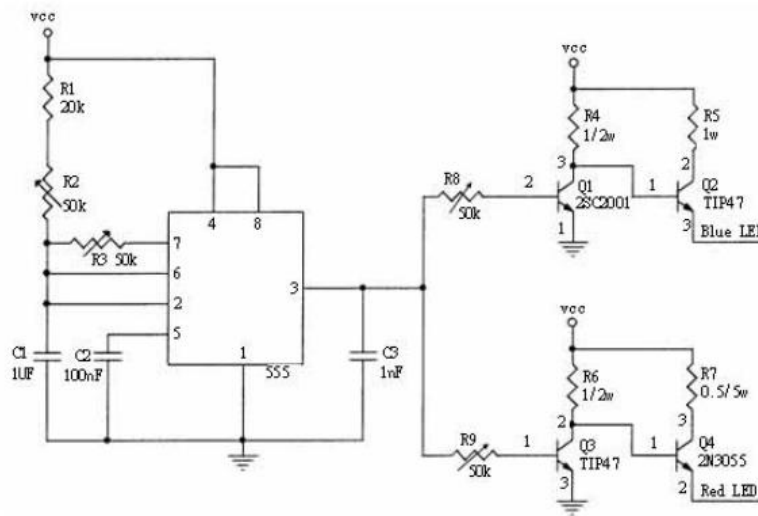


Figure 2.17: LEDSet control circuit design (Jao and Fang 2004)

2.5 LED drivers and design topology

The brightness of LED depends on the driving current during forward bias. An effective way to ensure that each LED produces similar luminous flux output is to connect them in series. There are many LED driver design topologies from a basic straightforward linear regulation to a more complicated switching mode, but all have a common goal to generate consistent current source to drive variable number of LEDs in the same circuit. One simple approach is employing a linear current regulator which has a lower cost but suffers from poor operating efficiency. An improved LED driver with self-adaptive drive voltage proposed by Hu and Jovanovic (2008) consists of an output voltage preregulator that is always self-adjusted. The voltage across the linear current regulator of the LED string with the highest voltage drops is kept at the minimum voltage in order to maximize the driver efficiency. The proposed LED driver eliminated the sensing voltage dropped across the linear regulator by removing the external voltage feedback for adjusting the output voltage of preregulator, in replacement was the preregulators and linear current regulators connected in series with the LED strings as shown in Figure 2.18.

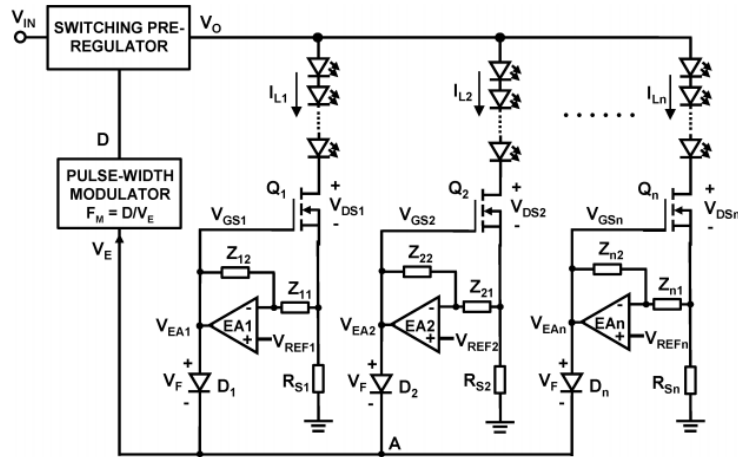


Figure 2.18: LED driver with adaptive drive voltage for linear current regulators (Hu and Jovanovic 2008)

Lu and Wu (2009) implemented pulse width modulation (PWM) controller for LED driver with two main operation modes, the current feedback mode and the constant current mode, for different PWM DC-DC converter topologies like buck, boost, buck-boost and flyback. A special error amplifier with adaptability to different DC-DC was introduced for different application. Figure 2.19 shows one of the LED driver design for buck-boost circuit where constant current mode is operated in peak current mode (PCM) and current feedback mode senses the current across the sense resistor R_{S2} in series with LED load and converts to offset voltage.

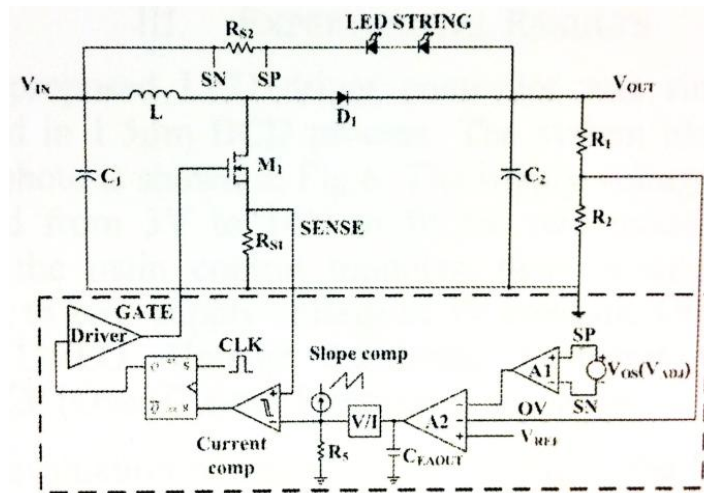


Figure 2.19: Buck-boost LED driver (Lu and Wu 2009)

The difference between offset voltage, output feedback voltage and reference voltage is then amplified and later converted to current signal by V/I converter. The current signal will act as the reference of the current comparator and the LED current will be regulated when the SENSE current is equally level with the LED current.

Leung et al. (2008) designed a power efficient LED-current sensing LED driver without using any sensing resistor but extracts LED-current value from the output capacitor of the driver. The sensing circuit is implemented in buck-boost topology and measurement results indicate 92% of power conversion efficiency and at least 90 times power reduction in sensing compared to existing approach. The proposed sensing circuit in Figure 2.20 senses a feedback LED voltage using resistive potential divider and amplifies the difference of the feedback voltage and the input voltage, which then to be

confirmed with target set current by the error amplifier to regulate the LED current to reasonable sensing accuracy and line/load regulation.

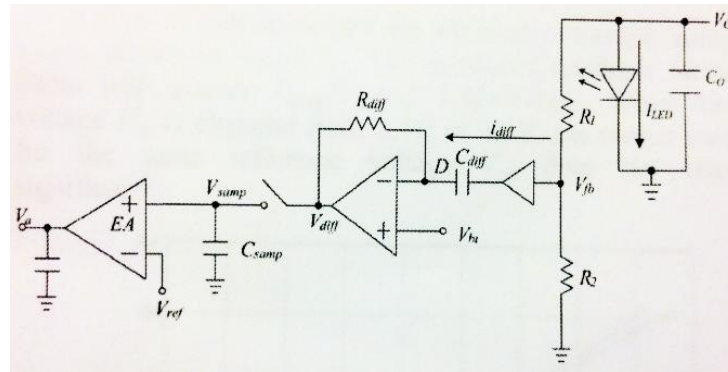


Figure 2.20: System diagram of LED-current sensing circuit (Leung et al., 2008)

Another low cost method of self-oscillating zero voltage switching clamped-voltage (ZVS-CV) LED driver implemented by Mineiro Sa et al. (2008) showed that no current sensor was required to stabilize the average current through the LED string. This is achieved by using the simplified mathematical model to characterize the series resonant converter for the power LED driver from the series resonant network of LED, inductor and capacitor. In the experiment, the load of eight power LED of Luxeon III (LXHL-PW09) were powered by ZVS-CV driver at 650 mA average current with ripple factor of 15 % obtained 81 % power efficiency. With the simplified design to produce good power efficiency, it is cost effective to replace the actual fluorescent lamps to the power LED lighting. Figure 2.21 shows the proposed

self-oscillating ZVS-CV LED driver circuit and Figure 2.22 shows the prove of 8 series LED is powered by self-oscillating ZVS-CV LED driver.

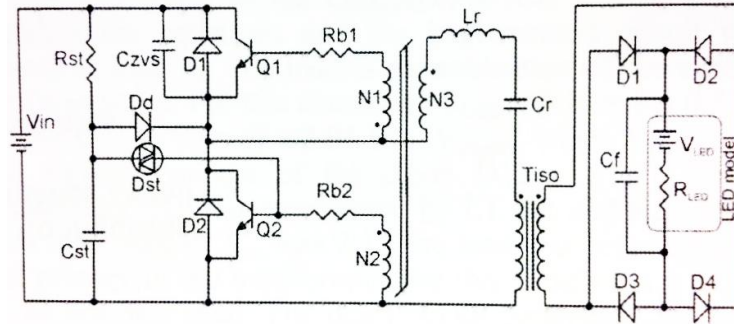


Figure 2.21: The BJT half bridge self-oscillating ZVS-CV LED driver circuit (Mineiro Sa et al., 2008)

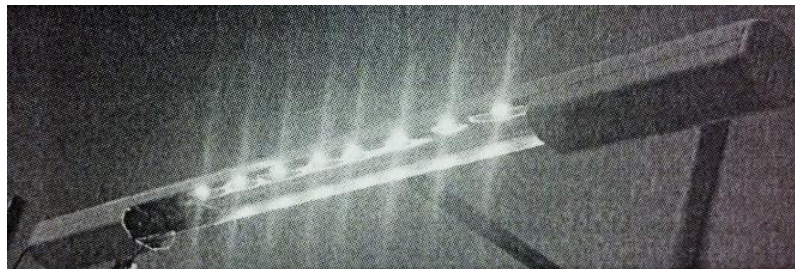


Figure 2.22: Self-oscillating ZVS-CV LED driver drives 8 series power LEDs (Mineiro Sa et al., 2008)

In general, the self-adaptive and self oscillating drive methods are typical low cost LED drivers that require modification on current sensing or current regulation components when there is a change in the LED string in order to

deliver the same target drive current. This has limited the design flexibility when variable LED strings and different LED model or made is applied where total LED forward voltage in the circuit has changed. While PWM controller topology provides the design flexibility advantage on the variable LED string but the current feedback resistor in the PWM controller circuit normally contributes in system power lost and it becomes more significant when lower output current is designed. To increase the LED driver efficiency and flexibility, a switch mode topology LED driver is preferred as a very low value of feedback resistor is used to reduce the system power lost.

2.6 LED and Printed Circuit Board

High power LED typically consumes minimum of 350 mA current or more than 1 W of electrical power. Only small percentage of this electrical energy is transformed into luminous light, while other huge portion of energy will become conduction heat as waste energy. This waste thermal energy must be extracted out from the high power LED to a heat sink in order to reduce the LED optical degradation and LED failure rate; as such it is important the printed circuit board (PCB) which mounts the high power LED must have low thermal resistance and good thermal flow features to help removing the heat from the high power LED to the heat sink attached to it as fast as possible. Commonly, there are two types of good thermal conductive the PCB including metal core PCB (MCPCB) and ceramic PCB for mounting the high power LED. Metal core PCB means the base material for PCB is metalized material

as heat spreader and usually is made from Copper alloy or Aluminum alloy and the latter material is more economy and easy to obtain. While for ceramic PCB, the base material is made from Alumina (96% Al_2O_3) and has lower thermal conductivity than MCPCB but it has better coefficient of thermal expansion (CTE) than the MCPCB which is an important factor for mounting high power LED of ceramic substrate body.

There was a study on enhancing the thermal conductivity of the insulation layer between the circuitry and the metal base plate of the MCPCB for better heat dissipation by Yung (2010). They added boron nitride into the dielectric substance to maximize the formation of conductive paths and to minimize the thermal barrier. The research showed that for any given percentage of boron nitride, the larger the size of boron nitride, the higher the thermal conductivity will be. In addition, a higher percentage of boron nitride as filler also gave higher thermal conductivity. The study proved that more and larger boron nitride particles helped to shorten the low thermal conductive path of the dielectric material (i.e. epoxy matrix) and establish a high thermal conductive network (i.e. boron nitride) for heat conduction. Figure 2.23 shows 4 μm filler size has the highest thermal conductivity as compared to the smaller filler size of boron nitride and the thermal conductivity increase with the higher percentage of boron nitride content.

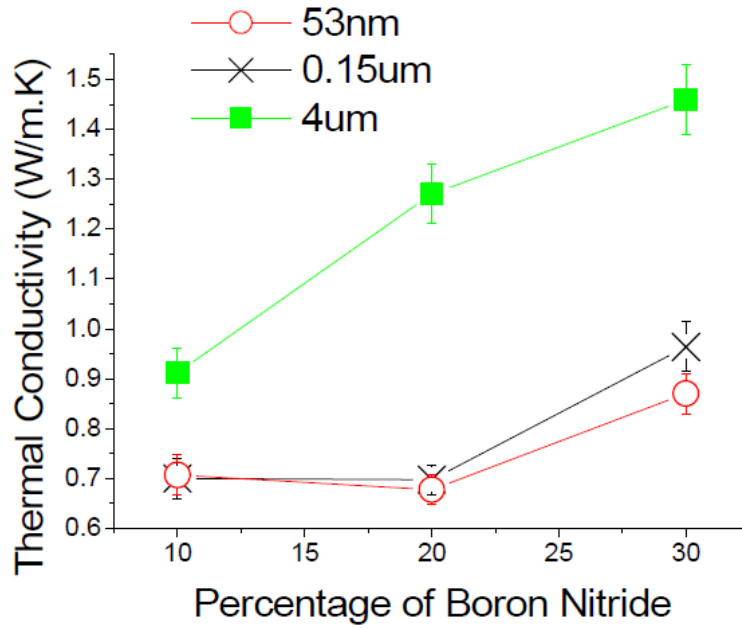


Figure 2.23: Thermal conductivity of dielectric with varying filler sizes and percentages of the boron nitride (Yung 2010)

Lee et al. (2010) have studied the MCPCB with anodized pattern to improve thermal dissipation by reducing the thermal resistance and increasing the thermal flow. From their findings the patterned anodizing could connect the lead frame of high power LED package to the metal substrate directly without any thermal loss through the dielectric layer and higher efficient thermal management is expected since the thermal resistance has reduced.

CHAPTER 3.0

METHODOLOGY

In this research, a study was conducted on the novel of high power LED solid state lighting in accelerating the plant growth rate for indoor cultivation (Chin and Chong 2012). An energy efficient solid state lamp (SSL) has been designed and constructed, which was based on high power LEDs and high efficient reflectors to produce high density luminous flux of Photosynthetic Photon Flux (PPF) from 400nm to 700nm wavelengths. The operating temperature of the energy efficient solid state lamp was controlled and maintained at good thermal efficiency level to ensure the luminous flux of PPF production is consistent throughout the study. Low light plant of *Lactuca sativa* (Romanian Lettuce) was chosen as the test specimen because of its high commercial value, short life cycle and easy to obtain from the local farmers.

The focus of energy efficient solid state lighting design could be divided into three main areas: high power LED module, alloy fixture LED lamp and LED driver. There were total of 18 pieces of high power LEDs, 18 pieces of ceramic PCBs, 18 pieces of high efficient reflectors, 3 units of LED drivers, 1 piece of step down transformer, 2 units of alloy fixture casing and some wires to build an energy efficient solid state lighting.

3.1 High power LED module

The high power LED made from AlInGaP with wavelength ranging from 620 to 645 nm for red radiation and the high power LED made from InGaN with wavelength ranging from 440 to 490 nm for blue radiation were adopted. Both kinds of high power LEDs provide high photon extraction efficiency (WPE) in which both are supplied by Philips Lumileds under the product range of Luxeon Rebel Direct Color family. The selected Luxeon Rebel red LED was LXML-PD01-0030 which could produce a minimum of 40 lumens of luminous flux per watt and was able to reach 65 lumens of luminous flux output when driven by 700 mA current; while the selected Luxeon Rebel royal blue LED is LXML-PR01-0175 which produced a minimum 175 mW of deep blue luminous flux per watt when driven with 350 mA current and it was able to produce 325 mW of luminous flux at 700 mA drive current (Philips Lumileds DS65, 2011).

All the Luxeon Rebel LEDs used in making the solid state lamp originally were in a bare emitter form and it was required to be mounted on the PCB for electrical connection. Figure 3.1 shows that the electrical connections of anode and cathode pads are located under the bare emitter of ceramic based body.

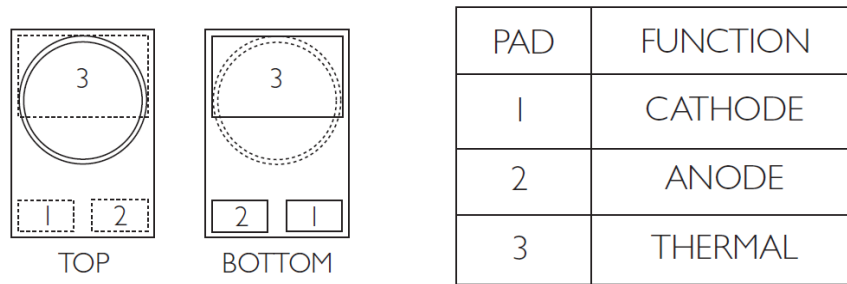


Figure 3.1: Diagrams show the Luxeon Rebel pads functions

With the recommendation pads layout design on gerber format given by Philips Lumileds, two small rectangular pads for anode and cathode electrical connections were drawn at the lower section and one big rectangular pad for thermal dissipation function was drawn at the upper section of a hexagon shaped PCB keep out layout. Two soldering pads that had bigger size than the cathode contact pad were electrical connected to the cathode contact pad and were placed at the left end of the hexagon PCB, similarly another two same size soldering pads were also connected with each other and were placed at the right end of the hexagon PCB to make electrical connection to the anode contact pad. The final PCB design was then sent to the ceramic PCB manufacturer, Hokuriku Sdn Bhd located in Shah Alam of Selangor state of Malaysia, to fabricate the actual ceramic PCB. Aluminum Oxide (Al_2O_3) based ceramic PCB was chosen for its good thermal conductivity, excellent thermal cycling stability, high electrical insulation and more importantly, to minimize the coefficient of thermal expansion (CTE) mismatch with the Luxeon Rebel LED emitter which was built on the ceramic substrate too (Philips Lumileds AB32, 2012). Silver material based circuit track using thick

film technology was printed on the ceramic PCB for its good adhesion force on ceramic surface and better electrical conductivity. When the hexagon shaped ceramic PCB fabricated with Luxeon Rebel emitter footprint was done and ready, the Luxeon Rebel LED emitter was then placed to the prepared location on the hexagon shaped ceramic PCB. The Luxeon Rebel emitter silicone lens is a fragile material. Thus, when placing the Luxeon Rebel emitter, a twizzer tool was used to help holding the Luxeon Rebel emitter body edge to avoid touching the soft silicone lens that might cause defect and lead to decrease the overall optical output performance and reliability as shown in Figure 3.2. The hexagon shaped ceramic PCB with Luxeon Rebel emitter sitting on it was then transferred to a hot plate soldering machine with the temperature control at 260 °C for few seconds to solder the Luxeon Rebel emitter on the ceramic PCB and formed a LED module as showed in Figure 3.3. After the soldering process, the soft silicone dome lens was gently cleaned by a cotton swab with isopropyl alcohol (IPA) to remove any dirt from the lens.



Figure 3.2: Correct way of manual handling of Luxeon Rebel emitter

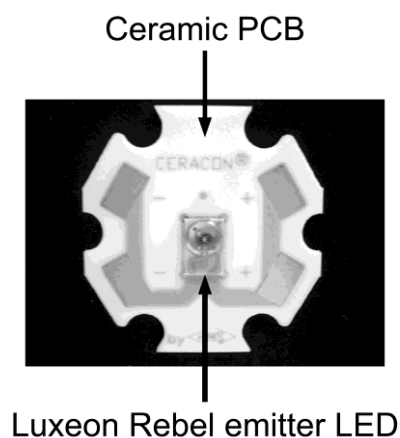


Figure 3.3: Luxeon Rebel LED module in which a Luxeon Rebel emitter is mounted at the centre of a hexagonal shaped ceramic PCB. The positive and negative pads are printed on the surface of the ceramic PCB for electrical connection.

From the ceramic PCB manufacturer specification, the ceramic substrate of PCB has thermal resistance of $0.12\text{ }^{\circ}\text{C}/\text{W}$. Luxeon Rebel red LED and royal blue LED have thermal resistances of $12\text{ }^{\circ}\text{C}/\text{W}$ and $10\text{ }^{\circ}\text{C}/\text{W}$ respectively (Philips Lumileds DS65, 2011), therefore the total thermal resistance of Luxeon Rebel red LED module and Luxeon Rebel royal blue LED module is $12.12\text{ }^{\circ}\text{C}/\text{W}$ and $10.12\text{ }^{\circ}\text{C}/\text{W}$, respectively.

The completed Luxeon Rebel LED module has a typical 120° radiation viewing angle which is the off axis angle from lamp centerline where the luminous intensity is half of the peak value at initial. In this wide distribution angle, only small amount of PPF radiation would reach the target test specimen target (young *Lactuca sativa* plants). The long light source distance from the target specimen caused a lot of waste PPF radiation. To increase the

radiation reception efficiency, open-ended parabolic profile with high precision optical surface reflectors that has two different slope angles of 25° and 52° supplied by Diffractive Optics were applied to focus the LEDs lights to the target plants. These reflectors have good optical efficiency of minimum 85% and it is dedicated design for Luxeon Rebel emitter that generates lambertian distribution pattern as shown in Figure 3.4. By using these optic reflectors, it could help focusing the original wide lambertian distribution pattern into narrow and reasonably uniform light illumination onto the young *Lactuca sativa* test plants.

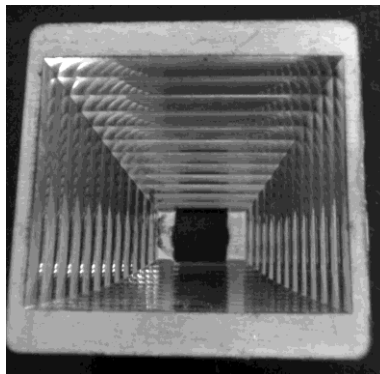


Figure 3.4: An open-ended pyramidal reflector with two different slope angles of 25° and 52° supplied by Diffractive Optics. The reflector is mounted on each of the LED module using the high temperature grade thermal adhesive in order to produce collimated light with reasonably uniform illumination

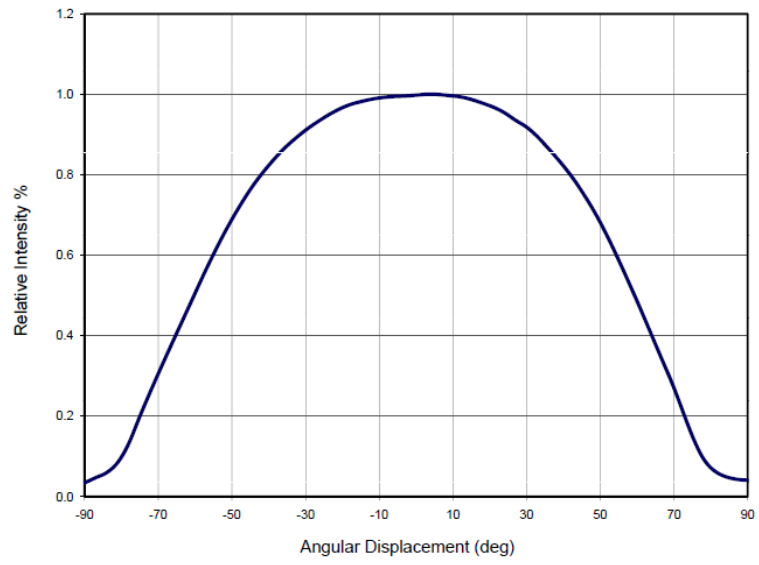


Figure 3.5: Lambertian radiation pattern of Luxeon Rebel royal-blue

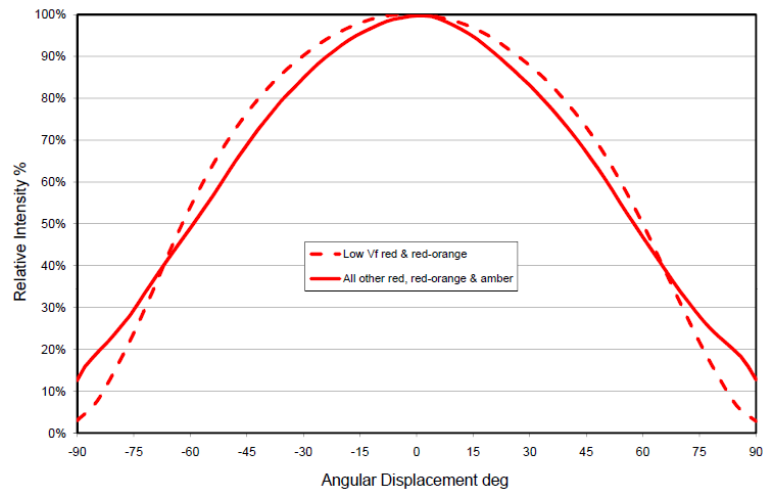


Figure 3.6: Lambertian radiation pattern of Luxeon Rebel red

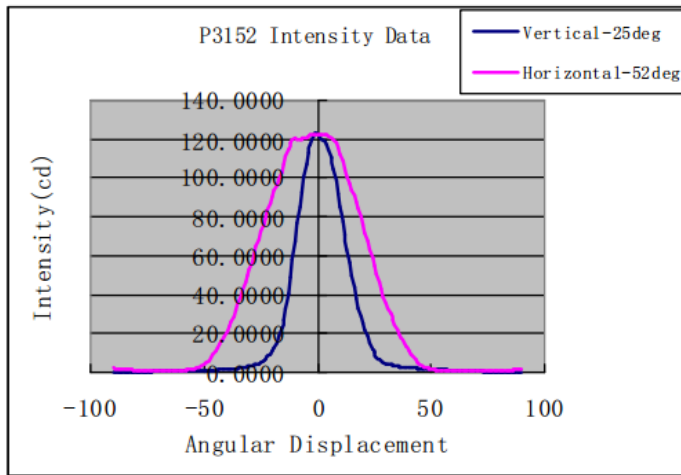


Figure 3.7: Typical 25° x 52° reflector radiation distribution pattern

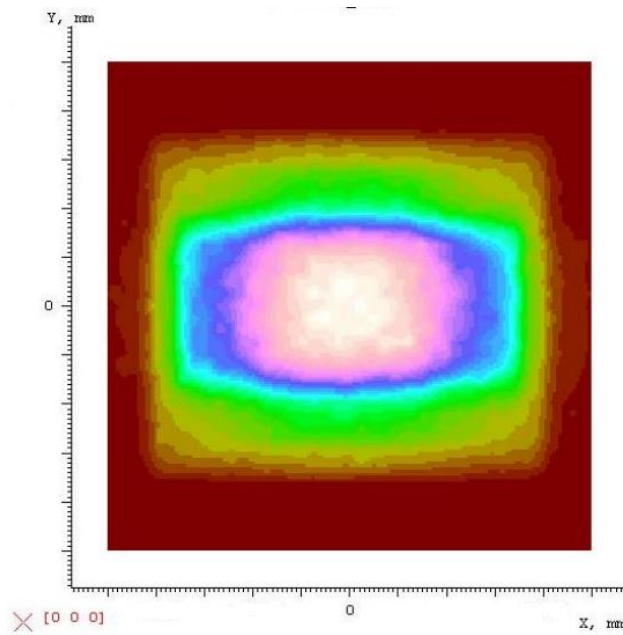


Figure 3.8: Optical simulation result shows uniform light distribution reflected by Diffractive Optics reflector

To mount the reflector onto the high power LED module, a high temperature grade thermal adhesive (Loctite Hysol 9340) was used to bond the polycarbonate (PC) plastic surface of the reflector to the ceramic PCB surface of high power LED module. Special attention on holding the reflector is needed and it is advised to wear gloves when handling the reflector to avoid the finger-print oil contamination on the aluminum coating surface that will degrade the light reflection efficiency. The completed Luxeon Rebel LED module assembly will then be installed to an alloy fixture to make solid state LED lamp.

3.2 Alloy fixture LED lamp

Two units of Luxeon Rebel Red LED panels and two units of Luxeon Rebel Blue LED module assemblies were constructed to make a LED lamp in this study. Each high power LED panel consists of an array of 4×2 units of Luxeon Rebel Red LED module assemblies that are fixed into the alloy fixture. Each high power LED module assembly consists of the Luxeon Rebel Red or Blue LED module and the open-ended square reflector. Figure 3.9 shows the flow diagram of how the LED panel was constructed.

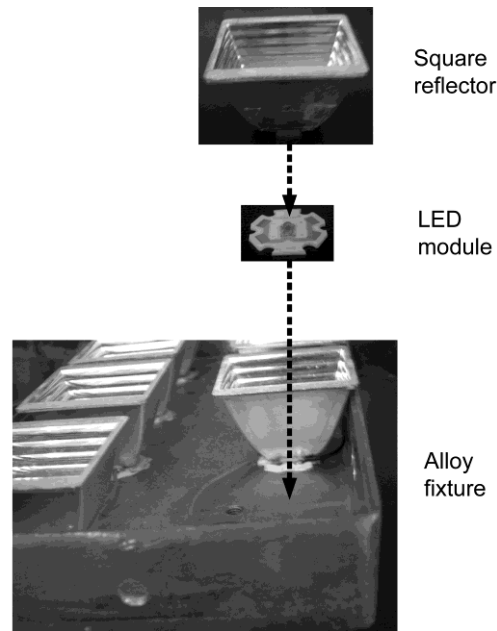


Figure 3.9: A flow diagram indicating how the LED panel was constructed. The opened reflector is mounted to the LED module before they are fixed into an alloy fixture.

The attachment of the Luxeon Rebel Red LED module assemblies into the alloy fixture was done with the use of Dow Corning SE4486 adhesive, which has a good thermal conductivity of 1.53 W/mK. The thermal resistance contributed by the adhesive is as low as 0.4 °C/W when 0.2 mm maximum thickness of adhesive was applied to bond the high power LED module to the surface of inner part of alloy fixture. On the other hand, Luxeon Rebel Blue LED module assemblies were attached to 20 mm x 20 mm aluminum sheet to assist heat dissipation and were placed at both end of the alloy fixture. Since the luminous flux output of AlInGaP LED is dependent on temperature, hence thermal management is required and it is important to ensure Luxeon Rebel Red LED operates in the optimal performance, as such Philips Lumileds's thermal management concept was adopted in this case. The high power LED

module assemblies that were attached to the alloy fixture with thermal resistance of 0.8 °C/W could create temperature as high as 80.4 °C at the LED junction when the LED was driven by constant input current of 700 mA at ambient temperature of 25 °C.

All the eight Luxeon Rebel Red LED module assemblies in the panel were electrical connected in series with the maximum forward voltage of 3.51 V each and hence it created the total forward voltage of 28.08 V for each panel. The calculation of total input electrical power of each panel is shown as follow:

$$P_{tot_LED} = V_f \times I = 28.08 \text{ V} \times 0.7 \text{ A} = 19.66 \text{ W} \quad (1)$$

(where V_f is the total maximum forward voltage of Luxeon Rebel Red LED in serial connection in the panel.)

The calculation of the LED temperature in the panel is as follow:

$$T_{j-a} = P_{tot_LED} \times (R\Theta_{LED_module}) / 8 \quad (2)$$

$$T_{j-a} = 19.66 \times [(12 + 0.12 + 0.4 + 0.8) \times 3.51 \times 0.7] / 8 = 80.4 \text{ °C} \quad (3)$$

$$(\textit{where } R\Theta_{LED_module} = R\Theta_j + R\Theta_{pcb} + R\Theta_{ads} + R\Theta_f) \quad (4)$$

provided that :

thermal resistance of LED die junction-slug, $R\Theta_j = 12 \text{ °C/W}$;

thermal resistance of PCB of ceramic substrate, $R\Theta_{pcb} = 0.12 \text{ °C/W}$;

thermal resistance of silicone adhesive with 0.2 mm thickness, $R\theta_{ads} = 0.4$ °C/W;

thermal resistance of alloy fixture, $R\theta_f = 0.8$ °C/W;

Note: Solder has extremely low thermal resistance of less than 0.001 °C/W and has been ignored in the calculation (Bai et al., 2004).

Temperature at outer surface of the alloy fixture was measured and recorded as 53 °C at the ambient temperature of 25 °C. By using the system thermal resistance model of Philips Lumileds AB05, the junction temperature of Luxeon Rebel Red LED should be;

$$53 \text{ °C} + (12 + 0.12 + 0.4 + 0.8) \text{ °C/W} \times (3.51 \times 0.7) \text{ W} = 85.7 \text{ °C}$$

This value was quite close to the calculated temperature value in equation (3); this temperature was still well below the maximum operating temperature of 135 °C. Based on Luxeon Rebel Red LED luminous flux versus temperature chart in Figure 3.10, when the Luxeon Rebel Red LED junction temperature reached 85.7 °C the thermal pad at that moment would be;

$$85.7 \text{ °C} - (12 \text{ °C/W} \times 3.51 \text{ V} \times 0.7 \text{ A}) = 56.2 \text{ °C}$$

This value has maintained 80% of the initial luminous flux. With this thermal pad temperature value and Luxeon Rebel Red LED has 0.05 nm/°C thermal coefficient of dominant wavelength as stated in Table 2, the wavelength shift will have $(56.2 - 25) \text{ °C} \times 0.05 \text{ nm/°C} = 1.56 \text{ nm}$ small different near to 629 nm.

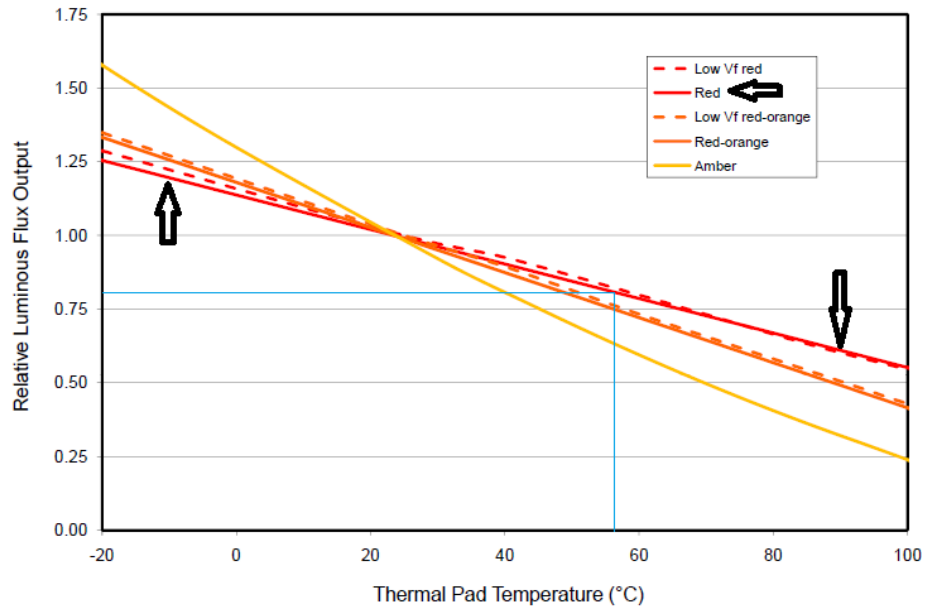


Figure 3.10: Relative light output vs. thermal pad temperature for red, red-orange & amber

Table 2: Optical characteristic of Luxeon Rebel LED

Color	Dominant Wavelength ^[2] λ_D , or Peak Wavelength ^[3] λ_p			Typical Spectral Half-width ^[4] (nm) $\Delta\lambda_{1/2}$	Typical Temperature Coefficient of Dominant Wavelength (nm/°C) $\Delta\lambda_D / \Delta T_J$	Typical Total Included Angle ^[5] (degrees) $\theta_{0.90V}$	Typical Viewing Angle ^[6] (degrees) $2\theta_{1/2}$
	Min.	Typ.	Max.				
Green ^[7]	520.0 nm	530.0 nm	550.0 nm	30	0.05	160	120
Cyan ^[7]	490.0 nm	505.0 nm	520.0 nm	30	0.04	160	120
Blue ^[7]	460.0 nm	470.0 nm	490.0 nm	20	0.05	160	120
Royal-Blue ^[3] ^[7]	440.0 nm	447.5 nm	460.0 nm	20	0.04	160	120
Red ^[8]	620.0 nm	627.0 nm	645.0 nm	20	0.05	160	120
Red-Orange ^[8]	610.0 nm	617.0 nm	620.0 nm	20	0.08	160	120
Amber ^[8]	584.5 nm	590.0 nm	597.0 nm	20	0.10	160	120

Similarly for the Luxeon Rebel Blue LED, the temperature recorded at the aluminum sheet surface it attached to was 64 °C and based on Luxeon Rebel Blue LED luminous flux versus temperature chart in Figure 3.11, when the

junction temperature of Luxeon Rebel Blue LED reached $64\text{ }^{\circ}\text{C} + (10 + 0.12 + 0.4 + 0.8)\text{ }^{\circ}\text{C}/\text{W} \times (3.51 \times 0.7)\text{ W} = 91.8\text{ }^{\circ}\text{C}$ the temperature of thermal pad at that moment would be $91.8\text{ }^{\circ}\text{C} - (10\text{ }^{\circ}\text{C}/\text{W} \times 3.51\text{ V} \times 0.7\text{ A}) = 67.2\text{ }^{\circ}\text{C}$; only less than 1% of the luminous flux degradation occurred. With $0.04\text{ nm}/^{\circ}\text{C}$ thermal coefficient of dominant wavelength as stated in Table 2, for Luxeon Rebel Blue LED the wavelength shift would have $(67.2 - 25)\text{ }^{\circ}\text{C} \times 0.04\text{ nm}/^{\circ}\text{C} = 1.69\text{ nm}$ delta different and near to 449 nm .

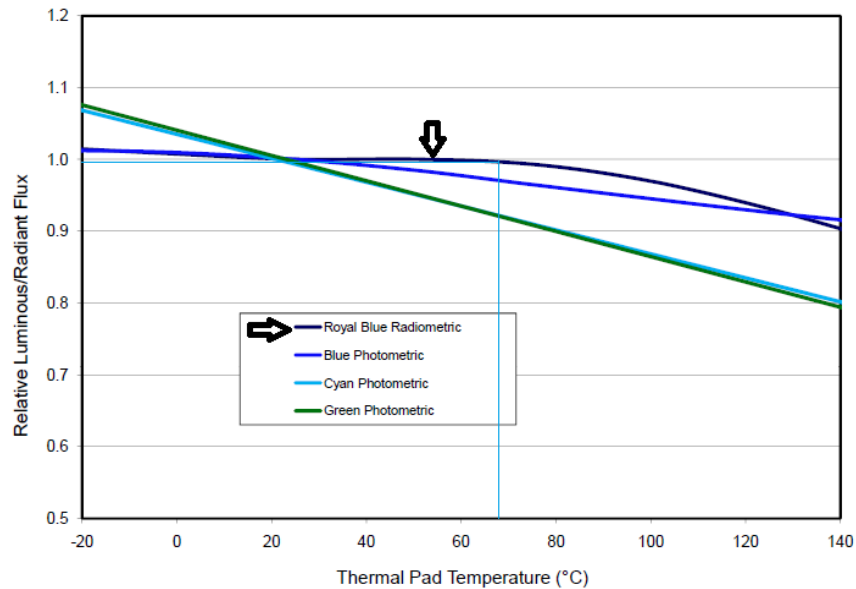


Figure 3.11: Relative light output vs. thermal pad temperature for royal blue, blue, cyan & green

3.3 LED driver

From the completed LED panels for red illumination and LED module assemblies for blue illumination, the highest numbers of serial LEDs in the circuit could be found in LED panels. There were eight Luxeon Rebel LEDs in each LED panel connected in serial connection that obtained 28.08 V total forward voltage as in section 3.2 equation (1); in which to turn on the LED panel, a LED driver that can deliver a DC output voltage of greater than 28.1 V is needed. The LED driver design in this study was based on switch mode buck topology where the LM3404 (Figure 3.12) made from National Semiconductor was selected for this reason. The LM3404 was capable to generate more than 40 V of DC voltage and maximum 1.0 A of current output which was greater than 28.08 V and 700 mA requirement. Besides, it also provided high power conversion efficiency at high switching frequency where part of this achievement was contributed from its integrated 1.5 A MOSFET switch. This switch could reduce the switching loss to the minimal and indirectly increasing the overall efficiency.

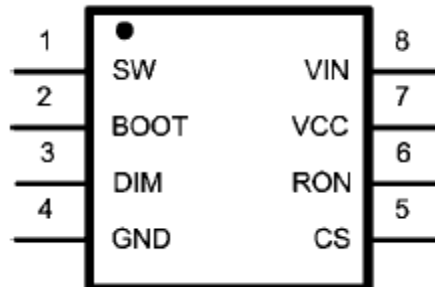


Figure 3.12: Pins function of LM3404

For driving Luxeon Rebel Red LED, only 700 mA maximum current was allowed and the LM3404 based LED driver was designed accordingly as shown in Figure 3.13. A feedback resistor of $0.33\ \Omega$ was calculated to convert the output current value to voltage value to allow the current feedback control to regulate 700 mA constant current. In this LED driver design, two Surface Mount Device (SMD) resistors of 1206 package with the resistance value of $0.68\ \Omega$ each were connected in parallel to have a total resistance of $0.34\ \Omega$. Two resistors instead of one were used for the reason of increasing the heat dissipation capacity when high current of 700 mA passing through them in the feedback loop. A step down transformer was used to step down the AC voltage from 240 V to 24 V. The 24V AC voltage then was converted to DC voltage through a bridge rectifier and filter circuit consisted of 4 diodes namely D2, D3, D4, D5 and two bypass capacitors C1, C4 before it supplied to LM3404 as shown in Figure 3.13. A $150\ \text{k}\Omega$ resistor was placed at the R_{on} and V_{in} pins to configure 1.4MHz high switching frequency in order to have higher efficiency operation. As a result, a smaller inductor size was required and lesser heat was generated from the whole LED driver.

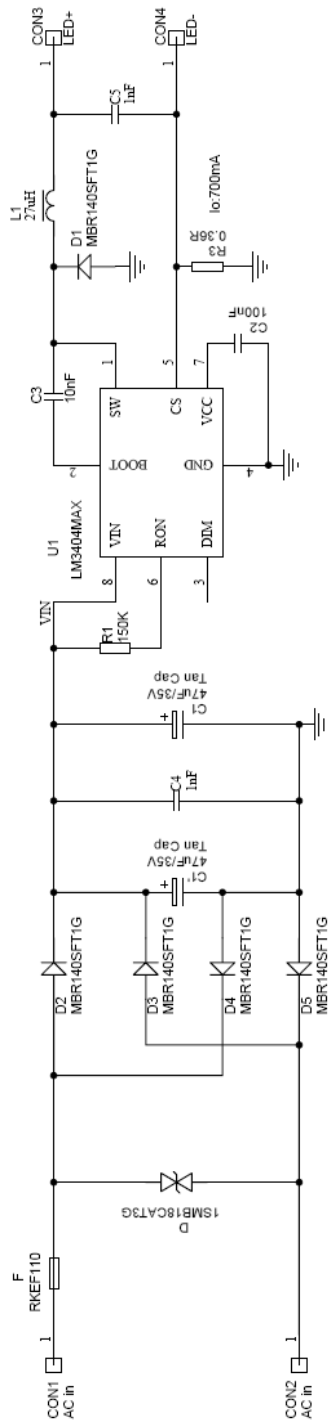


Figure 3.13: Circuit diagram shows a 24 V AC input LED driver based on LM3404IC that is capable of supplying constant output current of 700 mA and DC output voltage greater than 28.1 V in order to drive a maximum of eight Luxeon Rebel LEDs in series.

Total of three LED drivers were prepared for the energy efficient solid state lighting: two LED drivers supplied the power to two LED panels of eight series of Luxeon Rebel Red LED each and one LED driver supplied the power to two LED module assemblies of Luxeon Rebel Blue LED. All the three LED drivers were placed separately from the solid state lighting to avoid any heat interference with high power LED ambient temperature.

3.4 Luminous flux and PPF of solid state lighting

The completed solid state lighting was functionally tested to ensure working in good manner before starting the experiments. When all the LEDs of the solid state lamp were turned on, the illuminous recorded by Konica Minolta CL200 was 7200 lux in photometric at the center while 5190 lux and 5670 lux in photometric were recorded at the left and right sides of the illumination area as shown in Figures 3.14(a)-(c).



Figure 3.14(a): Illuminance recorded at center



Figure 3.14(b): Illuminance recorded at left edge



Figure 3.14(c): Illuminance recorded at right edge

There was higher illuminance obtained at the center of the target area. This was due to some radiation focus overlapped from LED panels and the LED module assemblies. This issue could be minimized by having more accurate reflectors mounting and placement adjustment of the LED modules in the LED panels.

The energy efficient solid state lamp produced minimum light radiation energy of 4.404 W of red radiation from 600-700 nm and 650 mW of blue radiation from 400-500 nm that would be focused to an area of 30 cm x 40 cm. The test specimen of young *Lactuca sativa* plants would be grown on the pallet placing at this area with 213.23 $\mu\text{mol}/\text{m}^2/\text{s}$ of PPF density. Below computation states the detail derivation.

Lumen output generated by LED panels at temperature stated in Figure 3.10;

$$\text{LM}_{\text{red}} = (\text{number of panels}) \times (\text{number of LED per panel}) \times (\text{radiant flux per LED}) \quad (5)$$

$$\text{LM}_{\text{red}} = 2 \times 8 \times 52 \text{ lm} = 832 \text{ lm} \quad (6)$$

Radiometric energy generated by LED panels is:

$$\text{RM}_{\text{red}} = \text{LM}_{\text{red}} / (\text{photopic conversion value at wavelength 629 nm}) \quad (7)$$

$$\text{RM}_{\text{red}} = 832 \text{ lm} / 188.92 \text{ lm/W} = 4.404 \text{ W} \quad (8)$$

Note : wavelengths in (6) - (8) are based on 629 nm and has Photopic Conversion of 188.92 lm/W

Radiometric energy output generated by LED module assemblies at temperature stated in Figure 3.11 is:

$$RM_{\text{blue}} = (\text{number of LED module assemblies}) \times (\text{radiant flux per LED}) \quad (9)$$

$$RM_{\text{blue}} = 2 \times 325 \text{ mW} = 650 \text{ mW} \quad (10)$$

Total irradiance energy output from solid state lighting is:

$$RM_{\text{tot}} = RM_{\text{red}} + RM_{\text{blue}} = 5.054 \text{ W} \quad (11)$$

Since energy per photon is $E = hv = hc/\lambda$, so total photons per second, n , will be:

$$n \text{ (photons/sec)} = Q_e / (h \times v) = Q_e / ((h \times c) / \lambda) = (Q_e \times \lambda) / (h \times c) \quad (12)$$

Photosynthetic Photon Flux, PPF, can be calculated as:

$$PPF \text{ (mol/sec)} = (Q_e \times \lambda) / (h \times c \times \text{Navogadro}) \quad (13)$$

where

$Q_e = \text{irradiance energy};$

$\lambda = \text{photon wavelength};$

$h = 6.63 \times 10^{-34};$

$c = 3.00 \times 10^8;$

$\text{Navogadro} = 6.02 \times 10^{23};$

For PPF of 600-700 nm;

$$PPF_{\text{red}} \text{ (mol/sec)} = (RM_{\text{red}} \times \lambda_{\text{red}}) / (h \times c \times \text{Navogadro}) \quad (14)$$

$$PPF_{\text{red}} \text{ (mol/sec)} = 23.149 \text{ } \mu\text{mol/s} \quad (15)$$

where $\lambda_{red} = 629 \text{ nm}$;

For PPF of 400-500 nm;

$$\text{PPF}_{\text{blue}} (\text{mol}/\text{sec}) = (\text{RM}_{\text{blue}} \times \lambda_{\text{blue}}) / (h \times c \times \text{Navogadro}) \quad (16)$$

$$\text{PPF}_{\text{blue}} (\text{mol}/\text{sec}) = 2.439 \text{ } \mu\text{mol}/\text{s} \quad (17)$$

where $\lambda_{\text{blue}} = 449 \text{ nm}$;

Total PPF of (400-500 nm) & (600-700 nm) is:

$$\text{PPF}_{\text{tot}} (\text{mol}/\text{sec}) = \text{PPF}_{\text{red}} + \text{PPF}_{\text{blue}} = 25.588 \text{ } \mu\text{mol}/\text{s} \quad (18)$$

PPF density in 30cm \times 40cm area, PPFD is:

$$\text{PPFD} = \text{PPF}_{\text{tot}} / \text{Area} \quad (19)$$

$$\text{PPFD} = (25.588 \text{ } \mu\text{mol}/\text{s}) / (0.3 \text{ m} \times 0.4 \text{ m}) \quad (20)$$

$$\text{PPFD} = 213.23 \text{ } \mu\text{mol}/\text{m}^2/\text{s} \quad (21)$$

CHAPTER 4.0

EXPERIMENTAL SETUP

The young *Lactuca sativa* seedlings were grown in pallet tray and two leaf stage plantlets germinated from the seeds were used as shown in Figure 4.1(a) & (b). Each pallet contained thirty three germinated two-leaf stage *Lactuca sativa*.

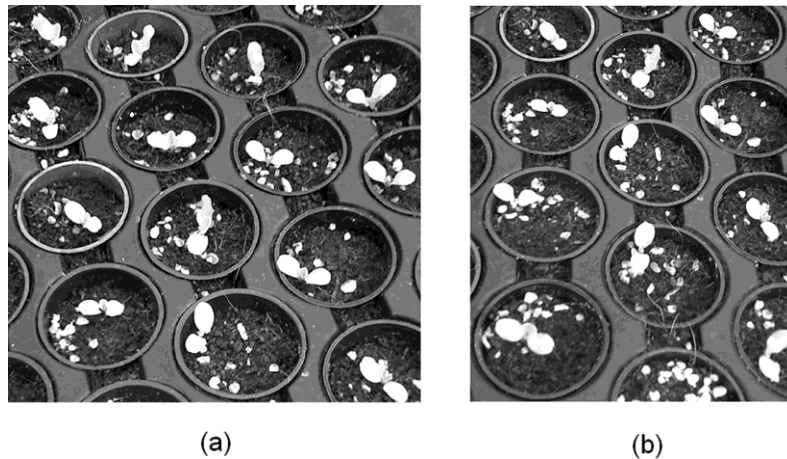


Figure 4.1: The two leaf stage *Lactuca sativa* seedlings were grown in pallets

The experiments were carried out in a green house of lettuce farm at Kampung Raja, Cameron Highland in Malaysia with altitude of 1311 m, latitude of 4.57 °N and longitude of 101.40 °E which lies entirely in the equatorial region. In the experiments, two pallets of young *Lactuca sativa* plants were cultivated

under two different illumination conditions for a comparison study. One pallet was placed inside a dark room equipped with energy efficient of high power LED solid state lighting system and another pallet was placed outside the dark room to be exposed to the normal solar irradiance. The pallet of young *Lactuca sativa* in the dark room was aligned well under the solid state LED lamp that was hung at the height of 20 cm above the plants, so that the light cone irradiated from the high power LED was sufficient to cover all the plants as shown in Figure 4.2.

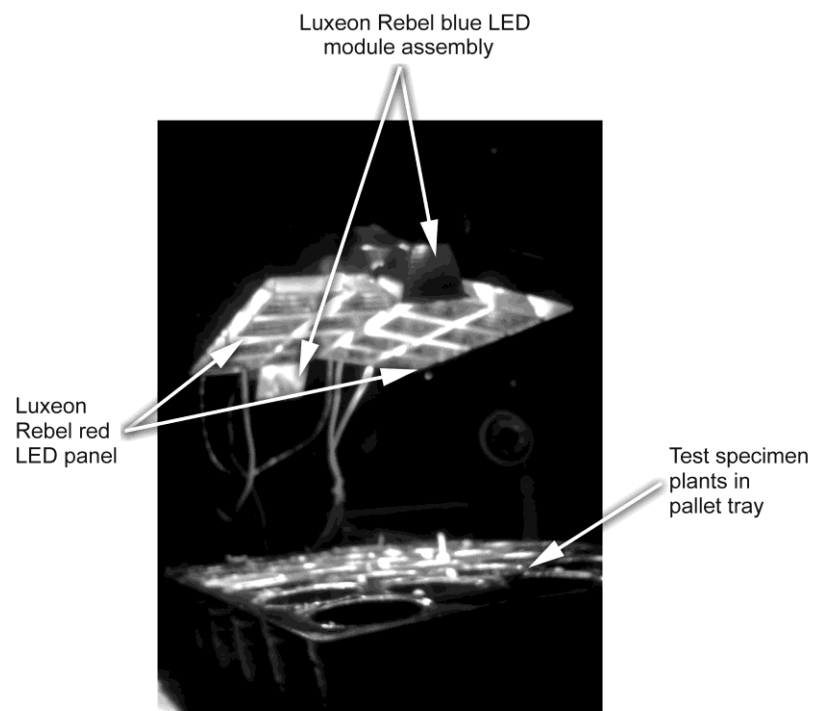


Figure 4.2: The experimental setup in a dark room. The energy efficient solid state lighting is placed at 20 cm above the test specimen plants.

The ambient temperature was recorded ranging from 18 °C to 26 °C during the testing period in which the lowest temperature happened in the midnight whilst the highest temperature happened in the sunny afternoon. The energy efficient solid state lighting system was powered up by a 24 V AC and the operating time was set from 8.00 am to 12.00 am (or 16 hours of photo-period) per day with the use of a timer control. Both the young *Lactuca sativa* plants cultivated in the dark room and under the normal solar irradiance were watered twice daily, i.e. in the morning and in the afternoon. The average illuminance under the energy efficient solid state lamp was 6020 lux while average illuminance under the normal sun was 36515 lux. The plantlets were grown under the above described conditions for 11 days. This experiment was repeated, however, due to unexpected electric power supply failure, it was performed for eight days. The whole plant growth and development of the *Lactuca sativa* was monitored and recorded by CCD cameras.



Figure 4.3(a): Solar illumination in the morning.



Figure 4.3(b): Solar illumination in the afternoon.

CHAPTER 5.0

RESULTS AND DISCUSSION

To prove the energy efficient of high power LED based solid state lighting is capable to accelerate the growth of indoor plants cultivation, two experiments were conducted and their results were presented in this study.

5.1 Physical observation of *Lactuca sativa* plants

From the observation, the specimens of young *Lactuca sativa* plants cultivated under the energy efficient solid state lighting showed faster growth rate than that of the plants cultivated under the normal solar irradiance. From the recorded video, Figures 5.1(a) – (k) show the *Lactuca sativa* plant growth from day 1 to day 11 for experiment 1 while Figures 5.2(a) – (h) show the *Lactuca sativa* plant growth from day 1 to day 8 for experiment 2. In the observations, the young *Lactuca sativa* plants cultivated under the energy efficient solid state lighting were observed to have larger leaf area and taller stem than the young *Lactuca sativa* plants cultivated under normal solar irradiance.

To compare the results of plant cultivation under the two different illumination conditions quantitatively, ten *Lactuca sativa* plants were

randomly selected from each pallet to measure the leaf width, total leaf area index per plant and plant fresh weight. The results are shown in Tables 3 and 4 for experiments 1 and 2, respectively. As a summary of experiment 1, most of the plants cultivated under energy efficient solid state lighting system had four big leaves with average leaf width of 21.8 mm, and average total leaf area index per plant of 1400.1 mm². The average plant fresh weight obtained was 2.39 g. For the plants cultivated under solar irradiance, the average leaf width measured was 13.6 mm, with the average total leaf area index per plant of 458.8 mm². A much lower average plant fresh weight (0.64 g) was obtained if compared with plants cultivated under the energy efficient solid state lighting. For experiment 2, the plants cultivated under the energy efficient solid state lighting system had two big leaves with average leaf width of 13.7 mm, and average total leaf area index per plant of 625.5 mm². The average plant fresh weight was 0.76 g. For plants cultivated under solar irradiance, the average leaf width and average total leaf area index per plant were 0.97 mm and 341.7 mm², respectively, with the average plant fresh weight of 0.37 g (Figure 5.3). By comparing the leaf size and plant fresh weight of the grown plants in Figures 5.3, the *Lactuca sativa* plants cultivated under the energy efficient solid state lighting system showed a faster growth rate than the plants cultivated under normal solar irradiance.

However, the plant growth is also affected by the physical environment where the plants are grown. Thus, the slower growth rate observed after the plants were kept under the normal sunlight condition might cause by other factors. In order to conclude the solid state lighting system would be able to

enhance the growth of plant in this study, further study needs to be performed in the future to grow the plants in a controlled environment where all samples will be grown under similar environment except the light source used will be varied. The current results showed the potential enhance effect of the solid state lighting on the plant growth.



(a)



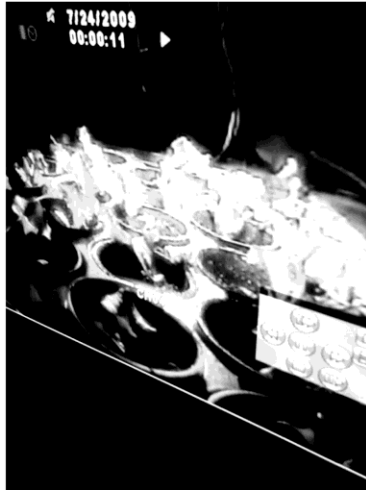
(b)



(c)



(d)



(e)



(f)



(g)



(h)



(i)



(j)



(k)

Figure 5.1: Images of grown *Lactuca sativa* plantlets captured by CCD video camera for 11 days to monitor the progress of plant growth under the energy efficient solid state lighting system in the dark room: (a) Day 1, (b) Day 2, (c) Day 3, (d) Day 4, (e) Day 5, (f) Day 6, (g) Day 7, (h) Day 8, (i) Day 9, (j) Day 10 and (k) Day 11.



(a)



(b)



(c)



(d)



(e)



(f)



(g)



(h)

Figure 5.2: Images of grown *Lactuca sativa* plantlets captured by CCD video camera for 8 days to monitor the progress of plant growth under the energy efficient solid state lighting system in the dark room: (a) Day 1, (b) Day 2, (c) Day 3, (d) Day 4, (e) Day 5, (f) Day 6, (g) Day 7, (h) Day 8.



(a)



(b)



(c)

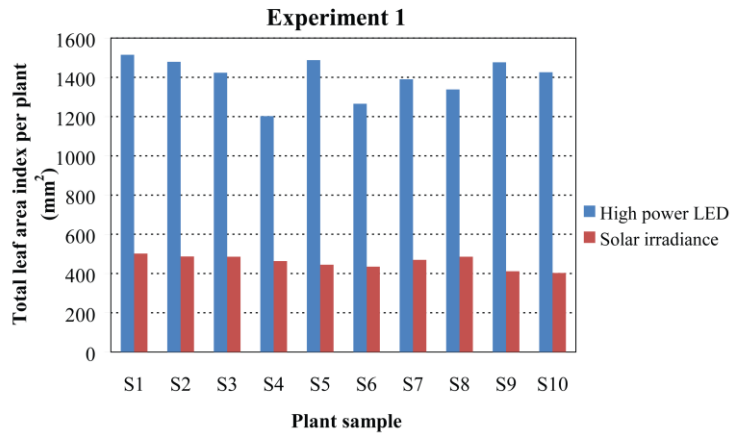
Figure 5.3: The comparisons of *Lactuca sativa* plantlets growth under the solar irradiance and the energy efficient solid state lighting: (a) *Lactuca sativa* plants cultivated under the energy efficient solid state lighting in experiment 1, (b) *Lactuca sativa* plants cultivated under solar irradiance in experiment 1, (c) *Lactuca sativa* cultivated under the energy efficient solid state lighting in left pallet and cultivated under solar irradiance in right pallet in experiment 2.

Table 3: Measurement result of total leaf area index, plant fresh weight and leaf width of the ten randomly selected samples in experiment 1

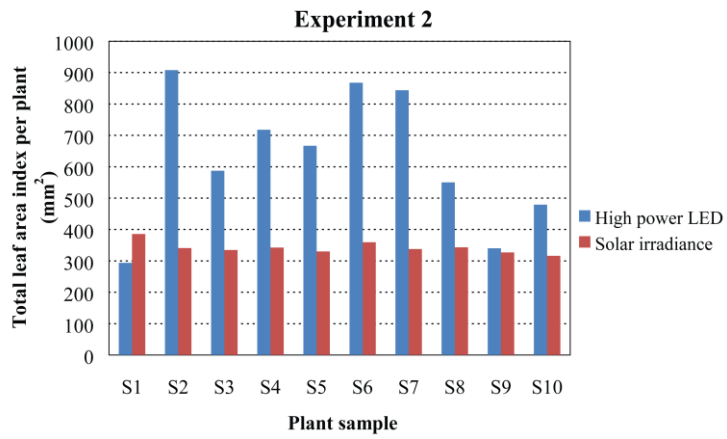
Plant sample	Experiment 1 (11 days of plant)					
	Total leaf area index per plant (mm ²)		Plant fresh weight (g)		Leaf width (mm)	
	High power LED	Solar irradiance	High power LED	Solar irradiance	High power LED	Solar irradiance
S1	1515	502	3.0	0.8	36, 33, 28, 24, 10	22, 20, 19, 11, 6
S2	1479	487	2.8	0.7	34, 28, 26, 25, 10	22, 20, 18, 10, 5
S3	1423	485	2.5	0.7	30, 27, 26, 18, 9	22, 19, 18, 10, 6
S4	1202	463	1.7	0.6	29, 24, 16, 8, 8	21, 18, 17, 9, 5
S5	1487	445	2.7	0.6	32, 27, 27, 24, 10	19, 17, 15, 8, 5
S6	1265	435	1.8	0.6	29, 24, 18, 10, 9	18, 16, 13, 8, 5
S7	1390	470	2.2	0.7	29, 27, 19, 17, 9	21, 20, 18, 9, 5
S8	1338	486	2.0	0.7	29, 25, 20, 14, 8	21, 20, 18, 10, 6
S9	1476	412	2.8	0.5	33, 30, 26, 24, 10	16, 14, 12, 8, 5
S10	1426	403	2.4	0.5	30, 28, 23, 18, 10	15, 14, 12, 7, 5
Average	1400.1	458.8	2.39	0.64	21.8	13.6
Max	1515	502	3.0	0.8	36	22
Min	1202	403	1.7	0.5	8	5

Table 4: Measurement result of total leaf area index, plant fresh weight and leaf width of the ten randomly selected samples in experiment 2

Plant sample	Experiment 2 (8 days of plant)					
	Total leaf area index per plant (mm ²)		Plant fresh weight (g)		Leaf width (mm)	
	High power LED	Solar irradiance	High power LED	Solar irradiance	High power LED	Solar irradiance
S1	294	386	0.3	0.4	17, 4, 4	18, 16, 7, 6
S2	908	341	1.2	0.4	28, 24, 7, 6	16, 12, 4, 4
S3	587	335	0.8	0.4	24, 20, 5, 5	15, 14, 5, 4
S4	718	342	0.9	0.4	24, 24, 5, 5	16, 10, 6, 5
S5	667	330	0.8	0.3	23, 20, 6	14, 14, 4, 4
S6	868	359	1.1	0.4	28, 23, 5, 6	15, 14, 5, 4
S7	844	338	1.0	0.4	23, 25, 6, 6	16, 12, 5, 4
S8	550	343	0.6	0.4	18, 22, 5, 5	15, 14, 5, 5
S9	340	327	0.4	0.3	20, 14, 6	21, 7, 4
S10	479	316	0.5	0.3	10, 21, 5, 6	17, 6, 6
Average	625.5	341.7	0.76	0.37	13.7	9.7
Max	908	386	1.2	0.4	28	21
Min	294	316	0.3	0.3	4	4

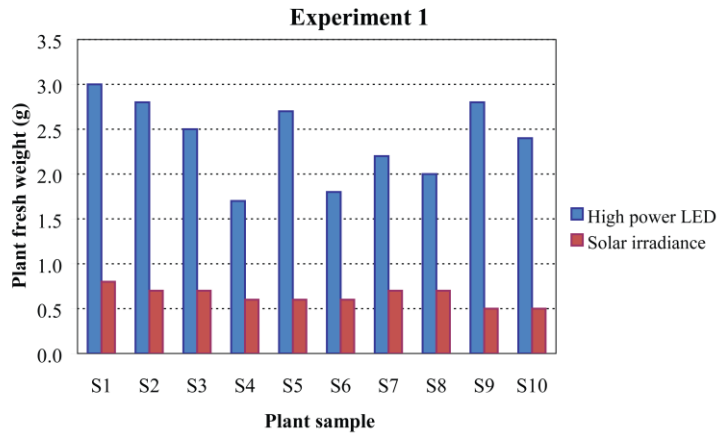


(a)

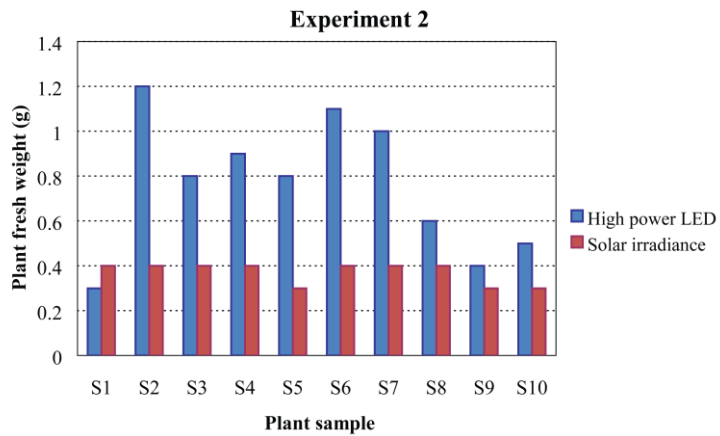


(b)

Figure 5.4: The total leaf area index per plant were measured from 10 randomly selected plants to compare the *Lactuca sativa* plants cultivated under the solar irradiance and the energy efficient solid state lighting system, (a) experiment 1 and (b) experiment 2.

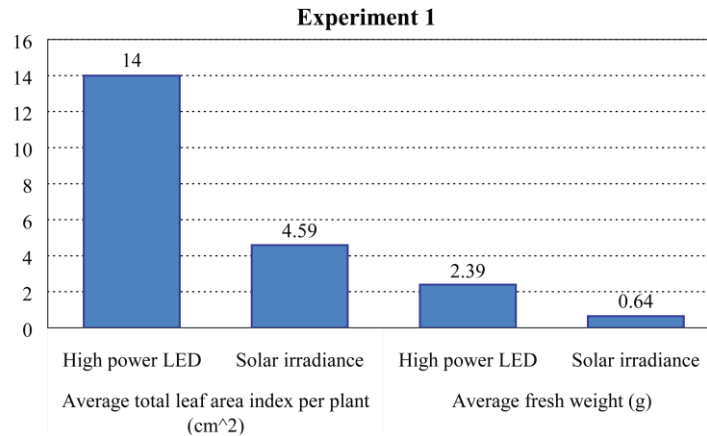


(a)

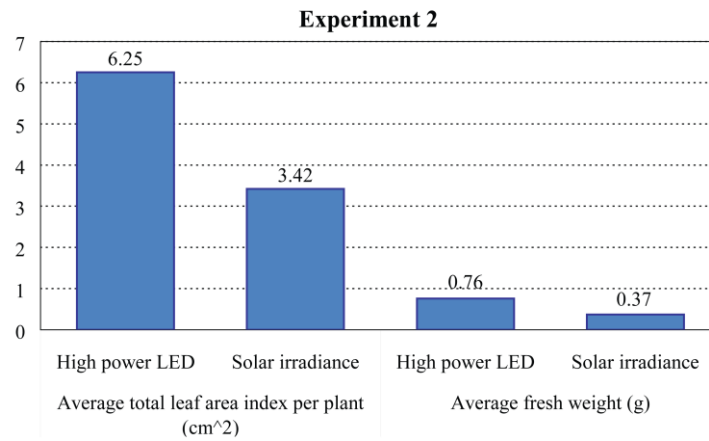


(b)

Figure 5.5: The fresh weight were measured from 10 randomly selected plants to compare the *Lactuca sativa* plants cultivated under the solar irradiance and the energy efficient solid state lighting system, (a) experiment 1 and (b) experiment 2.



(a)



(b)

Figure 5.6: The average values of both total leaf area index per plant and fresh weight were measured from 10 randomly selected plants to compare the *Lactuca sativa* plants cultivated under the solar irradiance and the energy efficient solid state lighting system, (a) experiment 1 and (b) experiment 2.

5.2 Energy efficiency and growth rate analysis

For the analysis of energy efficient method to cultivate the *Lactuca sativa* plants, three major parameters were computed which include Photosynthetic Active Radiation (PAR) energy efficiency, external power conversion efficiency and growth rate.

Firstly, to calculate PAR energy efficiency, the spectrums of various light sources are required. AvaSpec-256-NIR1.7 spectrometer with the resolution of 0.6 nm supplied by Avantes was employed to acquire the spectrums for high power LED based solid state lighting, Cool White Fluorescent Lamp (CWFL) and solar irradiance. To understand how effective the light source is in producing the irradiance within the wavelengths required for the photosynthesis process, PAR energy efficiency is defined as the ratio of PAR spectral intensity with the wavelengths ranging from 400 to 500 nm (red light) and from 600 to 700 nm (blue light) to the total spectral intensity with the wavelengths ranging from 200 to 900 nm. From the spectrums shown in Figures 5.7 – 5.9, the PAR energy efficiency for different light sources could compute for the comparison study. The applied equations in computation are as follow:

Spectral intensity with the wavelengths in the range of 400-500 nm:

$$I_{400-500nm} = \int_{400nm}^{500nm} I(\lambda) d\lambda \quad (22)$$

Spectral intensity with the wavelengths in the range of 600-700 nm:

$$I_{600-700nm} = \int_{600nm}^{700nm} I(\lambda) d\lambda \quad (23)$$

Total spectral intensity with the wavelengths in the range of 200-900 nm:

$$I_{200-900nm} = \int_{200nm}^{900nm} I(\lambda) d\lambda \quad (24)$$

PAR (400-500 nm & 600-700 nm) spectral intensity:

$$I_{PAR} = I_{400-500nm} + I_{600-700nm} \quad (25)$$

PAR energy efficiency,

$$\eta_{PAR} = (I_{PAR} / I_{200-900nm}) \times 100\% \quad (26)$$

From the computed results as listed in Table 5, the high power LED based solid state lighting had very good PAR energy efficiency of 95.54 % (PAR spectral intensity of 55.77 Wm^{-2} and total spectral intensity of 58.37 Wm^{-2}) when compared with the PAR energy efficiency of CWFL with 47.11 % (PAR spectral intensity of 9.07 Wm^{-2} and total spectral intensity of 19.2545 Wm^{-2}) as an alternative PAR source to solar irradiance. Figures 5.7 – 5.9 show the spectrum of energy efficient of high power LED based lighting system, CWFL lamp and solar irradiance, respectively.

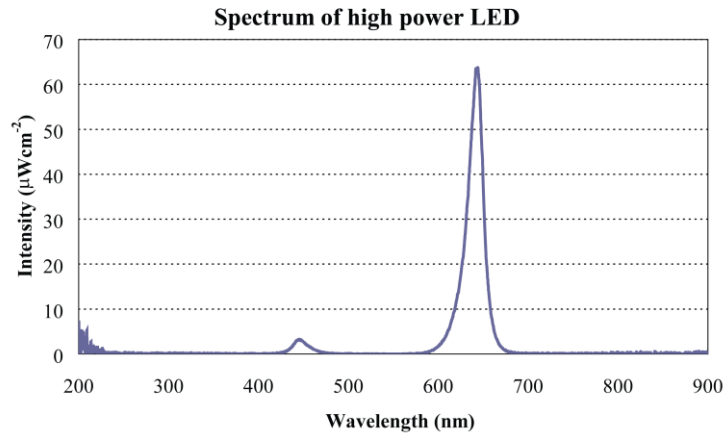


Figure 5.7: The spectrum of energy efficient of high power LED based lighting system ranging from 200nm to 900nm acquired using AvaSpec-256-NIR1.7 spectrometer with the resolution of 0.6 nm.

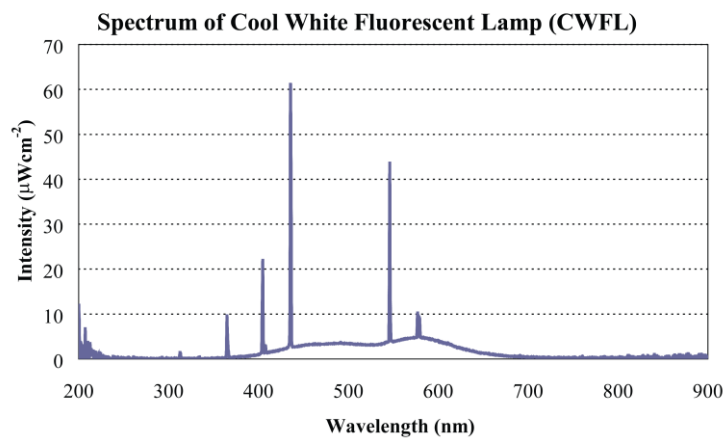


Figure 5.8: The spectrum of Cool White Fluorescent Lamp (CWFL) ranging from 200nm to 900nm acquired using AvaSpec-256-NIR1.7 spectrometer with the resolution of 0.6 nm.

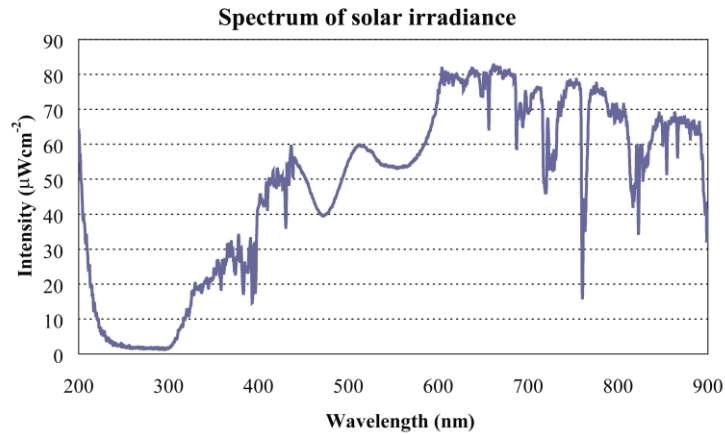


Figure 5.9: The spectrum of solar irradiance at 12pm sunny day ranging from 200nm to 900nm was acquired using AvaSpec-256-NIR1.7 spectrometer with the resolution of 0.6 nm.

Secondly, the external power conversion efficiency can be calculated as a ratio of the output PAR spectral power that is illuminated on the focus area of 0.12 m^2 to the input electrical power. The calculated results are listed in Table 5 where the conversion efficiency of high power LED based solid state lighting with 15.81 % is much more superior to that of the CWFL with 3.03 %; indirectly showing that the high power LED based solid state lighting could provide higher amount of PAR energy with lower electrical energy power consumption. Thus, this also shows that the high power LED based solid state lighting provides higher energy efficient than the CWFL.

Lastly, the growth rate (η_{Gr}) of the *Lactuca sativa* plants was also computed for the comparison study. The growth rate (η_{Gr}) is defined as the average plant fresh weight divided by the total radiometric power consumption

per plant. Total radiometric power consumption per plant can be obtained as follow:

$$E = I_{200-900nm} \times t \times A \quad (27)$$

where

$I_{200-900nm}$ is the irradiance of the light source;

t is the total hours of the plant being illuminated by the light source throughout the whole cultivation process (or total days of plant \times total hours of photo-period per day);

A is the total illuminated area.

The growth rate for the plants cultivated under the high power LED based solid state lighting and solar irradiance in experiments 1 and 2 were calculated and listed in Table 5. The calculation of total radiometric power consumption per plant for solar irradiance is based on the average daily solar irradiation of 6000 Wh/m^2 for the months of July and August in the zone of Cameron Highland provided by Ayu Wazira et al. (2008). In experiment 1, the growth rate of *Lactuca sativa* plants cultivated under high power LED based solid state lighting with $63.97 \times 10^{-3} \text{ gram/Wh}$ was much higher compared to that of solar irradiance of $2.67 \times 10^{-3} \text{ gram/Wh}$. Similarly in experiment 2, the growth rate of *Lactuca sativa* plants cultivated under high power LED based solid state lighting with $27.97 \times 10^{-3} \text{ gram/Wh}$ was also much higher compared to that of solar irradiance of $2.12 \times 10^{-3} \text{ gram/Wh}$.

Conclusively, all the data listed in Table 5 have clearly explained that the cultivation of *Lactuca sativa* plants under high power LED based solid state lighting has higher growth rate than cultivation under solar irradiance.

Table 5: PAR energy efficiency, external power conversion efficiency and growth rate for different light sources: solar irradiance, high power LED based energy efficient solid state lighting and CWFL

	Solar irradiance	High power LED	CWFL
$I_{200-900\text{nm}}$ (μWcm^{-2})	59892.65	5837.15	1925.45
$I_{400-500\text{nm}}$ (μWcm^{-2})	8157.97	265.24	617.63
$I_{500-600\text{nm}}$ (μWcm^{-2})	9996.95	50.78	768.38
$I_{600-700\text{nm}}$ (μWcm^{-2})	13757.95	5311.42	289.35
PAR energy efficiency, η_{PAR} (%)	36.59	95.54	47.11
Electrical power (W)	-	42.32	36
PAR spectral intensity (W/m^2)	219.16	55.77	9.07
PAR spectral power illuminated to the area of 0.12 m^2 (W)	26.30	6.69	1.09
External power conversion efficiency (%)	-	15.81	3.03
Experiment 1			
Average plant fresh weight (gram)	0.64	2.39	-
Total radiometric power consumption per plant (Wh)	(*6000 \times 11 \times 0.12)/33	(58.37 \times 16 \times 11 \times 0.12)/33	-
Growth rate η_{Gr} (gram/(Wh))	2.67×10^{-3}	63.97×10^{-3}	-
Experiment 2			
Average plant fresh weight (gram)	0.37	0.76	-

Total radiometric power consumption per plant (Wh)	$(*6000 \times 8 \times 0.12) / 33$	$(58.37 \times 16 \times 8 \times 0.12) / 33$	-
Growth rate η_{Gr} (gram/(Wh))	2.12×10^{-3}	27.97×10^{-3}	-

Note: * Average daily solar irradiation of 6000 Wh/m² for the month of July and August in the zone of Cameron Highland that is provided by Ayu Wazira et al. (2008)

CHAPTER 6

CONCLUSION

The energy efficient solid state lighting which consists of AlInGaP and InGaN high power LEDs that produces effective 400-500 nm and 600-700 nm PPF, was successfully designed and constructed. This novel energy efficient of high power LED based solid state lighting only uses 18 pieces of high power LEDs to generate high PPFD of 213.23 $\mu\text{mol}/\text{m}^2/\text{s}$. From the experimental results shown, the young *Lactuca sativa* (the test plants) cultivated under the energy efficient solid state lighting had higher growth rate when compared to those plants cultivated under normal solar irradiance in terms of total leaf area index per plant and average fresh weigh. Since the energy efficient solid state lighting only consumes less than 20 W of electric power energy, a simple passive cooling method is sufficient to retain the high power LED in good operating condition for less optical degradation. As such, this will increase the solid state lighting lumen maintenance and directly reduces the agriculture maintenance costs to a very minimal level for a long period of time. Besides, it can be easily controlled to operate longer than normal sun irradiance period which might be able to increase plants photosynthesis for higher agriculture economy. To conclude, the research has verified the energy efficient solid state lighting is highly energy efficient for the in indoor plant cultivation. The energy efficient solid state lighting is also capable in accelerating the growth rate of *Lactuca sativa*.

The government is recommended to set policy to use energy efficient and green solid state lighting system replacing the current conventional lighting system for indoor cultivation. For future study, more study on cost and benefits of solid state lighting should be conducted to convince the farmer in using high efficient LED for indoor cultivation.

REFERENCES

- Ayu Wazira, Azhari et al., 2008. A New Approach For Predicting Solar Radiation In Tropical Environment Using Satellite Images – Case Study Of Malaysia. *WSEAS Transactions on Environment and Development*, 4(4), pp. 373-378.
- Bai, J.G. et al., 2005. Measurement of Solder/Copper Interfacial Thermal Resistance by the Flash Technique. *Int. J. Thermophys.*, 26(5), pp. 1607-1615.
- Brown, C.S., Schuerger, A.C. and Sager J.C., 1995. Growth and photomorphogenesis of pepper plants under red light-emitting diodes with supplemental blue or far-red lighting. *Journal Amer. Soc. Hort. Sci.*, 120(5), pp. 808-813.
- Bula, R.J. et al., 1991. Light-emitting diodes as a radiation source for plants. *HortScience*, 26(2), pp. 203-205.
- Chin, L.Y. and Chong, K.K., 2012. Study of high power light emitting diode (LED) lighting system in accelerating the growth rate of *Lactuca sativa* for indoor cultivation. *International Journal of Physical Sciences*, 7(11), pp. 1773-1781.

Craford, M.G., 2007, *Current State of the Art in High Brightness LEDs*
[Online]. Available at:

[http://www.aps.org/meetings/multimedia/march2007/upload/craford.p](http://www.aps.org/meetings/multimedia/march2007/upload/craford.pdf)

[df](http://www.aps.org/meetings/multimedia/march2007/upload/craford.pdf) [Accessed: 31st August 2012].

Farabee M.J., 2001, *Photosynthesis* [Online]. Available at:

<http://ridge.icu.ac.jp/biobk/BioBookPS.html> [Accessed: 31st August

2012].

Goins, G.D. et al., 1997. Photomorphogenesis, photosynthesis, and seed yield of wheat plants grown under red light-emitting diodes (LEDs) with and without supplemental blue lighting. *Journals of Experimental Botany*, 48(7), pp.1407-1413.

High power LEDs, 2010, *Luxeon Star LED* [Online]. Available at:

http://www.rabtron.co.za/high_power_leds [Accessed: 31st August

2012].

Hoenecke, M.E., Bula, R.J., and Tibbitts, T.W., 1992. Importance of blue photon levels for lettuce seedlings grown under red-light-emitting diodes. *HortScience*, 27(5), pp. 427-430.

Holonyak, N. and Bevacqua, S.F., 1962. Coherent (visible) Light Emission From Ga(As_{1-x}P_x) Junctions. *Applied Physics Letters*, 1, pp. 82-83.

- Hu, Y. and Jovanovic, M.M., 2008. LED Driver With Self-Adaptive Drive Voltage. *IEEE Transactions On Power Electronics*, 23(6), pp. 3116-3125.
- Jao, R.C. and Fang, Wei, 2004. Effects of Frequency and Duty Ratio on the Growth of Potato Plantlets In Vitro Using Light-emitting Diodes. *HortScience*, 39(2), pp. 375-379.
- Kim, A.Y. et al., 2001. Performance of High-Power AlInGaN Light Emitting Diodes. *Physica Status Solidi A*, 188(1), pp. 15-21.
- Lee, C.G. and Palsson, B., 1994. High-density algal photobioreactors using light-emitting diodes. *Biotechnology & Bioengineering*, 44, pp. 1161-1167.
- Lee, M.H. et al., 2010. Design and fabrication of metal PCB based on the patterned anodizing for improving thermal dissipation of LED lighting. *Microsystems Packaging Assembly and Circuits Technology Conference (IMPACT)*, 2010 5th International, 20-22 October 2010 Taipei, pp. 1-4.
- Leung, W.Y., Man, T.Y. and Chan, Mansun, 2008. A high power LED driver with power efficient LED-current sensing circuit. *34th European Solid State Circuits Conference*, 15-19 September 2008 Edinburgh, pp. 354-357.

Lu, J.Y. and Wu, X.B., 2009. A PWM controller IC for LED driver used to multiple DC–DC topologies. *Proceedings of Asia Pacific power and energy engineering conference*, 27- 31 March 2009 Wuhan, pp. 1-4.

Lumileds AB12, 2005, *Custom Luxeon Design Guide* [Online]. Available at: <ftp://ftp.sic.rm.cnr.it/incoming/ifa.rm.cnr.it/Maurizio.Viterbini/Public/SuperLED/AB12.pdf> [Accessed: 31st August 2012].

Luxeon 1-Watt Star, 2002, *Power Light Source – Luxeon 1 Watt Star* [Online]. Available at: <http://www.maruka-denki.co.jp/images/DS23.pdf> [Accessed: 31st August 2012].

Matthijs, H.C.P. et al., 1996. Application of light-emitting diodes in bioreactors: flashing light effects and energy economy in Algal culture (*Chlorella pyrenoidosa*). *Biotechnology & Bioengineering*, 50(1), pp. 98-107.

Mineiro Sa, E., Antunes, F.L.M., and Perin, A.J., 2008. Low Cost Self-Oscillating ZVS-CV Driver for Power LEDs. *Power Electronics Specialists Conference*, 15-19 June 2008 Rhodes, pp. 4196-4201.

Nakamura, S., Mukai, T. and Senoh, M., 1991. High-Power GaN P-N-Junction Blue-Light Emitting Diodes. *Japanese Journal of Applied Physics Part 2 Letters*, 30(12A), pp. L1998-L2001.

Nave, C.R., 2012, *Light Absorption for Photosynthesis* [Online]. Available at:

<http://hyperphysics.phy-astr.gsu.edu/hbase/biology/ligabs.html>.

[Accessed: 31st August 2012].

Nedbal, L. et al., 1996. Microscopic green algae and cyanobacteria in high-frequency intermittent light. *Journal of Applied Phycology*, 8, pp. 325-333.

Nhut, D.T. et al., 2000. Light emitting diodes (LEDs) as a radiation source for micropropagation of strawberry. *Transplant production in the 21st century : proceedings of the International Symposium on Transplant Production in Closed System for Solving the Global Issues on Environmental Conservation, Food, Resources and Energy*, 28 February – 2 March 2000 Japan, pp. 114-118.

Okamoto, K., Yanagi, T. and Kondo, S., 1997. Growth and morphogenesis of lettuce seedlings raised under different combinations of red and blue light. *Acta Horticulture*, 435, pp. 149-157.

Philips Lumileds AB32, 2012. Luxeon LED Assembly and Handling Information. *Philips Lumileds*, pp. 3-13.

Philips Lumileds DS64, 2012. Luxeon Rebel General Purpose White Portfolio. *Philips Lumileds*, pp. 3-10.

Philips Lumileds DS65. 2011. Luxeon Rebel Direct Color Portfolio. *Philips Lumileds*, pp. 3-13.

Round, H.J., 1907. A note on Carborundum. *Electrical World*, 49, pp. 309.

Tennessee, D.J., Singaas, E.L. and Sharkey, T.D., 1994. Light-emitting diodes as a light source for photosynthesis research. *Photosynthesis Research*, 39, pp. 85-92.

Yanagi, T. and Okamoto, K., 1994. Super-bright light emitting diodes as an artificial light source for plant growth. *Abstract of 3rd international symposium on artificial lighting in horticulture*, pp. 19.

Yung, Winco, 2010, *A Cost-effective Advanced Thermal Material for Metal-Core Printed Circuit Board (MCPCB)* [Online]. Available at: <http://www.ektpcb.com/Uploadfile/file/download/A%20Costeffective%20Advanced%20Thermal%20Material.pdf> [Accessed: 31st August 2012].

APPENDIX A

Current state of the art in high brightness LEDs

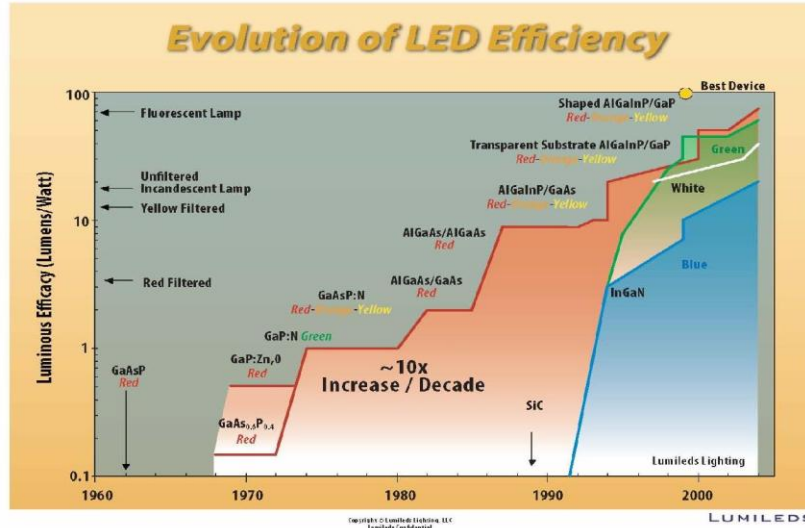
PHILIPS

Current State of the Art in High Brightness LEDs

LUMILEDS
LIGHT FROM SILICON VALLEY

M. George Craford, CTO
American Physical Society
Solid State Lighting Session
March 6, 2007

Evolution of LED Efficiency



APPENDIX B

Full spectrum lighting

IRC Internal Report No. 659
Page 30

Is Full-Spectrum Lighting Special?

Peter R. Boyce, Ph.D.
Lighting Research Center
Rensselaer Polytechnic Institute
Troy, NY 12180-3590 U.S.A.

Definition

There is no "official" definition of full spectrum lighting. What there is, is a de facto definition related to the use of full-spectrum fluorescent lamps. Specifically, full-spectrum lighting consists of interior lighting provided exclusively by full-spectrum fluorescent lamps. Such lamps are designed to mimic daylight. They have spectral emissions in all parts of the visible spectrum and some emission in the ultra-violet, mainly the near ultra-violet. Quantitatively, they have a correlated colour temperature greater than 5000 K and a CIE General Colour Rendering Index of greater than 90. The correlated colour temperature specifies the apparent colour of light emitted by the lamp; the higher the colour temperature, the cooler (or more blue) the apparent colour of the light. The CIE Colour Rendering Index quantifies the ability of the lamp to render colours as well as a standard lamp with the same colour temperature. The CIE General Colour Rendering Index has a value of 100 when the match between the test lamp and the standard is perfect. Therefore, the full-spectrum fluorescent lamp is cool in colour appearance and has good colour rendering properties.

Claims

Lighting using full-spectrum fluorescent lamps has been the subject of many claims. The level of support for these claims varies. For example, full-spectrum lamps have repeatedly been shown to be effective in the treatment of seasonal affective disorder (Rosenthal & Blehar, 1989). Less well established are the effects of working under full-spectrum fluorescent lamps on fatigue, task performance and mood; some authors achieving statistically significant improvements under full spectrum lighting (Maas, Jayson & Kleiber, 1974) while others fail to find any effects (Berry, 1983; Boray, Gifford & Rosenblood, 1989). Even more controversial are studies of the effects of full-spectrum lighting on hyperactivity in children (Mayron, Ott, Nations & Mayron, 1974; O'Leary, Rosenbaum & Hughes, 1978a; Mayron, 1978; O'Leary, Rosenbaum & Hughes, 1978b).

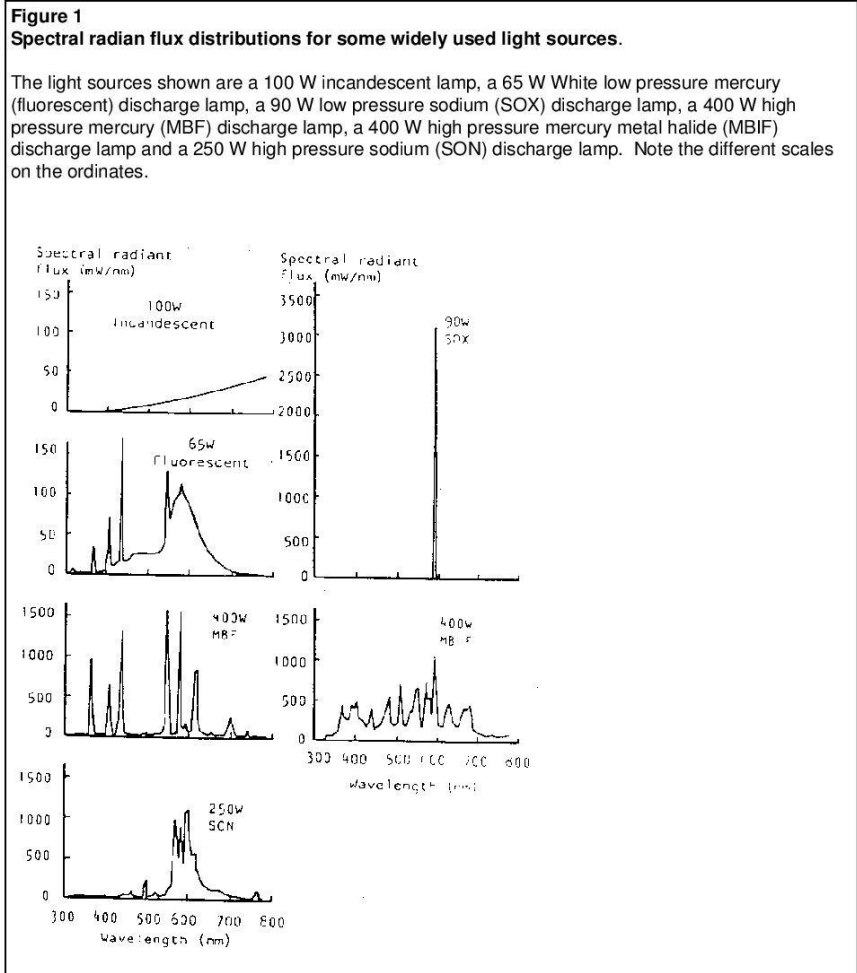
The result of this diversity of findings is that the whole field of full-spectrum lighting has become clouded with controversy. The objective of this symposium is to clarify some of the arguments involved in this controversy and to set down what steps are needed to resolve it.

The objective of this presentation is to place full-spectrum fluorescent lamps in context with other light sources available to the lighting designer and to predict what would be expected from full-spectrum fluorescent lamps on the basis of current knowledge.

Full-Spectrum Fluorescent Lamps in Context

There are two broad classes of electric light sources available for interior lighting; incandescent light sources and discharge light sources. Incandescent light sources produce light by heating a filament, the spectrum of the light being determined by the temperature of the filament. Discharge light sources produce light by passing an electric current through an ionized gas; the spectrum of the light being determined by the gas used, the gas pressure, the other elements in the discharge and the presence or absence of a phosphor coating. Full-spectrum fluorescent lamps are low pressure, mercury discharge lamps with a phosphor coating. The discharge in the mercury atmosphere produces mainly ultra-violet radiation. This ultra-violet radiation is largely absorbed by the phosphor coating lining the walls of the discharge tube and reradiated as light. Incandescent lamps have a continuous spectrum in the visible region, dominated by the long wavelengths (see Figure 1). Discharge lamps typically have a spectrum consisting of strong single wavelengths amongst a

continuous background (see Figure 1). The spectrum emitted by one type of full-spectrum fluorescent lamp is shown in Figure 2.



It is the emission spectrum which defines each lamp type. Different lamp types have different luminous flux outputs but these can be compensated by adjusting the number of lamps used in an installation. The spectral emission cannot be compensated in this way. Figure 1 shows emission spectra, over the visible spectrum, for a number of light sources. All the light sources shown are commonly used for lighting in homes, offices, factories and on roads. It should be apparent from

APPENDIX C

Ceracon product specification

CERACON®

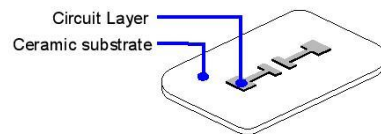
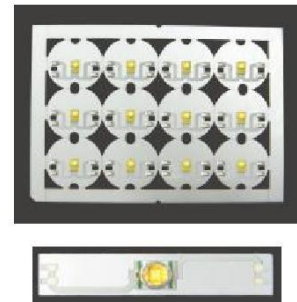
We Produce Competitive Printed Circuit Substrate for LEDs Lighting

CERACON® is the latest launched product for LEDs application. We offer affordable and competitive price of CERACON® without compromising its quality and functional features. The cost is comparatively lower than metal core circuit boards.

With our past 17 years of good quality control experiences and exposure in ceramic printing, we are proud to be renowned as a reliable and trustworthy thin film processes technology producer.

Physically white in nature, CERACON® is able to provide good lighting reflection to enhance brightness. By allowing direct fired on ceramic surface, elimination of heat barrier and directly generates better heat dissipation and thermal management, thus longer LED life span is assured.

CERACON® is excellent used for ceramic-based LED as it is able to reduce TCE mismatch. Thus solder stretch problem will be minimum or negligible. As CERACON® has high electrical insulation, it widely used for high voltage applications.



RoHS Compliant

Benefits

- * High electrical insulation
- * Thermal cycling stability
- * Better light reflection of its natural color.
- * Reduce TCE mismatch (*excellent used for ceramic-based LEDs such as Rebel*).
- * Good thermal conductivity
- * Low cost
- * Flexible shape and design capability

Product Specification

Technical Specification:

Maximum Operating voltage	: 250 VAC
Maximum Operating Temperat	: 150° C
Breakdown Voltage	: 15KV/mm
Conductor Trace Resistivity	: < 5.5 mΩ/in ²
Fired Conductor Thickness	: 10.0μm ± 2.5μm
Maximum Substrate Size	: 100mm X 100mm
Conductor Trace Resolution (line/space)	: 200μm X 200μm
Conductor Adhesion Force (Initial - 2mm X 2mm pad)	: >6.0 kgf



Property	Units	Ceracon® 96% Al ₂ O ₃
Color	-	White
Thermal conductivity 20-100°C	W/m °K	24
Thermal expansion 20-600°C	10 ⁻⁶ /°K	7.3
Dielectric constant		
-1 MHz		9.8 ± 10%
-1 GHz		10.0 ± 10%
Volume resistivity		
20°C	Ohm x cm	10 ¹³
200°C		10 ¹²

APPENDIX D

Dow Corning adhesive thermal management



Electronics
Solutions

Dow Corning LED
SOLUTIONS
Lighting the way
to advanced materials and solutions

LED Thermal Management

Advanced silicone technology for LED applications

Dow Corning is a global technology innovator for the LED marketplace, delivering high-performance solutions developed to meet the unique demands of LED assembly, from general illumination to specific automotive applications.

We deliver a comprehensive line of wet dispensed and fabricated thermal management material.

Features

- Excellent thermal transfer
- Good thermal and aging stability
- Flexible, stress relieving
- Outstanding gap fill

Benefits

- Easy application (heat cured or screen printing)
- Pre-cured materials can be cold applied
- Good dielectric properties
- Available in various forms: adhesive, gels, grease, thermal pad

Thermal Interface Materials – Wet Dispensed: Dispensable, printable and curable materials effective as heat transfer media.

Product Family	Material	Description/Color	Cure Conditions		Thermal Conductivity at 25°C (77°F), Watt/meter-K	Viscosity (cP)
			Room Temperature Cure, Time	Heat Cure, Time		
Adhesive/Sealant	Dow Corning® SE 4486 CV Thermally Conductive Adhesive	Flowable; one-part moisture cure; white	120 hr	—	1.53	19,000
	Dow Corning® SE 9184 CV Thermally Conductive Adhesive	One-part; non-flow; moisture cure; white	48 hr	—	0.84	non-flowing
	Dow Corning® 1-4173 Thermally Conductive Adhesive	One-part; low-flow; rapid-heat cure; grey	—	90 min@100°C 30 min@125°C 20 min@150°C	1.9	58,000
	Dow Corning® Q1-9226 Thermally Conductive Adhesive	Two-part; semi-flowable; self-priming; grey	—	60 min@100°C 30 min@150°C	0.74	50,000
Compound	Dow Corning® SC 102 Thermally Conductive Compound	One-part; gap fill material; white	—	—	0.8	non-flowing
	Dow Corning® TC-5625 Thermally Conductive Compound	One-part; silicone paste; grey	—	—	2.5	127,725
Gel	Dow Corning® SE 4445 CV Thermally Conductive Gel	Two-part; UL 94 V-0 rating; grey	—	45 min@125°C	1.26	14,000
Encapsulant	Sylgard® Q3-3600 A&B Thermally Conductive Encapsulant	Two-part encapsulant; grey	—	60 min@100°C 30 min@150°C	0.77	4,700

NOTE: Please check with your local Dow Corning office for a full product range and availability in your area.

APPENDIX E

Luxeon Thermal Design using Luxeon Power Light Source

Application Brief AB05



Thermal Design Using LUXEON® Power Light Sources

Introduction

LUXEON® Power Light Sources provide the highest light output with the smallest footprint of any Light Emitting Diodes (LEDs) in the world. This is due, in part, to LUXEON's ground breaking thermal design. LUXEON is the first LED solution to separate thermal and electrical paths, drawing more heat away from the emitter core and significantly reducing thermal resistance. As a result, LUXEON packages handle significantly more power than competing LEDs. LUXEON's larger, brighter emitters together with its unique high-power capabilities provide a tremendous amount of light in a small, durable package. This, in turn, provides lighting designers with a unique opportunity to explore new designs and product ideas and to improve the quality, energy-efficiency, safety and longevity of existing products.

Lighting designers working with LUXEON Power Light Sources do need to consider some potentially unfamiliar factors, such as the impact of temperature rise on optical performance. Proper thermal design is imperative to keep the LED emitter package below its rated operating temperature. This application note will assist design engineers with thermal management strategies.

We recommend taking the time to develop a thermal model for your application before finalizing your design. The LUXEON Custom Design Guide provides important details about operating temperatures for each LED emitter package. Once you determine your target temperature, a thermal model will allow you to consider the impact of factors such as size, type of heat sink, and airflow requirements.

Lighting designers needing additional development support for thermal management issues will find ample resources. The thermal management industry has grown along side advances in electronics design. The thermal analysis resources section at the end of this document provides a useful introduction to some industry resources.

Index

Introduction	1
Minimum Heat Sink Requirements	2
Thermal Modeling	2
Inputs/Output of the Thermal Model	4
Heat Sink Characterization	4
Attachment to Heat Sinks	7
Best Practices for Thermal Design	8
Evaluating Your Design	8
Validation of Method	11



Minimum Heat Sink Requirements

All LUXEON products mounted on an aluminum, metal-core printed circuit board (MCPCB, also called Level 2 products) can be lit out of the box, though we do not recommend lighting the Flood for more than a few seconds without an additional heat sink.

As a rule, product applications using LUXEON Power Light Sources require mounting to a heat sink for proper thermal management in all operating conditions. Depending on the application, this heat sink can be as simple as a flat, aluminum plate.

The LUXEON Star, Line and Ring products consist of LEDs mounted on MCPCB in various configurations (see the *LUXEON Product Guide*). These products have 1 in² of MCPCB per emitter. The MCPCB acts as an electrical interconnect, as well as a thermal heat sink interface. While we recommend using an additional heat sink, these products can be operated at 25°C without one. The MCPCB can get very hot (~70°C) without a heat sink. Use appropriate precautions.

A LUXEON Flood should be mounted to a heat sink before being illuminated for more than a few seconds. A flat aluminum plate with an area of about 36 in² (6" x 6" x 0.0625" thick) is adequate when operating at 25°C.

Thermal Modeling

The purpose of thermal modeling is to predict the junction temperature (T_{Junction}). The word "junction" refers to the p-n junction within the semiconductor die. This is the region of the chip where the photons are created and emitted. You can find the maximum recommended value for each LUXEON product in your data sheet. This section describes how to determine the junction temperature for a given application using a thermal model.

A. Thermal Resistance Model

One of the primary mathematical tools used in thermal management design is thermal resistance (R θ). Thermal resistance is defined as the ratio of temperature difference to the corresponding power dissipation. The overall R $\theta_{\text{Junction-Ambient (J-A)}}$ of a LUXEON Power Light Source plus a heat sink is defined in Equation 1:

Equation 1. Definition of Thermal Resistance

$$R_{\theta_{\text{Junction-Ambient}}} = \frac{\Delta T_{\text{Junction-Ambient}}}{P_d}$$

Where:

$\Delta T = T_{\text{Junction}} - T_{\text{Ambient}}$ (°C)

P_d = Power dissipated (W)

$P_d = \text{Forward current (If)} * \text{Forward voltage (Vf)}$

Heat generated at the junction travels from the die along the following simplified thermal path: junction-to-slug, slug-to-board, and board-to-ambient air.

For systems involving conduction between multiple surfaces and materials, a simplified model of the thermal path is a series-thermal resistance circuit, as shown in Figure 1A. The overall thermal resistance (R $\theta_{\text{J-A}}$) of an application can be expressed as the sum of the individual resistances of the thermal path from junction to ambient (Equation 2). The corresponding components of each resistance in the heat path are shown in Figure 1B. The physical components of each resistance lie between the respective temperature nodes.

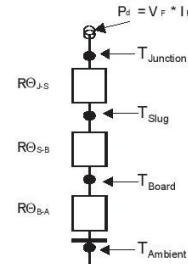


Figure 1A. Series Resistance Thermal Count

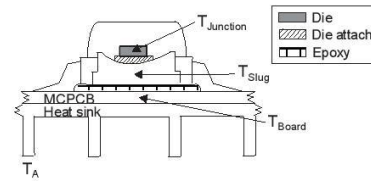


Figure 1B. Emitter Cut-Away

Equation 2. Thermal Resistance Model

$$R_{\theta_{\text{Junction-Ambient}}} = R_{\theta_{\text{Junction-Slug}}} + R_{\theta_{\text{Slug-Board}}} + R_{\theta_{\text{Board-Ambient}}}$$

Where:

R $\theta_{\text{Junction-Slug (J-S)}}$ = R θ of the die attach combined with die and slug material in contact with the die attach.

R $\theta_{\text{Slug-Board (S-B)}}$ = R θ of the epoxy combined with slug and board materials in contact with the epoxy.

R $\theta_{\text{Board-Ambient (B-A)}}$ = the combined R θ of the surface contact or adhesive between the heat sink and the board and the heat sink into ambient air.

Equation 3, derived from Equation 1 can be used to calculate the junction temperature of the LUXEON device.

Equation 3. Junction Temperature Calculation

$$T_{\text{Junction}} = T_A + (P_d)(R_{\theta_{J-A}})$$

Where:

- T_A = Ambient temperature
- P_d = Power Dissipated (W) = Forward current (I_f) * Forward voltage (V_f)
- $R_{\theta_{J-A}}$ = Thermal resistance junction to ambient

B. Thermal Resistance of LUXEON Light Sources

In LUXEON Power Light Sources, Philips Lumileds has optimized the junction-to-board thermal path to minimize the thermal resistance. The thermal resistance of a LUXEON emitter (not mounted on an MCPCB, also called a Level 1) is represented by $R_{\theta_{J-S}}$.

The thermal resistance of LUXEON Power Light Sources (MCPCB mounted, also called a Level 2) representing by $R_{\theta_{J-B}}$, equal to:

$$R_{\theta_{J-B}} = R_{\theta_{J-S}} + R_{\theta_{S-B}}$$

Typical values for R_{θ} are shown in Table 2.

Table 2 Typical LUXEON Thermal Resistance

Enter Description	LUXEON Power Light Sources ($R_{\theta_{J-B}}$) MCPCB Mounted Level 2	LUXEON Emitter ($R_{\theta_{J-S}}$) MCPCB Mounted Level 1
	Batwing (all colors)	
Lambertian (Green, Cyan, Blue, Royal Blue)	17°C/W	15°C/W
Lambertian (Red, Red-orange, Amber)	20°C/W	18°C/W

°C/W = °Celsius (ΔT) / Watts (P_d)

Note: Consult current data sheet for $R_{\theta_{J-S}}$ and $R_{\theta_{J-B}}$

C. Thermal Resistance of Multiple LUXEON Products

The total system thermal resistance of multiple-emitter LUXEON Products such as the LUXEON Line, Ring or multiple Stars can be determined using the parallel thermal resistance model as shown in Figure 2. In this model, each emitter is represented by individual, parallel thermal resistances.

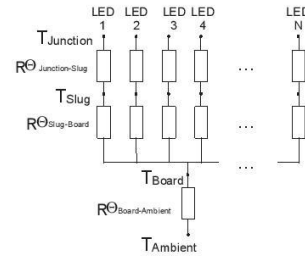


Figure 2. Parallel Thermal Resistance Model of Multiple Emitter Products

The $R_{\theta_{J-B}}$ of the multiple-emitter array is obtained by using the parallel resistance equation:

$$\frac{1}{\text{Total_Array_}R_{\theta_{\text{Junction-Board}}}} = \frac{1}{\text{LED}(1)_R_{\theta_{\text{Junction-Board}}}} + \dots + \frac{1}{\text{LED}(N)_R_{\theta_{\text{Junction-Board}}}}$$

All the parallel resistances can be assumed equivalent, so the equation becomes:

$$\frac{1}{\text{Total_Array_}R_{\theta_{\text{Junction-Board}}}} = \frac{N}{\text{LED_Emitter_}R_{\theta_{\text{Junction-Board}}}}$$

or:

Equation 4. Multiple Emitter to Single Emitter Thermal Resistance Relation

$$\text{Total_Array_}R_{\theta_{\text{Junction-Board}}} = \frac{\text{LED_Emitter_}R_{\theta_{\text{Junction-Board}}}}{N}$$

Where:

- LED Emitter $R_{\theta_{\text{Junction-Board}}}$ = $R_{\theta_{\text{Junction-Slug}}} + R_{\theta_{\text{Slug-Board}}}$
- N = Number of emitters

For example, in a LUXEON Line, there are 12 emitters, N=12. The LUXEON Line uses a batwing emitter; therefore, the Total Array $R_{\theta_{J-B}}$ is: (17°C/W)/12 = 1.42°C/W.

The Total Array $R_{\theta_{\text{Junction-Ambient}(J-A)}}$ for the LUXEON Line is:

$$\text{Total_Array_}R_{\theta_{\text{Junction-Ambient}}} = 1.42 + R_{\theta_{\text{Board-Ambient}}}$$

The Total Array Dissipated Power must be used in any calculations when using a Total Array thermal resistance model. The Total Array Dissipated Power is the sum of $V_e * I_e$ for all the emitters.

Equation 5. Thermal Resistance of a Multiple Emitter Array

$$\text{Total Array } R_{\theta_{J-A}} = \frac{\Delta T}{P_{d_Total}}$$

Where:

- ΔT = $T_{\text{Junction}} - T_{\text{Ambient}}$ (°C)
- P_{d_Total} = Total Array Dissipated Power (W)

Inputs/Output of the Thermal Model

You can use a thermal model to predict the junction temperature (T_J) for your application. This section discusses setting a goal for a maximum T_J as well as the variables in the right-hand-side of Equation 3 below. You can use variables in the thermal model as control factors in your application design.

$$T_{\text{Junction}} = T_{\text{Ambient}} + (P_d)(R\theta_{\text{Junction-Ambient}})$$

A. Set Limit for Junction Temperature (T_J)

Good thermal design incorporates T_J limits based on three factors:

1. Light output with T_J rise
2. Color shift with T_J rise
3. Reliability

Consult *LUXEON Custom Design Guide* for more detailed information on light output and color shift with rise in T_J .

1. Light Output with Temperature Rise

LEDs experience a reversible loss of light output as the T_J increases. The lower the T_J is kept, the better the luminous efficiency of the product (i.e. the better the light output). Light output from red, red-orange and amber emitters (based on AlInGaP LED technology) are more sensitive to increases in junction temperature than other colors.

An example of light output loss associated with temperature rise occurs with traffic signals. Signals that are simply retro-fitted with LED sources may not account adequately for heat dissipation. As temperatures rise during the day, the signals may dim. Redesigning the signal housing to provide airflow to cool the components alleviates this condition.

The chart on the LUXEON product data sheet will help you determine a maximum T_J based on the light output requirements of your application.

2. Color Shift with Temperature Rise

Emitter color can shift slightly to higher wavelengths with T_J rise. Shift values quantifying this effect are included in the LUXEON Custom Design Guide. Red, Red-Orange and Amber color emitters are the most sensitive to this effect, although the human eye is more sensitive to color changes in the amber region. The importance of this effect depends on the color range requirements for the application. If the allowed color range is very small, you will need to account for color shift when setting your maximum T_J goal.

3. Reliability-Based Temperature Ratings

To ensure the reliable operation of LUXEON Power Light Sources, observe the absolute maximum thermal ratings for the LEDs provided in Table 1. The maximum T_J is based on the allowable thermal stress of the silicone encapsulate that surrounds die.

Table 1. Maximum Thermal Ratings.

Parameter	Maximum
LED Junction Temperature	120
Aluminum-Core PCB Temperature	105
Storage/Operating Temperature:	
LUXEON Products without optics (Star, Star/C)	-40 to 105
LUXEON Products with optics (Star/O, Line, Ring)	-40 to 75

B. Assess Ambient Temperature Conditions

The designer must take into account the maximum ambient temperature (T_A) the LUXEON Power Light Source will experience over its lifetime. In most cases, you can use product standards to determine the worst case T_A . Otherwise, use representative maximum T_A measurements. Please note that the ambient temperatures should include other sources of heat such as electronics or heating due to sun exposure.

C. Power Dissipated

The dissipated power (P_d) can be determined as the forward voltage (V_f) of the emitter times the forward current (I_f). The portion of power emitted as visible light (about 10%) is negligible for thermal design.

D. Add Heat Sink to Model

The $R\theta_{B-A}$ component of $R\theta_{J-A}$ (see Figure 1A) represents the heat sink and attachment interface. The responsibility for the proper selection of the heat sink thermal resistance, $R\theta_{B-A}$, lies with the engineer using the product. A process for selecting $R\theta_{B-A}$ is explained in the examples that follow. Many resources exist to assist with this selection. Some are listed in the resources section at end of this document. The following section provides additional guidance to help you determine the most suitable heat sink for your application.

Heat Sink Characterization

A. Explanation of Data Charts

1. Test Set Up

We tested some typical heat sink configurations on LUXEON Stars and Floods including both finned and flat heat sinks. We used the following test conditions: free (or natural) convection environment with no fan (Figures 3A, 3B, 3C and 3D) and forced convection in a small wind tunnel (Figure 3E). The LUXEON Stars tested did not have optics. The optics do not affect the $R\theta_{J-B}$ of the LUXEON emitter; however, depending on the orientation, they may affect the convection flow over the attached heat sink.

APPENDIX F

Heat transfer fundamentals

HEAT TRANSFER FUNDAMENTALS

Introduction

The objective of thermal management programs in electronic packaging is the efficient removal of heat from the semiconductor junction to the ambient environment. This process can be separated into three major phases:

- 1) heat transfer within the semiconductor component package;
- 2) heat transfer from the package to a heat dissipater (the initial heat sink);
- 3) heat transfer from the heat dissipater to the ambient environment (the ultimate heat sink)

The first phase is generally beyond the control of the system level thermal engineer because the package type defines the internal heat transfer processes. In the second and third phases, the packaging engineer's goal is to design an efficient thermal connection from the package surface to the initial heat spreader and on to the ambient environment. Achieving this goal requires a thorough understanding of heat transfer fundamentals as well as knowledge of available interface materials and how their key physical properties affect the heat transfer process.

Basic Theory

The rate at which heat is conducted through a material is proportional to the area normal to the heat flow and to the temperature gradient along the heat flow path. For a one dimensional, steady state heat flow the rate is expressed by Fourier's equation:

$$(1) \quad Q = kA \frac{\Delta T}{d}$$

Where:

- k** = thermal conductivity, W/m-K
- Q** = rate of heat flow, W
- A** = contact area
- d** = distance of heat flow
- ΔT = temperature difference

Thermal conductivity, k, is an intrinsic property of a homogeneous material which describes the material's ability to conduct heat. This property is independent of material size, shape or orientation. For non-homogeneous materials, those having glass mesh or polymer film reinforcement, the term "*relative thermal conductivity*" is appropriate because the thermal conductivity of these materials depends on the relative thickness of the layers and their orientation with respect to heat flow.

Another inherent thermal property of a material is its *thermal resistance, R*, as defined in Equation 2.

$$(2) \quad R = A \frac{\Delta T}{Q}$$

This property is a measure of how a material of a specific thickness resists the flow of heat. The relationship between **k** and **R** is shown by substituting Equation (2) into (1) and rearranging to form (3)

$$(3) \quad k = \frac{d}{R}$$

Equation 3 shows that for homogeneous materials, thermal resistance is directly proportional to thickness. For non-homogeneous materials, the resistance generally increases with thickness but the relationship may not be linear.

Thermal conductivity and thermal resistance describe heat transfer within a material once heat has entered the material. Because real surfaces are never truly flat or smooth, the contact plane between a surface and a material can also produce a resistance to the flow of heat. This contact plane is depicted in **Figure 1**. Actual contact occurs at the high points, leaving air-filled voids where the valleys align. The air voids resist the flow of heat and force more of the heat to flow through the

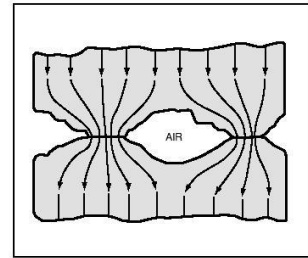


Figure 1a. Schematic representation of two surfaces in contact and heat flow across the interface.

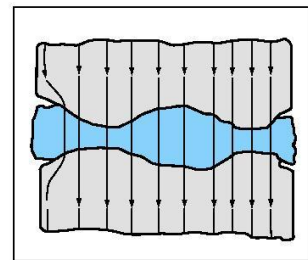


Figure 1b. Interface material compressed between two contacting surfaces.

contact points. This constriction resistance is referred to as surface contact resistance and can be a factor at all contacting surfaces.

The *thermal impedance, θ* , of a material is defined as the sum of its thermal resistance and any contact resistance between it and the contacting surfaces as defined in Equation (4).

$$(4) \quad \theta = R_{\text{material}} + R_{\text{contact}}$$

Surface flatness, surface roughness, clamping pressure, material thickness and compressive modulus have a major impact on contact resistance. Because these surface conditions can vary from application to application, the thermal impedance of a material will also be application dependent.

Thermal Interface Materials

Heat generated by a semiconductor must be removed to the ambient environment to maintain the junction temperature of the component within safe operating limits. Often this heat removal process involves conduction from a package surface to a heat spreader that can more efficiently transfer the heat to the ambient environment. The spreader has to be carefully joined to the package to minimize the thermal resistance of this newly formed thermal joint.

Attaching a heat spreader to a semiconductor package surface requires that two commercial grade surfaces be brought into intimate contact. These surfaces are usually characterized by a microscopic surface roughness superimposed on a macroscopic non-planarity that can give the surfaces a concave, convex or twisted shape. When two such surfaces are joined, contact occurs only at the high points. The low points form air-filled voids. Typical contact area can consist of more than 90 percent air voids, which represents a significant resistance to heat flow.

Thermally conductive materials are used to eliminate these interstitial air gaps from the interface by conforming to the rough and uneven mating surfaces. Because the material has a greater thermal conductivity than the air it replaces, the resistance across the joint decreases, and the component junction temperature will be reduced.

A variety of material types have been developed in response to the changing needs of the electronic



THERMFLOW™ T310 Phase-Change Material

packaging market. These materials can be categorized as follows:

Phase-Change Materials. THERMFLOW™ products provide a combination of grease-like thermal performance with pad-like convenience when used between high performance microprocessors and heat sinks.

- Can achieve less than 0.05°C-in²/W thermal impedance
- Conform at operating temperature to minimize thermal path thickness
- Excellent surface "wetting" eliminates contact resistance

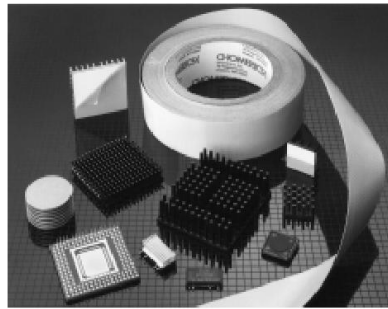
Phase-change materials behave like thermal greases after they reach their melt temperature. Their viscosity rapidly diminishes and they flow throughout the thermal joint to fill the gaps that were initially present. This process requires some compressive force, usually a few psi, to bring the two surfaces together and cause the material to flow. This process continues until the two surfaces come into

contact at a minimum of three points, or the joint becomes so thin that the viscosity of the material prevents further flow. These materials do not provide electrical isolation because they may allow the two surfaces to make contact.

Thermal Tapes. THERMATTACH tapes are a family of acrylic and silicone pressure-sensitive adhesive tapes designed to securely bond heat sinks to power dissipating components.

- Acrylic based adhesives for metal or ceramic packages
- Silicone based adhesive for bonding plastic packages to heat sinks
- Ionically pure formulations for use inside component packages and on printed circuit boards
- Limited gap filling properties require reasonable surface flatness
- High shear strength at elevated temperatures

Thermal tapes are used primarily for their mechanical adhesive properties, and to a lesser extent for their thermal properties. The thermal conductivity of these tapes is moderate and their thermal performance in an application is dependent on the contact area that can be achieved between the bonding surfaces.



THERMATTACH® Adhesive Tapes

HEAT TRANSFER FUNDAMENTALS



CHO-THERM® Insulating Pads

Insulating Pads. CHO-THERM® insulating pads were developed as a user-friendly alternative to greased mica insulators to be used between discrete power devices and heat sinks.

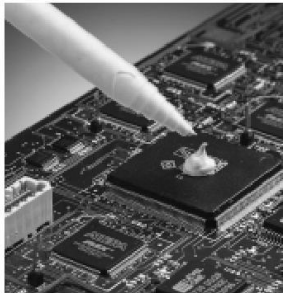
- Silicone binder provides high temperature stability and good electrical insulation properties
- Glass mesh reinforcement provides cut-through resistance
- High mounting pressure required to minimize contact resistance
- U.L. Recognized

This class of product is characterized by high thermal conductivity, very high dielectric strength and volume resistivity. Pads must conduct very large heat loads from discrete power semiconductors to heat sinks, while providing long-term electrical insulation between the live component case and the grounded heat sink.

Gap Fillers. THERM-A-GAP™ gap fillers provide a family of low modulus (soft), thermally conductive silicone elastomers for applications where heat must be conducted over a large and variant gap between a semiconductor component and a heat dissipating surface.

- Soft silicone gel binder provides low modulus for conformability at low pressures
- Low modulus allows materials to make up for large tolerance stack ups
- Low pressure applications

Gap fillers are used to bridge large gaps between hot components and a cold surface. The gaps are not only large, but their tolerances can be +/-20 % or greater. This means that the gap filler must have sufficient pliancy to fill such spaces without stressing components beyond their safe limits. The thermal conductivity of these materials is in the moderate range and their use is typically limited to moderate-to-low power dissipation components.



THERM-A-FORM™ Compounds

Cure In Place Compounds. THERM-A-FORM™ compounds are reactive, two-component silicone RTVs* that can be used to form thermal pathways in applications where the distance between a component and a cold surface is highly variable.

- Boron nitride or aluminum oxide-filled low modulus silicone resins

- Fill gaps ranging from 0.005 to 0.25 inch without stressing components
- Can cure at room temperature
- Localized encapsulating of components

*Room temperature vulcanizing materials.

Key Properties of Thermal Interface Materials

Thermal Properties

The key properties of interface materials are thermal impedance and thermal conductivity.

Thermal Impedance. This is the measure of the total resistance to the flow of heat from a hot surface through an interface material into a cold surface. Thermal impedance is measured according to the ASTM D5470 test method. Although the current version of this method is specific to high durometer insulating pad materials tested at high clamping forces, the method has been successfully adapted for use with low durometer materials as well as fluid compounds.

Thermal impedance can be measured using D5470 at several clamping forces to generate a pressure versus thermal impedance plot as shown in **Figure 2**. This type of data can be used to generate information about the ability of a material to conform to surfaces to minimize contact resistance. Care must be taken with this type of data because contact resistance is also highly influenced by surface characteristics. To minimize the impact of test equipment variations, this type of work is best performed with the same test surfaces for all materials being tested.

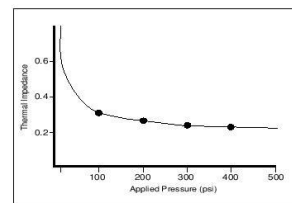


Figure 2. Thermal Impedance vs. pressure for CHO-THERM 1671 material.

Thermal Conductivity. Thermal impedance data measured according to ASTM D5470 can be used to calculate the thermal conductivity of an interface material. Rearranging Equation (3) to give Equation (5)

$$(5) \quad R_{\text{material}} = \frac{d}{k}$$

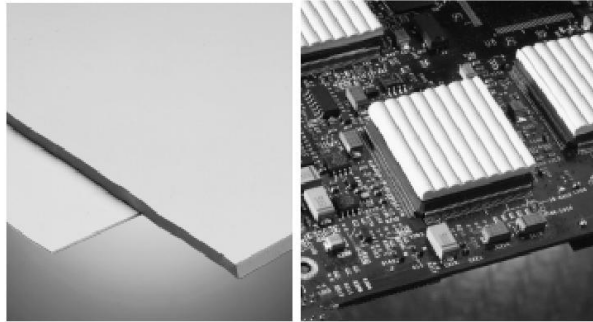
and substituting into Equation (4) yields Equation (6).

$$(6) \quad \theta = \frac{d}{k} + R_{\text{contact}}$$

Equation (6) shows that for a homogeneous material, a plot of thermal impedance (θ) versus thickness (d) is a straight line whose slope is equal to the inverse of the thermal conductivity and the intercept at zero thickness is the contact resistance. Thickness can be varied by either stacking up different layers of the material or by preparing the material at different thicknesses.

Electrical Properties

Voltage Breakdown. This is a measure of how much voltage difference a material can withstand under a specific set of test conditions. This property is usually measured using ASTM D149 where a test specimen is subjected to ramped alternating current voltage such that dielectric failure is reached within twenty seconds after the start of the test. Five specimens are tested and the average voltage breakdown is calculated and reported. The value is an average, not a minimum. Voltage Breakdown can be converted to Dielectric Strength by dividing the voltage breakdown value by the specimen thickness where the dielectric failure occurred. This test is an indication of the ability of a material to withstand high voltages, but does not guarantee how a material will behave over time in a real application. The value is influenced by several factors. Humidity and elevated temperature will reduce the voltage breakdown because absorbed water will degrade the electrical properties of the material. The size of the test elec-



THERM-A-GAP™ Interface Materials (flat and ribbed)

trode will affect the observed breakdown voltage. A larger test electrode will typically yield a lower breakdown voltage. The presence of partial discharge, as well as mechanical stresses imposed on the interface material, also reduce voltage breakdown.

Volume Resistivity. Volume resistivity is a measure of the bulk electrical resistance of a unit cube of a material. When determined per ASTM D257, volume resistivity can give an indication of how well an interface material can limit leakage current between an active component and its grounded metal heat sink. As with voltage breakdown, volume resistivity can be significantly lowered by humidity and elevated temperature.

Elastomeric Properties

Interface materials exhibit properties typical of highly filled elastomers, namely compression deflection, compression set and stress relaxation.

Compression Deflection. Unlike foams, a solid elastomer can not be compressed under normal compressive loads. As a compressive load is applied, the material is deformed but the volume of the material remains constant.

Stress Relaxation. When a compressive load is applied to an interface material, there is an initial deflection followed by a slow relaxation process whereby some of the load is relaxed. This process continues until the compressive load is balanced by the cohesive strength of the material.

Compression Set. Compression set is the result of stress relaxation. After a material has been subjected to a compressive load for an extended time, part of the deflection becomes permanent and will not be recoverable after the load is reduced.

Thermal Conductivity Conversion Guide

From	Cal sec-cm-°C		BTU-in hr-ft²-°F		Watt m-K	
	Multiplier	4.2 x 10 ²	2.9 x 10 ³	0.14	3.4 x 10 ⁻⁴	6.94
To	Watt m-K	BTU-in hr-ft²-°F	Watt m-K	Cal sec-cm-°C	BTU-in hr-ft²-°F	Cal sec-cm-°C

APPENDIX G

Luxeon Rebel technical datasheet



LUXEON® Rebel

Direct Color Portfolio

Introduction

LUXEON® Rebel Direct Color portfolio LEDs are ideal for a wide variety of lighting, signaling, signage and entertainment applications. These flux differentiated parts, like all other LUXEON Rebel LEDs, provide the industry's best lumen maintenance, superior reliability and quality light. Using the information in this document you can begin designing applications to your unique specifications.

LUXEON Rebel Direct Color LEDs

- deliver more usable light and higher flux density
- optimize applications to reduce size and cost
- tightly pack the LEDs for mixing
- engineer more robust applications
- utilize standard FR4 PCB technology
- simplify manufacturing through the use of surface mount technology
- recognized under the Component Recognition Program of Underwriters Laboratories Inc. UL listing E327436.

PHILIPS
LUMILEDS

General Product Information

Product Nomenclature

LUXEON Rebel Direct Color is tested and binned at 350 mA.

The part number designation is explained as follows:

L X M L - A B C D - E F G H

L X M 2 - A B C D - E F G H

Where:

A — designates radiation pattern (value P for Lambertian)

B — designates color (see LUXEON Rebel Binning and Labeling section)

C — designates color variant (0 for direct colored variants)

D — designates test current (value I for 350 mA)

E — reserved for future product offerings

FGH — minimum luminous flux (lm) or radiometric power (mW) performance

Therefore products tested and binned at 350 mA follow the part numbering scheme:

L X M L - P x 0 I - x x x x

L X M 2 - P x 0 I - x x x x

Average Lumen Maintenance Characteristics

LUXEON Rebel Direct Color emitters are tested and binned at 350 mA, with current pulse duration of 20 ms. All characteristic charts where the thermal pad is kept at constant temperature (25°C typically) are measured with current pulse duration of 20 ms. Under these conditions, junction temperature and thermal pad temperature are the same.

Philips Lumileds projects that green, cyan, blue and royal-blue LUXEON Rebel Direct Color products will deliver, on average, 70% lumen maintenance (B50, L70) at 50,000 hours of operation at a forward current of 700 mA. This projection is based on constant current operation with junction temperature maintained at or below 135°C.

Philips Lumileds projects that red, red-orange and amber LUXEON Rebel Direct Color products will deliver, on average, 70% lumen maintenance (B50, L70) at 50,000 hours of operation at a forward current of 350 mA. This projection is based on constant current operation with junction temperature maintained at or below 110°C.

This performance is based on independent test data, Philips Lumileds historical data from tests run on similar material systems, and internal LUXEON reliability testing. Observation of design limits included in this data sheet is required in order to achieve this projected lumen maintenance.

Environmental Compliance

Philips Lumileds is committed to providing environmentally friendly products to the solid-state lighting market. LUXEON Rebel products are compliant to the European Union directives on the restriction of hazardous substances in electronic equipment, namely REACH and the RoHS directive. Philips Lumileds will not intentionally add the following restricted materials to the LUXEON Rebel: lead, mercury, cadmium, hexavalent chromium, polybrominated biphenyls (PBB) or polybrominated diphenyl ethers (PBDE).

Flux Characteristics

Luminous Flux Characteristics for LUXEON Rebel, Thermal Pad Temperature=25°C

Table 1.

Performance at Test Current				Typical Performance at Indicated Current	
Color	Part Number	Minimum Luminous Flux (lm) or Radiometric Power (mW)		Typical Luminous Flux (lm) or Radiometric Power (mW)	
		$\Phi_v^{[1]}$	Test Current (mA)	$\Phi_v^{[2]}$	Drive Current (mA)
Green	LXML-PM01-0070	70	350	123	700
	LXML-PM01-0080	80	350	139	700
	LXML-PM01-0090	90	350	150	700
	LXML-PM01-0100	100	350	166	700
Cyan	LXML-PE01-0050	50	350	91	700
	LXML-PE01-0060	60	350	107	700
	LXML-PE01-0070	70	350	120	700
	LXML-PE01-0080	80	350	129	700
Blue	LXML-PB01-0013	13.9	350	28	700
	LXML-PB01-0018	18.1	350	37	700
	LXML-PB01-0023	23.5	350	48	700
	LXML-PB01-0030	30.0	350	58	700
	LXML-PB01-0040	40.0	350	70	700
Royal-Blue	LXML-PR01-0350	350 mW	350	625 mW	700
	LXML-PR01-0425	425 mW	350	740 mW	700
	LXML-PR01-0500	500 mW	350	875 mW	700
Red	LXML-PD01-0030	30	350	65	700
	LXML-PD01-0040	40	350	85	700
	LXM2-PD01-0040*	40	350	90	700
	LXM2-PD01-0050*	50	350	102	700
Red-Orange	LXML-PH01-0040	40	350	85	700
	LXML-PH01-0050	50	350	100	700
	LXM2-PH01-0060*	60	350	122	700
	LXM2-PH01-0070*	70	350	134	700
Amber	LXML-PL01-0023	23.5	350	50	700
	LXML-PL01-0030	30.0	350	65	700
	LXML-PL01-0040	40.0	350	86	700

* Low Vf parts.

See table notes on next page.

Optical Characteristics

LUXEON Rebel at Test Current ^[1] Thermal Pad Temperature = 25°C

Table 2.

Color	Dominant Wavelength ^[2] λ_D , or Peak Wavelength ^[3] λ_p			Typical Spectral Half-width ^[4] (nm) $\Delta\lambda_{1/2}$	Typical Temperature Coefficient of Dominant Wavelength (nm/°C) $\Delta\lambda_D / \Delta T_j$	Typical Total Included Angle ^[5] (degrees) $\theta_{0.90V}$	Typical Viewing Angle ^[6] (degrees) $2\theta_{1/2}$
	Min.	Typ.	Max.				
Green ^[7]	520.0 nm	530.0 nm	550.0 nm	30	0.05	160	120
Cyan ^[7]	490.0 nm	505.0 nm	520.0 nm	30	0.04	160	120
Blue ^[7]	460.0 nm	470.0 nm	490.0 nm	20	0.05	160	120
Royal-Blue ^{[3] [7]}	440.0 nm	447.5 nm	460.0 nm	20	0.04	160	120
Red ^[8]	620.0 nm	627.0 nm	645.0 nm	20	0.05	160	120
Red-Orange ^[8]	610.0 nm	617.0 nm	620.0 nm	20	0.08	160	120
Amber ^[8]	584.5 nm	590.0 nm	597.0 nm	20	0.10	160	120

Notes for Table 2:

1. Test current is 350 mA for all LXML-PxxI-0xxx and LXM2-PxxI-0xxx products.
2. Dominant wavelength is derived from the CIE 1931 Chromaticity diagram and represents the perceived color. Philips Lumileds maintains a tolerance of ± 0.5 nm for dominant wavelength measurements.
3. Royal-Blue product is binned by radiometric power and peak wavelength rather than photometric lumens. Philips Lumileds maintains a tolerance of ± 2 nm for peak wavelength measurements.
4. Spectral width at $1/2$ of the peak intensity.
5. Total angle at which 90% of total luminous flux is captured.
6. Viewing angle is the off axis angle from lamp centerline where the luminous intensity is $1/2$ of the peak value.
7. All green, cyan, blue and royal-blue products are built with Indium Gallium Nitride (InGaN).
8. All red, red-orange, and amber are built with Aluminum Indium Gallium Phosphide (AlInGaP).

Electrical Characteristics

Electrical Characteristics at 350 mA for LUXEON Rebel, Part Numbers LXML-PxxI-0xxx and LXM2-PxxI-0xxx, Thermal Pad Temperature = 25°C

Table 3.

Color	Forward Voltage V_f ^[1] (V)			Typical Temperature Coefficient of Forward Voltage ^[2] (mV/°C) $\Delta V_f / \Delta T_j$	Typical Thermal Resistance Junction to Thermal Pad (°C/W) $R\theta_{jc}$
	Min.	Typ.	Max.		
Green	2.55	3.05	3.51	- 2.0 to - 4.0	10
Cyan	2.55	3.05	3.51	- 2.0 to - 4.0	10
Blue	2.55	3.10	3.51	- 2.0 to - 4.0	10
Royal-Blue	2.55	3.05	3.51	- 2.0 to - 4.0	10
Red	2.31	2.90	3.51	- 2.0 to - 4.0	12
Red (Low Vf)	1.80	2.10	2.80	- 2.0 to - 4.0	8
Red-Orange	2.31	2.90	3.51	- 2.0 to - 4.0	12
Red-Orange (Low Vf)	1.80	2.10	2.80	- 2.0 to - 4.0	8
Amber	2.31	2.90	3.51	- 2.0 to - 4.0	12

Notes for Table 3:

1. Philips Lumileds maintains a tolerance of $\pm 0.06V$ on forward voltage measurements.
2. Measured between 25°C = T_j = 110°C at I_f = 350 mA.

Typical Electrical Characteristics at 700 mA for LUXEON Rebel, Part Numbers LXML-PxxI-0xxx and LXM2-PxxI-0xxx, Thermal Pad Temperature = 25°C

Table 4.

Color	Typical Forward Voltage V_f (V)
Green	3.40
Cyan	3.40
Blue	3.40
Royal-Blue	3.40
Red	3.60
Red (Low Vf)	2.30
Red-Orange	3.60
Red-Orange (Low Vf)	2.30
Amber	3.60

Absolute Maximum Ratings

Table 5.

Parameter	Green / Cyan / Blue / Royal-Blue	Red / Red-Orange / Amber
DC Forward Current (mA)	1000	700
Peak Pulsed Forward Current (mA)	1000	700
Average Forward Current (mA)	1000	700
ESD Sensitivity	< 8000V Human Body Model (HBM) Class 3A JESD22-A114-B	< 8000V Human Body Model (HBM) Class 3A JESD22-A114-B
LED Junction Temperature ^[1]	150°C	135°C
Operating Case Temperature at 350 mA	-40°C - 135°C	-40°C - 120°C
Storage Temperature	-40°C - 135°C	-40°C - 135°C
Soldering Temperature	JEDEC 020c 260°C	JEDEC 020c 260°C
Allowable Reflow Cycles	3	3
	Autoclave Conditions 121°C at 2 ATM 100% Relative Humidity for 96 Hours Maximum	Autoclave Conditions 121°C at 2 ATM 100% Relative Humidity for 96 Hours Maximum
Reverse Voltage (Vr)	See Note 2	See Note 2

Notes for Table 5:

1. Proper current derating must be observed to maintain junction temperature below the maximum.
2. LUXEON Rebel LEDs are not designed to be driven in reverse bias.

JEDEC Moisture Sensitivity

Table 6.

Level	Floor Life		Soak Requirements	
	Time	Conditions	Standard	
			Time (hours)	Conditions
I	unlimited	≤ 30°C / 85% RH	168 + 5 / -0	85°C / 85% RH

Reflow Soldering Characteristics

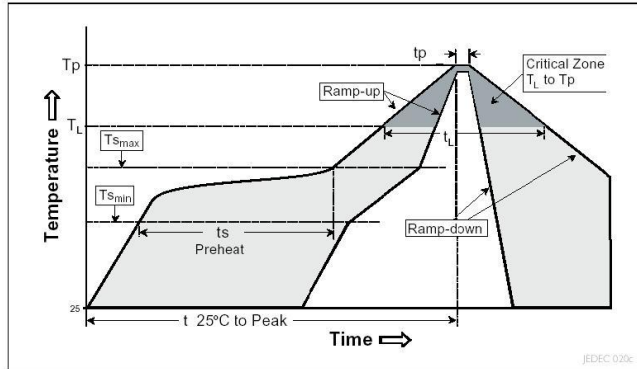


Table 7.

Profile Feature	Lead Free Assembly
Average Ramp-Up Rate ($T_{s_{max}}$ to T_p)	3°C / second max
Preheat Temperature Min ($T_{s_{min}}$)	150°C
Preheat Temperature Max ($T_{s_{max}}$)	200°C
Preheat Time ($t_{s_{min}}$ to $t_{s_{max}}$)	60 - 180 seconds
Temperature T_L (t_L)	217°C
Time Maintained Above Temperature T_L (t_L)	60 - 150 seconds
Peak / Classification Temperature (T_p)	260°C
Time Within 5°C of Actual Peak Temperature (t_p)	20 - 40 seconds
Ramp-Down Rate	6°C / second max
Time 25°C to Peak Temperature	8 minutes max

Note for Table 7:

- All temperatures refer to the application Printed Circuit Board (PCB), measured on the surface adjacent to the package body.

Pad Configuration

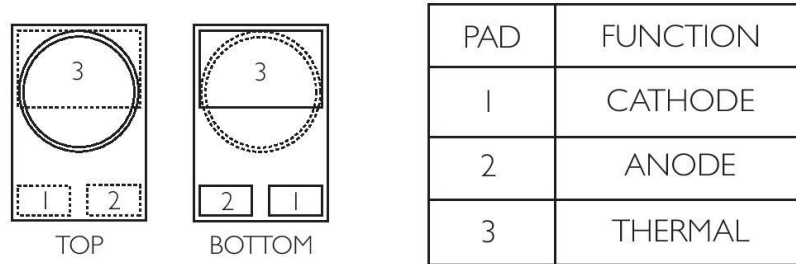


Figure 2. Pad configuration.

Note for Figure 2:

- The thermal pad is electrically isolated from the anode and cathode contact pads.

Solder Pad Design

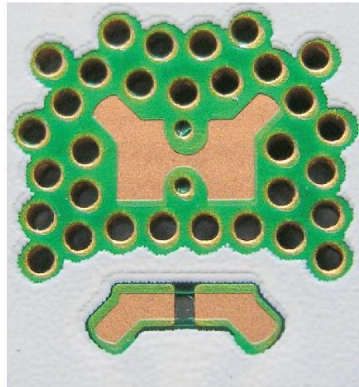


Figure 3. Solder pad layout.

Notes for Figure 3:

- The photograph shows the recommended LUXEON Rebel layout on printed circuit board (PCB). This design easily achieves a thermal resistance of 7K/W.
- Application Brief AB32 provides extensive details for this layout. The .dwg files are available at www.philipslumileds.com and www.philipslumileds.cn.com.

Typical Light Output Characteristics over Temperature

Cyan, Blue and Royal-Blue at Test Current

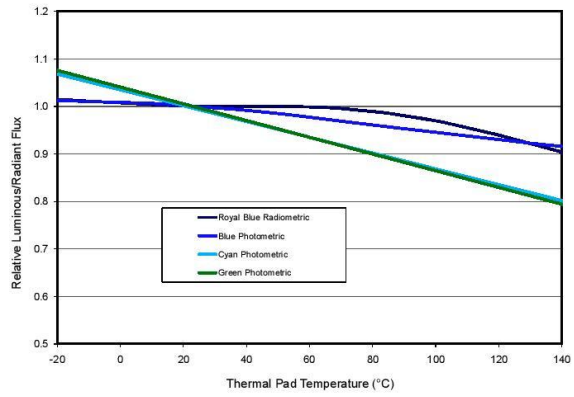


Figure 5. Relative light output vs. thermal pad temperature for green, cyan, blue and royal-blue.

Red, Red-Orange and Amber at Test Current

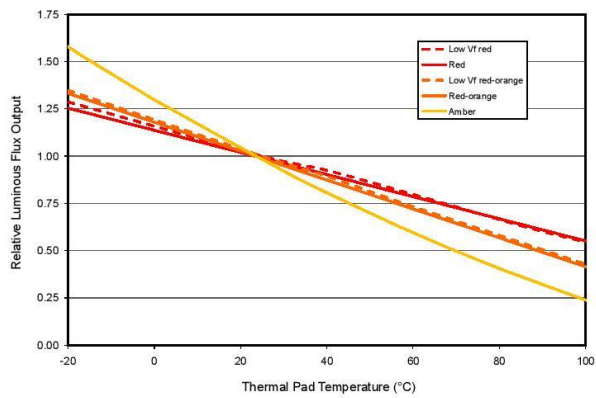


Figure 6. Relative light output vs. thermal pad temperature for red, red-orange and amber.

APPENDIX H

Diffraction Optics reflector product specification



Unit 531, Enterprise Place, Hong Kong Science Park, 5 Science Park West Avenue, Shatin, N.T., Hong Kong
Tel: (852) 27935976, Fax: (852)27931696
Website: <http://www.diffractive-optics.com>

Product Specification 产品说明书

Description/描述

- Name/名称: Reflector
- Construction/结构: Parabolic profile with high precision optical surface.
- Lens material/材料: Precision molded in optical grade PC with AL coating for thermal stability and system durability.
- Operating temperature range/操作温度: -20° C to +80° C
- Storage temperature range/储存温度: -20° C to +80° C



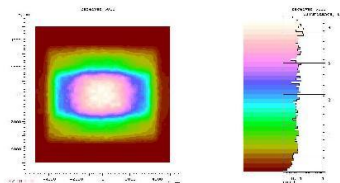
Part No.: P3152

Key Features/重要特征

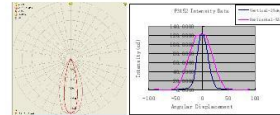
- Size/尺寸: 42 x 42mm diameter, 29.5mm tall
- Typical Dimensional Tolerance/公差: ± 0.1 mm
- Distortion/变形: Low
- Fit For/适用于: Luxeon emitter (Lambertian), K2 and Rebel
- Light Distribution/光的分布: Uniform
- Beam Angle/光束角度: Estimated 25 x 52° (Varies slightly with LED color)
- Efficiency/效率: $\geq 85\%$ of total flux
- High efficiency: more than 85% of total flux
- Performance/效果: ≥ 4 lx with 100 lm. LED at 1m.

(Performance values given are typical values and will vary dependant on LED binning, color and drive profile.)

Optical Performance/光学效果



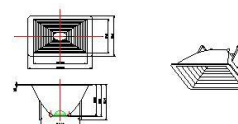
Optical simulation result with Rebel 100 lm. LED at 6m distance.



Application/应用

- Flash-lighting
- Reading lamps
- Architectural lighting
- Street lights
- Signaling
- Autom otive lighting
- Emergency lights
- General illumination

Dimensions/尺寸



Notes:
1.All dimensions in millimeters
2.Tolerance:0.1mm
3.The Reflector rim (42x42mm) may be used as a suspension feature to support the Reflector.
4.The LUXEON light sources must be precluded from any axial or lateral loads caused by the fit/force do not clamp the Reflector against the LUXEON emitter

IMPORTANT NOTE – Lenses handling

Handling: Always use gloves to handle lenses and/or handle the lenses only by the flange. Never touch the outside surfaces of the lenses with fingers, finger oils and contamination will absorb or refract light.

APPENDIX I

Loctite adhesive product specification

 <p>1001 Trout Brook Crossing Rocky Hill, CT 06067-3910 Telephone: (860) 571-5100 FAX: (860) 571-5465</p>	<p>Product Description Sheet</p> <p>Hysol® Product 9340</p> <p>Industrial Products, August 2001</p>
--	---

Description

Loctite® Hysol® 9340 is a general purpose adhesive with exceptional high temperature performance. This easy to use epoxy is can be used in many demanding applications where resistance to chemicals and heat extremes are required. Hysol 9340 can be used on many different substrates such as wood, metal, ceramics, and most plastics. This exceptional epoxy can be sanded and drilled and painted after curing making it ideal for finish work.

Features

Excellent Heat Resistance
Good Tensile Sheer Strength
Resistant to Automotive Fluids
Sandable
Easy to Mix

Typical Uncured Properties	Part A	Part B	Mixed
Pot Life @ 77°F, 100 grams mins	—	—	90
Color	Green	Grey	Grey
Viscosity, cP	Paste	Paste	Paste
Specific Gravity	—	—	—
Mix Ratio			
By weight	1	1	—
By volume	1	1	—

Typical Properties	Typical Value
Hardness, Shore D	>80

Shear Strength, psi, ASTM D 1002 Etched Aluminum		
Cure Schedule	Test Temp °F	Typical Value
3 Days @ 77°F	-40	2100
	77	2300
	180	1850

GENERAL INFORMATION

This product is not recommended for use in pure oxygen and/or oxygen rich systems and should not be selected as a sealant for chlorine or other strong oxidizing materials.

For safe handling information on this product, consult the Material Safety Data Sheet, (MSDS).

Handling

Mixing: Hysol 9340 requires mixing Part A and Part B together just prior to the application. Complete mixing of the two components is necessary.

Application

Mixing: Combine Part A (resin) and Part B (hardener) in the correct ratio and mix thoroughly. Continue to mix until all green and gray streaks are gone and mix is uniformly gray. This is important! Heat build-up during or after mixing is normal. Do not mix quantities greater than one pound as excessive exotherm or heat build-up will develop. Mixing smaller quantities will minimize the heat build-up.

Application: Bonding surfaces should be clean and dry. The bonded parts should be held in contact until the adhesive is set. It not necessary to maintain fixturing for the entire cure schedule but only until handling strength is achieved.

Cure: Hysol 9340 can be cured by a variety of cure schedules to meet processing requirements. Hysol 9340 will achieve handling strength in 6-8 hours at room temperature (note: this can vary with different bond configurations and ambient temperatures). Full cure time at 77°F is 24 hours. Heat cures can be used to shorten this time. For instance, one hour at 180 °F or 2 hours at 140 °F is sufficient to fully cure the adhesive.

Clean up: It is important to remove excess adhesive from the work area and application equipment before it hardens. Many common solvents and citrus cleaners are suitable for removing uncured adhesive. Consult with your solvent supplier for information pertaining to the safe and proper use of solvents.

Packaging

2.7 oz. Tube Kits
Quart, One Gallon Systems

Storage

Store product in unopened container in a cool dry location. Ideal conditions are within the range 8 to 21 degrees C (46 to 70 degrees F) and are recommended for long term storage. Exposure to higher temperatures (greater than 28 degrees C) for prolonged periods should be avoided as extended exposure to warm conditions can adversely affect product properties. For further specific shelf life information, contact your local Technical Service Center.


Note

The data contained herein are furnished for information only and are believed to be reliable. We cannot assume responsibility for the results obtained by others over whose methods we have no control. It is the user's responsibility to determine suitability for the user's purpose of any production methods mentioned herein and to adopt such precautions as may be advisable for the protection of property and of persons against any hazards that may be involved in the handling and use thereof. In light of the foregoing, **Loctite Corporation specifically disclaims all warranties expressed or implied, including warranties of merchantability or fitness for a particular purpose, arising from sale or use of Loctite Corporation's products. Loctite Corporation specifically disclaims any liability for consequential or incidental damages of any kind, including lost profits.** The discussion herein of various processes or compositions is not to be interpreted as representation that they are free from domination of patents owned by others or as a license under any Loctite Corporation patents that may cover such processes or compositions. We recommend that each prospective user test his proposed application before repetitive use, using this data as a guide. This product may be covered by one or more United States or foreign patents or patent applications.

NOT FOR PRODUCT SPECIFICATIONS
THE TECHNICAL DATA CONTAINED HEREIN ARE INTENDED AS REFERENCE ONLY.
PLEASE CONTACT LOCTITE CORPORATION QUALITY DEPARTMENT FOR ASSISTANCE AND RECOMMENDATIONS ON SPECIFICATIONS FOR THIS PRODUCT.
ROCKY HILL, CT FAX: +1 (860)-571-5473 DUBLIN, IRELAND FAX: +353-1-451-9959
Loctite and Hysol are Trademarks of Loctite Corporation USA

APPENDIX J

LM3404 LED driver datasheet



February 8, 2010

LM3404/04HV

1.0A Constant Current Buck Regulator for Driving High Power LEDs

General Description

The LM3404/04HV are monolithic switching regulators designed to deliver constant currents to high power LEDs. Ideal for automotive, industrial, and general lighting applications, they contain a high-side N-channel MOSFET switch with a current limit of 1.5A (typical) for step-down (Buck) regulators. Hysteretic controlled on-time and an external resistor allow the converter output voltage to adjust as needed to deliver a constant current to series and series-parallel connected LED arrays of varying number and type. LED dimming via pulse width modulation (PWM), broken/open LED protection, low-power shutdown and thermal shutdown complete the feature set.

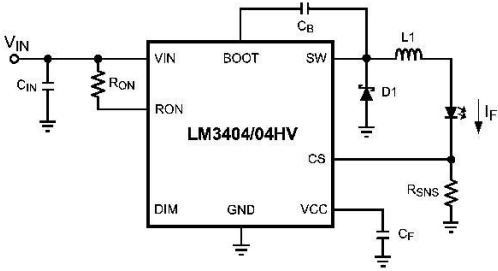
Features

- Integrated 1.0A MOSFET
- V_{IN} Range 6V to 42V (LM3404)
- V_{IN} Range 6V to 75V (LM3404HV)
- 1.2A Output Current Over Temperature
- Cycle-by-Cycle Current Limit
- No Control Loop Compensation Required
- Separate PWM Dimming and Low Power Shutdown
- Supports all-ceramic output capacitors and capacitor-less outputs
- Thermal shutdown protection
- SO-8 Package, PSOP-8 Package

Applications

- LED Driver
- Constant Current Source
- Automotive Lighting
- General Illumination
- Industrial Lighting

Typical Application

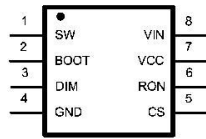


20205401

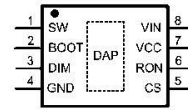
LM3404/04HV 1.0A Constant Current Buck Regulator for Driving High Power LEDs

© 2010 National Semiconductor Corporation 202054
www.national.com

Connection Diagrams



20205402
8-Lead Plastic SO-8 Package
NS Package Number M08A



20205456
8-Lead Plastic PSOP-8 Package
NS Package Number MRA08B

Ordering Information

Order Number	Package Type	NSC Package Drawing	Supplied As
LM3404MA	SO-8	M08A	95 units in anti-static rails
LM3404MAX			2500 units on tape and reel
LM3404HVMA			95 units in anti-static rails
LM3404HVMAX			2500 units on tape and reel
LM3404MR	PSOP-8	MRA08B	95 units in anti-static rails
LM3404MRX			2500 units on tape and reel
LM3404HVMR			95 units in anti-static rails
LM3404HVMRX			2500 units on tape and reel

Pin Descriptions

Pin(s)	Name	Description	Application Information
1	SW	Switch pin	Connect this pin to the output inductor and Schottky diode.
2	BOOT	MOSFET drive bootstrap pin	Connect a 10 nF ceramic capacitor from this pin to SW.
3	DIM	Input for PWM dimming	Connect a logic-level PWM signal to this pin to enable/disable the power MOSFET and reduce the average light output of the LED array.
4	GND	Ground pin	Connect this pin to system ground.
5	CS	Current sense feedback pin	Set the current through the LED array by connecting a resistor from this pin to ground.
6	RON	On-time control pin	A resistor connected from this pin to VIN sets the regulator controlled on-time.
7	VCC	Output of the internal 7V linear regulator	Bypass this pin to ground with a minimum 0.1 μ F ceramic capacitor with X5R or X7R dielectric.
8	VIN	Input voltage pin	Nominal operating input range for this pin is 6V to 42V (LM3404) or 6V to 75V (LM3404HV).
DAP	GND	Thermal Pad	Connect to ground. Place 4-6 vias from DAP to bottom layer ground plane.

Absolute Maximum Ratings

(LM3404) (1)

If Military/Aerospace specified devices are required, please contact the National Semiconductor Sales Office/Distributors for availability and specifications.

VIN to GND	-0.3V to 45V
BOOT to GND	-0.3V to 59V
SW to GND	-1.5V to 45V
BOOT to VCC	-0.3V to 45V
BOOT to SW	-0.3V to 14V
VCC to GND	-0.3V to 14V
DIM to GND	-0.3V to 7V
CS to GND	-0.3V to 7V
RON to GND	-0.3V to 7V
Junction Temperature	150°C

Storage Temp. Range	-65°C to 125°C
ESD Rating (2)	2kV
Soldering Information	
Lead Temperature (Soldering, 10sec)	260°C
Infrared/Convection Reflow (15sec)	235°C

Operating Ratings (LM3404)

(1)

V _{IN}	6V to 42V
Junction Temperature Range	-40°C to +125°C
Thermal Resistance θ_{JA} (SO-8 Package)	155°C/W
Thermal Resistance θ_{JA} (PSOP-8 Package) (5)	50°C/W

Absolute Maximum Ratings (LM3404HV) (1)

If Military/Aerospace specified devices are required, please contact the National Semiconductor Sales Office/Distributors for availability and specifications.

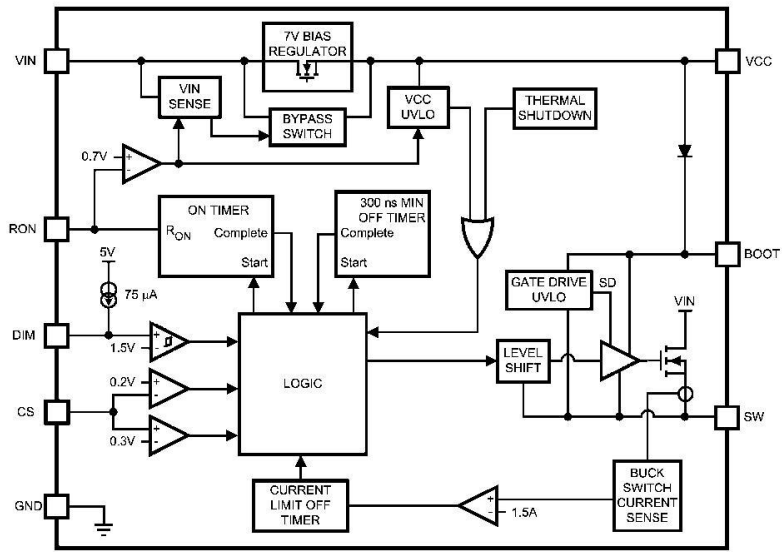
VIN to GND	-0.3V to 76V
BOOT to GND	-0.3V to 90V
SW to GND	-1.5V to 76V
BOOT to VCC	-0.3V to 76V
BOOT to SW	-0.3V to 14V
VCC to GND	-0.3V to 14V
DIM to GND	-0.3V to 7V
CS to GND	-0.3V to 7V
RON to GND	-0.3V to 7V
Junction Temperature	150°C

Storage Temp. Range	-65°C to 125°C
ESD Rating (2)	2kV
Soldering Information	
Lead Temperature (Soldering, 10sec)	260°C
Infrared/Convection Reflow (15sec)	235°C

Operating Ratings (LM3404HV)

(1)	
V _{IN}	6V to 75V
Junction Temperature Range	-40°C to +125°C
Thermal Resistance θ_{JA} (SO-8 Package)	155°C/W
Thermal Resistance θ_{JA} (PSOP-8 Package) (5)	50°C/W

Block Diagram



20205403

Application Information

THEORY OF OPERATION

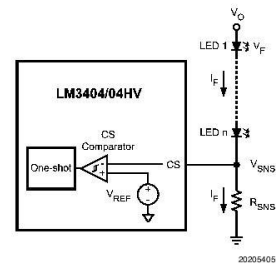
The LM3404 and LM3404HV are buck regulators with a wide input voltage range, low voltage reference, and a fast output enable/disable function. These features combine to make them ideal for use as a constant current source for LEDs with forward currents as high as 1.2A. The controlled on-time (COT) architecture is a combination of hysteretic mode control and a one-shot on-timer that varies inversely with input voltage. Hysteretic operation eliminates the need for small-signal control loop compensation. When the converter runs in continuous conduction mode (CCM) the controlled on-time maintains a constant switching frequency over the range of input voltage. Fast transient response, PWM dimming, a low power shutdown mode, and simple output overvoltage protection round out the functions of the LM3404/04HV.

CONTROLLED ON-TIME OVERVIEW

Figure 1 shows the feedback system used to control the current through an array of LEDs. A voltage signal, V_{SNS} , is created as the LED current flows through the current setting resistor, R_{SNS} , to ground. V_{SNS} is fed back to the CS pin, where it is compared against a 200 mV reference, V_{REF} . The on-comparator turns on the power MOSFET when V_{SNS} falls below V_{REF} . The power MOSFET conducts for a controlled on-time, t_{ON} , set by an external resistor, R_{ON} , and by the input voltage, V_{IN} . On-time is governed by the following equation:

$$t_{ON} = 1.34 \times 10^{-10} \times \frac{R_{ON}}{V_{IN}}$$

At the conclusion of t_{ON} the power MOSFET turns off for a minimum off-time, $t_{OFF-MIN}$, of 300 ns. Once $t_{OFF-MIN}$ is complete the CS comparator compares V_{SNS} and V_{REF} again, waiting to begin the next cycle.



20205405

FIGURE 1. Comparator and One-Shot

The LM3404/04HV regulators should be operated in continuous conduction mode (CCM), where inductor current stays positive throughout the switching cycle. During steady-state

CCM operation, the converter maintains a constant switching frequency that can be selected using the following equation:

$$f_{\text{SW}} = \frac{V_{\text{O}}}{1.34 \times 10^{-10} \times R_{\text{ON}}}$$

$$V_{\text{O}} = n \times V_{\text{F}} + 200 \text{ mV}$$

V_{F} = forward voltage of each LED, n = number of LEDs in series

AVERAGE LED CURRENT ACCURACY

The COT architecture regulates the valley of ΔV_{SNS} , the AC portion of V_{SNS} . To determine the average LED current (which is also the average inductor current) the valley inductor current is calculated using the following expression:

$$I_{\text{L-MIN}} = \frac{0.2}{R_{\text{SNS}}} \cdot \frac{V_{\text{O}} \times t_{\text{SNS}}}{L}$$

In this equation t_{SNS} represents the propagation delay of the CS comparator, and is approximately 220 ns. The average inductor/LED current is equal to $I_{\text{L-MIN}}$ plus one-half of the inductor current ripple, ΔI_{L} :

$$I_{\text{F}} = I_{\text{L}} = I_{\text{L-MIN}} + \Delta I_{\text{L}} / 2$$

Detailed information for the calculation of ΔI_{L} is given in the Design Considerations section.

MAXIMUM OUTPUT VOLTAGE

The 300 ns minimum off-time limits the maximum duty cycle of the converter, D_{MAX} , and in turn the maximum output voltage, $V_{\text{O(MAX)}}$, determined by the following equations:

$$D_{\text{MAX}} = \frac{t_{\text{ON}}}{t_{\text{ON}} + t_{\text{OFF-MIN}}}$$

$$V_{\text{O(max)}} = D_{\text{MAX}} \times V_{\text{IN}}$$

The maximum number of LEDs, n_{MAX} , that can be placed in a single series string is governed by $V_{\text{O(MAX)}}$ and the maximum forward voltage of the LEDs used, $V_{\text{F(MAX)}}$, using the expression:

$$n_{\text{MAX}} = \frac{V_{\text{O(max)}} - 200 \text{ mV}}{V_{\text{F(MAX)}}$$

At low switching frequency the maximum duty cycle and output voltage are higher, allowing the LM3404/04HV to regulate output voltages that are nearly equal to input voltage. The following equation relates switching frequency to maximum output voltage, and is also shown graphically in the Typical Performance Characteristics section:

$$V_{\text{O(MAX)}} = V_{\text{IN}} \times \frac{T_{\text{SW}} - 300 \text{ ns}}{T_{\text{SW}}}$$

$$T_{\text{SW}} = 1/f_{\text{SW}}$$

MINIMUM OUTPUT VOLTAGE

The minimum recommended on-time for the LM3404/04HV is 300 ns. This lower limit for t_{ON} determines the minimum duty cycle and output voltage that can be regulated based on input voltage and switching frequency. The relationship is determined by the following equation, shown on the same graphs as maximum output voltage in the Typical Performance Characteristics section:

$$V_{\text{O(MIN)}} = V_{\text{IN}} \times \frac{300 \text{ ns}}{T_{\text{SW}}}$$

HIGH VOLTAGE BIAS REGULATOR

The LM3404/04HV contains an internal linear regulator with a 7V output, connected between the VIN and the VCC pins. The VCC pin should be bypassed to the GND pin with a 0.1 μF ceramic capacitor connected as close as possible to the pins of the IC. VCC tracks VIN until VIN reaches 8.8V (typical) and then regulates at 7V as VIN increases. Operation begins when VCC crosses 5.25V.

INTERNAL MOSFET AND DRIVER

The LM3404/04HV features an internal power MOSFET as well as a floating driver connected from the SW pin to the BOOT pin. Both rise time and fall time are 20 ns each (typical) and the approximate gate charge is 6 nC. The high-side rail for the driver circuitry uses a bootstrap circuit consisting of an internal high-voltage diode and an external 10 nF capacitor, C_{B} . V_{CC} charges C_{B} through the internal diode while the power MOSFET is off. When the MOSFET turns on, the internal diode reverse biases. This creates a floating supply equal to the V_{CC} voltage minus the diode drop to drive the MOSFET when its source voltage is equal to V_{IN} .

FAST SHUTDOWN FOR PWM DIMMING

The DIM pin of the LM3404/04HV is a TTL compatible input for low frequency PWM dimming of the LED. A logic low (below 0.8V) at DIM will disable the internal MOSFET and shut off the current flow to the LED array. While the DIM pin is in a logic low state the support circuitry (driver, bandgap, VCC) remains active in order to minimize the time needed to turn the LED array back on when the DIM pin sees a logic high (above 2.2V). A 75 μA (typical) pull-up current ensures that the LM3404/04HV is on when DIM pin is open circuited, eliminating the need for a pull-up resistor. Dimming frequency, f_{DIM} , and duty cycle, D_{DIM} , are limited by the LED current rise time and fall time and the delay from activation of the DIM pin to the response of the internal power MOSFET. In general, f_{DIM} should be at least one order of magnitude lower than the steady state switching frequency in order to prevent aliasing.

PEAK CURRENT LIMIT

The current limit comparator of the LM3404/04HV will engage whenever the power MOSFET current (equal to the inductor current while the MOSFET is on) exceeds 1.5A (typical). The power MOSFET is disabled for a cool-down time that is approximately 75x the steady-state on-time. At the conclusion of this cool-down time the system re-starts. If the current limit condition persists the cycle of cool-down time and restarting will continue, creating a low-power hiccup mode, minimizing thermal stress on the LM3404/04HV and the external circuit components.

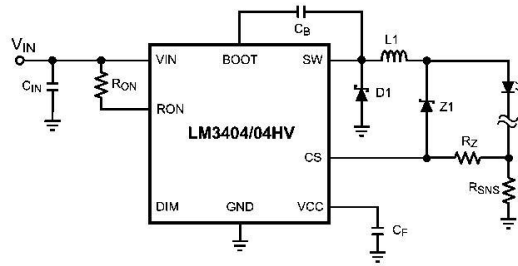
OVER-VOLTAGE/OVER-CURRENT COMPARATOR

The CS pin includes an output over-voltage/over-current comparator that will disable the power MOSFET whenever

V_{SNS} exceeds 300 mV. This threshold provides a hard limit for the output current. Output current overshoot is limited to $300\text{ mV} / R_{SNS}$ by this comparator during transients.

The OVP/OCF comparator can also be used to prevent the output voltage from rising to $V_{O(MAX)}$ in the event of an output open-circuit. This is the most common failure mode for LEDs, due to breaking of the bond wires. In a current regulator an output open circuit causes V_{SNS} to fall to zero, commanding maximum duty cycle. *F 2* shows a method using a zener diode, Z1, and zener limiting resistor, R_Z , to limit output voltage to the reverse breakdown voltage of Z1 plus 200 mV. The zener diode reverse breakdown voltage, V_Z , must be greater than the maximum combined V_f of all LEDs in the array. The maximum recommended value for R_Z is 1 k Ω .

As discussed in the Maximum Output Voltage section, there is a limit to how high V_O can rise during an output open-circuit that is always less than V_{IN} . If no output capacitor is used, the output stage of the LM3404/04HV is capable of withstanding $V_{O(MAX)}$ indefinitely, however the voltage at the output end of the inductor will oscillate and can go above V_{IN} or below 0V. A small (typically 10 nF) capacitor across the LED array dampens this oscillation. For circuits that use an output capacitor, the system can still withstand $V_{O(MAX)}$ indefinitely as long as C_O is rated to handle V_{IN} . The high current paths are blocked in output open-circuit and the risk of thermal stress is minimal, hence the user may opt to allow the output voltage to rise in the case of an open-circuit LED failure.



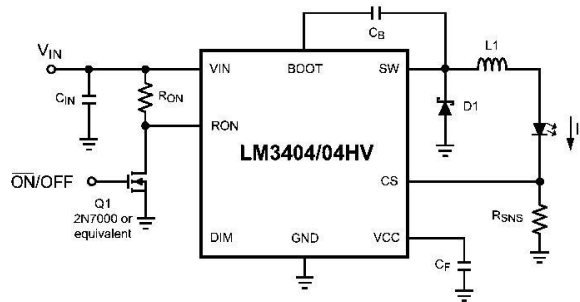
20205412

FIGURE 2. Output Open Circuit Protection

LOW POWER SHUTDOWN

The LM3404/04HV can be placed into a low power state ($I_{IN,SD} = 90\ \mu\text{A}$) by grounding the RON pin with a signal-level MOSFET as shown in *F 3*. Low power MOSFETs like the 2N7000, 2N3904, or equivalent are recommended devices for putting the LM3404/04HV into low power shutdown. Logic gates can also be used to shut down the LM3404/04HV as

long as the logic low voltage is below the over temperature minimum threshold of 0.3V. Noise filter circuitry on the RON pin can cause a few pulses with longer on-times than normal after RON is grounded or released. In these cases the OVP/OCF comparator will ensure that the peak inductor or LED current does not exceed $300\text{ mV} / R_{SNS}$.

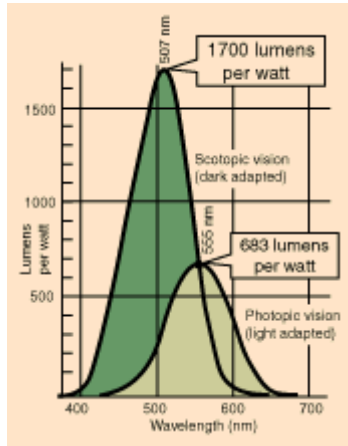


20205413

FIGURE 3. Low Power Shutdown

APPENDIX K

Photopic Luminous Conversion Table



Wavelength λ (nm)	Photopic Luminous Efficacy V_{λ}	Photopic Conversion lm/W	Scotopic Luminous Efficacy V'_{λ}	Scotopic Conversion lm/W
380	0.000039	0.027	0.000589	1.001
390	0.000120	0.082	0.002209	3.755
390	0.000120	0.082	0.002209	3.755
400	0.000396	0.270	0.009290	15.793
410	0.001210	0.826	0.034840	59.228
420	0.004000	2.732	0.096600	164.220
430	0.011600	7.923	0.199800	339.660
440	0.023000	15.709	0.328100	557.770
450	0.038000	25.954	0.455000	773.500
460	0.060000	40.980	0.567000	963.900
470	0.090980	62.139	0.676000	1149.200
480	0.139020	94.951	0.793000	1348.100
490	0.208020	142.078	0.904000	1536.800
500	0.323000	220.609	0.982000	1669.400
507	0.444310	303.464	1.000000	1700.000
510	0.503000	343.549	0.997000	1694.900
520	0.710000	484.930	0.935000	1589.500
530	0.862000	588.746	0.811000	1378.700
540	0.954000	651.582	0.655000	1105.000

550	0.994950	679.551	0.481000	817.700
555	1.000000	683.000	0.402000	683.000
560	0.995000	679.585	0.328800	558.960
570	0.952000	650.216	0.207600	352.920
580	0.870000	594.210	0.121200	206.040
590	0.757000	517.031	0.065500	111.350
600	0.631000	430.973	0.033150	56.355
610	0.503000	343.549	0.015930	27.081
620	0.381000	260.223	0.007370	12.529
630	0.265000	180.995	0.003335	5.670
640	0.175000	119.525	0.001497	2.545
650	0.107000	73.081	0.000677	1.151
660	0.061000	41.663	0.000313	0.532
670	0.032000	21.856	0.000148	0.252
680	0.017000	11.611	0.000072	0.122
690	0.008210	5.607	0.000035	0.060
700	0.004102	2.802	0.000018	0.030
710	0.002091	1.428	0.000009	0.016
720	0.001047	0.715	0.000005	0.008
730	0.000520	0.355	0.000003	0.004
740	0.000249	0.170	0.000001	0.002
750	0.000120	0.082	0.000001	0.001
760	0.000060	0.041	0.000000	0.000
770	0.000030	0.020	0.000000	0.000

Source: Table 6-1 of Williamson & Cummins, *Light and Color in Nature and Art*, Wiley, 1983. The Photopic conversion (lm/W) is obtained by multiplying V_{λ} by 683 and the Scotopic conversion is obtained by multiplying V'_{λ} by 1700 as suggested by those authors.

APPENDIX L

Philips Horticultural Lighting



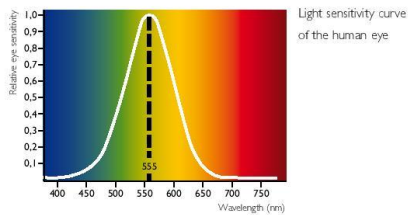
Growing your profits

Horticultural lighting

PHILIPS

GrowthLight

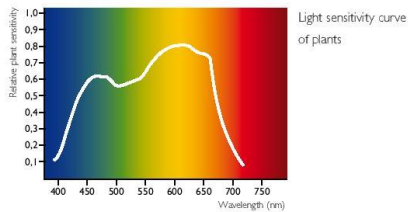
Light is, for the human eye, the visible part of electromagnetic radiation. Most products for lighting are developed for human applications. For these purposes the intensity of visible light is expressed in lux. Lux is a photometric unit and is based on the average sensitivity of the human eye.



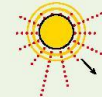
This sensitivity is maximal at green/yellow (555 nm) and is declining towards longer (red) and shorter wavelengths (blue).

Plants have a completely different sensitivity for light colours than the human eye. For plant growth it is important to define light as small light particles, also called photons or quantum. The energy content of photons is different, depending on wavelength (light colour). For one Watt of energy, almost twice as many red photons can be produced compared with blue. This means that although they still use the green and blue part for growth – or photosynthesis - they use the red part of the light much more efficiently. In fact we are dealing with a plant sensitivity curve for GrowthLight.

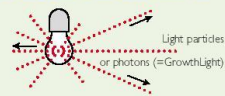
So, contrary to common belief, plant growth is not determined by lux or energy, but by photons from the blue to red (400-700 nm) part of the spectrum. This is called GrowthLight!



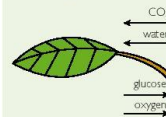
GrowthLight



Light source as GrowthLight



Photosynthesis



Suitability for photosynthesis

Research at universities and applied research stations has demonstrated that the rate of photosynthesis is related to the amount of photons between 400 – 700 nm. This is called 'Photosynthetic Photon Flux' (PPF). It is the only reliable way of measuring if a light source is suitable for photosynthesis.

The higher the PPF value per Watt, the more efficient the light source for plant growth. This is why Philips specifies on all his light sources for horticultural use, the PPF value. This is expressed in micromole photons per second ($\mu\text{mol/s}$).

The Philips MASTER GreenPower lamp is specially developed for maximal GrowthLight and has the highest PPF per Watt available for horticulture.



For supplemental GrowthLight applications Philips recommends:

- MASTER GreenPower



Artificial lighting

There are several ways in which artificial light can be used to improve growth and extend the growing season of commercial crops:

1. To supplement natural daylight and raise GrowthLight levels in order to enhance photosynthesis and thereby improve growth and quality of plants in greenhouses (supplemental GrowthLight).
2. To control the light period by extending the natural day length with artificial light (photoperiodic lighting).
3. To totally replace daylight with artificial light for ultimate climate control (cultivation without daylight).

Philips offers a wide range of lamps for all these horticultural applications.



Figure 1 shows an example of how natural daylight is supplemented with MASTER GreenPower during winter. In this example plants are illuminated with 105 $\mu\text{mol}/\text{m}^2\text{s}$ GrowthLight (= circa 8000 lux) during 20 hours/day from November until February. In the remaining lighting period the operating hours is less.

1. Supplemental GrowthLight in greenhouses

The amount of supplemental GrowthLight required very much depends on plant type, desired plant growth and availability of natural daylight. For this reason Philips has designed a tool that calculates how much additional GrowthLight is required in each individual situation. The tool is available at your local Philips office and allows you to calculate the optimal amount of light your greenhouse requires based on your wishes and/or possibilities.

Depending on plant type and desired plant growth for central European conditions, the following supplemental levels are suggested:

1. 15 – 30 $\mu\text{mol}/\text{m}^2\text{s}$ for improving quality, maintenance of the crop and limited production increase;
2. 30 – 45 $\mu\text{mol}/\text{m}^2\text{s}$ for seedlings, growth and production of pot plants;
3. 40 – 100 $\mu\text{mol}/\text{m}^2\text{s}$ for year-round cultivation, for example, of chrysanthemums and roses and multiple layer cultivation;
4. 100 – 200 $\mu\text{mol}/\text{m}^2\text{s}$ for production of plants with high light demand (fruit production of, for example, tomatoes and cucumbers);
5. 100 – 800 $\mu\text{mol}/\text{m}^2\text{s}$ for the production of plants under artificial light alone (for example growth chambers)

In the case of MASTER GreenPower 600W/400V:
1 $\mu\text{mol}/\text{m}^2\text{s}$ GrowthLight corresponds to 76 lux.



MASTER TL-D Reflex Super 80

Lamp

- MASTER TL-D Reflex lamps are fluorescent lamps with an internal reflector to concentrate the lamplight in the direction in which it is needed.

Features / Benefits

- Internal reflector with an opening angle of 160° increases the light intensity by 60%.
- High GrowthLight maintenance.
- MASTER TL-D Reflex lamps are 100% retrofit with all TL-D lamps with similar wattage.
- Recyclable; mercury, phosphor and glass can be re-used in production of new TL-D lamps.

- Lower initial investment because of built in reflector.
- Internal reflector reduces used space in multi layer cultivation.
- Light output is hardly affected in environments subject to dust accumulation due to internal reflector.

Comparison of MASTER TL-D Reflex with standard TL-D

- Up to 60% higher light output resulting in higher yield for existing installation or less battens for new installations.
- 60% longer service lifetime reduces the maintenance and relamping cost.

Applications

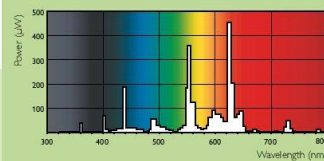
- Cultivation of plants without daylight.
- Growth chamber or cabinet with possibility to grow plants in multiple layers.

Gear

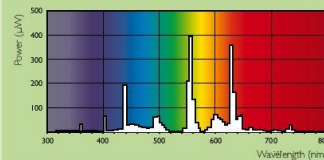
- Operates both on conventional but preferably on HF control gear.
- We recommend the Philips HF-P (see page 22).



MASTER TL-D Reflex/830



MASTER TL-D Reflex/840



Product Information

	GrowthLight PPF ^a (initial)	Lifetime	Maintenance (nominal)
MASTER TL-D Reflex Super 80 36W	47 µmol/sec	12.000 hrs	> 90% at 12.000 hrs
MASTER TL-D Reflex Super 80 58W	73 µmol/sec	12.000 hrs	> 90% at 12.000 hrs

* PPF information: see page 3

APPENDIX M

Study of high power light emitting diode (LED) lighting system in accelerating the growth rate of *Lactuca sativa* for indoor cultivation

International Journal of Physical Sciences Vol. 7(11), pp. 1773 - 1781, 9 March, 2012
Available online at <http://www.academicjournals.org/IJPS>
DOI: 10.5897/IJPS11.1568
ISSN 1992 - 1950 ©2012 Academic Journals

Full Length Research Paper

Study of high power light emitting diode (LED) lighting system in accelerating the growth rate of *Lactuca sativa* for indoor cultivation

Le-Yan Chin and Kok-Keong Chong*

Faculty of Engineering and Science, Universiti Tunku Abdul Rahman, Off Jalan Genting Kelang, Setapak, 53300 Kuala Lumpur, Malaysia.

Accepted 17 February, 2012

The experimental study of indoor cultivation using high power light emitting diode (LED) lighting system to accelerate the growth rate of *Lactuca sativa* plant is presented in this article. A novel high power LED lighting system with the use of aluminum indium gallium phosphide (AlInGaP) and indium gallium nitrate (InGaN) LEDs to produce photosynthetically active radiation (PAR) light source required for photosynthesis process of plant has been constructed. This study has verified that high power LED lighting system can accelerate the growth rate of *L. sativa* when compared with those plants cultivated under normal solar irradiance.

Key words: *Lactuca sativa*, high power LED, AlInGaP, InGaN, photosynthetically active radiation, indoor plant cultivation, Solar irradiance.

INTRODUCTION

Light emitting diode (LED) lighting is a promising artificial light source that is getting more attention for indoor plant cultivation. This is because the LED lighting can provide advantages including lower energy consumption, less heat generation and least insecticide used as compared to the conventional lighting, such as vapor sodium, metal halide or fluorescent lamp. Overall, the LEDs can be grouped into low power LED with current rating ranging from 1 to 20 mA, medium power LED with current rating around 100 mA and high power LED with current rating from hundreds of mA to more than an ampere.

In the early development, the only available type of LED was made from gallium arsenide (GaAs) material with illumination ranging from infrared to red. Advances in material science had then made possible the production of devices with ever-shorter wavelengths to produce light in a variety of colors (Yeh and Chung, 2009). In late 1960s, the first practical LED was invented by Nick Holonyak, Jr using gallium arsenide phosphide (GaAsP)

material to provide a 655 nm red light with low brightness levels of approximately 1 to 10 mcd at 20 mA. As LED technology progressed through the 1970s, additional colors and wavelengths became available, such as GaP for green and red lights, GaAsP for orange and high efficient red light, and GaAsP for yellow light, etc., (Yeh and Chung, 2009). In 1980s, a new material gallium aluminum arsenide (GaAlAs) was developed to provide superior performance over previously available LEDs with a minor improvement in brightness and efficiency. In the late 1980s, LED designers started to produce high-brightness and high reliability LEDs. This has led to the development of indium gallium aluminum phosphide (InGaAlP) LEDs that can have different color output via adjusting the energy bandgap.

The studies of indoor plant cultivation using low and medium power LED can be listed in the following. Schuerger and Brown (2004) applied LED arrays with different spectral qualities to determine the effect of light on the development of tomato mosaic virus in peppers and powdery mildew on cucumbers. Matthijs et al. (1996) used LED as sole light source in continuous culture of green algae. Goins et al. (1997) used plenty of LED

*Corresponding author. E-mail: chongkk@utar.edu.my.

arrays to study the wheat plants grown in Kennedy Space Center. Okamoto et al. (1997) used LED to study the lettuce seedling growth and morphogenesis. Strawberry micro-propagation study using LED as a light source was carried out by Nhut et al. (2000). Jao and Fang (2004) studied different frequency and duty ratio on the growth of potato plantlets *in vitro* by using LED light source. All these studies had to use a lot of normal low power LED or customized LED array to produce sufficient photosynthetically active radiation (PAR), which is not cost effective solution for commercial or mass agricultural production purpose.

Since year 2009, LED technology has been developing into a much more energy efficient with power conversion efficiency as high as 14.9% at 25°C temperature with the use new base materials, that is, aluminum indium gallium phosphide (AlInGaP), indium gallium nitrate (InGaN), etc. These base materials can produce much higher radiant flux at high operating current of 700 mA and operating temperature of 135°C for AlInGaP, while at 1000 mA of operating current and 150°C of operating temperature for InGaN (Philips Lumileds, 2011). These types of LEDs are also called high power LED because it consumes electrical energy power of 1 W or higher. A single AlInGaP LED (model LXML-PD01-0030 from Philips Lumileds) can produce a typical of 62 lumens of radiant flux at the dominant wavelength of 627 nm with the input current and forward voltage of 700 mA and 3.60 V, respectively at 25°C (Philips Lumileds, 2011). A normal type of low power LED, such as 5 mm cylindrical package LED from Avago Technology only produces typical of 1 lumen of radiant flux with 20 mA, which is a much lower flux production than that of a high power LED (Avago Technologies, 2009). The AlInGaP and InGaN LEDs produce the irradiance in the wavelengths of 620 to 645 nm and 440 to 490 nm, respectively, which are within the useful range of PAR of most plants' chlorophyll for photosynthesis process to produce glucose (Photosynthesis Timeline, 2008).

In this paper, the use of novel high power LEDs in accelerating the growth rate of plants for indoor cultivation has been studied. High energy efficient solid state lamp (SSL) has been designed and constructed using high power LEDs that consist of Luxeon Rebel Red (model LXML-PD01) and Luxeon Rebel Royal Blue (model LXML-PR01) LEDs by Philips Lumileds to produce high photosynthesis photon flux (PPF). In this study, low light *Lactuca sativa* (Romanian Lettuce) was chosen as test specimen in the experiment, because of its high commercial value, short test cycle and easy to grow under normal condition.

METHODOLOGY

The high power LED lighting system that was designed and constructed for indoor plant cultivation can be divided into three main components: LED module, alloy fixture of LED lamp and LED driver.

LED module and alloy fixture

AlInGaP LED as red radiation source (wavelength ranging from 620 to 645 nm) and InGaN LED as blue radiation source (wavelength ranging from 440 to 460 nm) in which both are supplied by Philips Lumileds under the product range of Luxeon Rebel have been employed.

Luxeon Rebel LED is in a bare emitter form and it is required to be mounted on printed circuit board (PCB) for electrical connection to the power supply. A hexagonal PCB with 20 mm in diameter was fabricated by printing the footprint layout on a raw ceramic substrate of PCB that contains both the anode and cathode pads where the bare emitter can be mounted on. PCB with ceramic based substrate was selected, because of both its good thermal conductivity and high electrical resistivity. The Luxeon Rebel LED was then soldered to the PCB using a hot plate soldering machine to form a LED module as shown in Figure 1.

During the process of assembling the LED module, special care was required to avoid touching on the Luxeon Rebel dome lens that could lead to defects in the LED as it is a fragile material. From the manufacturer specification of PCB, PCB with ceramic substrate has thermal resistance of 0.12°C/W (Hokuriku, 2009). Luxeon Rebel Red (AlInGaP) and Blue (InGaN) LEDs have thermal resistances of 12 and 10°C/W, respectively (Philips Lumileds, 2011) and therefore, the total thermal resistance of Luxeon Rebel Red and Blue LED modules can be obtained as 12.12 and 10.12°C/W, respectively. The completed LED modules were then installed to an alloy fixture.

In the preparation of LED module assembly, an open-ended pyramidal reflector with two different slope angles of 25 and 52° supplied by Diffractive Optics was mounted on each of the LED module using high temperature grade thermal adhesive in order to produce collimated light with reasonably uniform illumination onto the young *L. sativa*. Figure 2 shows the photo taken for the open-ended pyramidal reflector (Diffractive Optics, 2009).

Two units of Luxeon Rebel Red LED panel and two units of Luxeon Rebel Blue LED module assembly have been constructed in this study. Each LED panel consists of an array of 4 × 2 units of Luxeon Rebel Red LED module assembly fixed to the alloy fixture. Each LED module assembly consists of the LED module and the open-ended pyramidal reflector. Figure 3 shows the flow diagram of how the LED panel was constructed.

The attachment of the Luxeon Rebel Red LED modules to the alloy fixture was done with the use of Dow Corning SE4486 adhesive, which has a good thermal conductivity of 1.53 W/mK (Dow Corning, 2012). The thermal resistance contributed by the adhesive is as low as 0.4°C/W when 0.2 mm maximum thickness of adhesive was applied to bond the LED module to the inner part of alloy fixture. On the other hand, Luxeon Rebel Blue LED modules were attached to 20 × 20 mm aluminum sheet to assist heat dissipation and were placed at both sides of the alloy fixture. Since the efficiency of AlInGaP LED is dependent on temperature, thermal management is important to ensure Luxeon Rebel Red LED operating in the optimal performance, and hence, Philips Lumileds's thermal management concept was adopted in this case. The high power LED modules that are attached to the alloy fixture with thermal resistance of 0.8°C/W could create temperature as high as 80.4°C at the LED junction when the LED is driven by constant input current of 700 mA at ambient temperature of 25°C. The eight Luxeon Rebel Red LED modules in the panel were connected in series with the maximum forward voltage of 3.51 V each to form the total voltage of 28.08 V for each panel.

The calculation of total input electrical power of each panel can be shown as follow:

$$P_{\text{tot,LED}} = V_f \times I = 28.08 \text{ V} \times 0.7 \text{ A} = 19.66 \text{ W} \quad (1)$$

where V_f is the total maximum forward voltage of Luxeon Rebel Red LED panel.

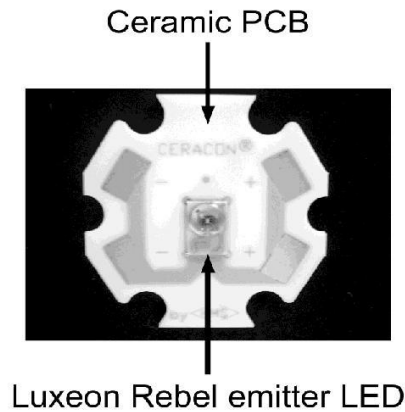


Figure 1. Luxeon Rebel LED module in which a Luxeon Rebel LED is mounted at the centre of a hexagonal ceramic PCB where positive and negative pads are printed on the surface.

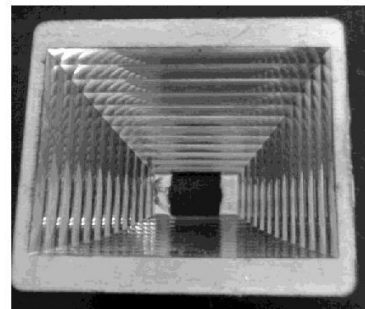


Figure 2. An open-ended pyramidal reflector with two different slope angles of 25 and 52° to be supplied by diffractive optics and it is mounted on each of the LED module using high temperature grade thermal adhesive in order to produce collimated light with reasonably uniform illumination.

The calculation of the LED temperature in the panel:

$$T_{J-a} = P_{\text{of_LED}} \times (R_{\Theta_{\text{LED_module}}})/8 \tag{2}$$

$$T_{J-a} = 19.66 \times [(12 + 0.12 + 0.4 + 0.8) \times 3.51 \times 0.7]/8 = 80.4^{\circ}\text{C} \tag{3}$$

where

$$R_{\Theta_{\text{LED_module}}} = R_{\Theta_j} + R_{\Theta_{\text{pcb}}} + R_{\Theta_{\text{ads}}} + R_{\Theta_f} \tag{4}$$

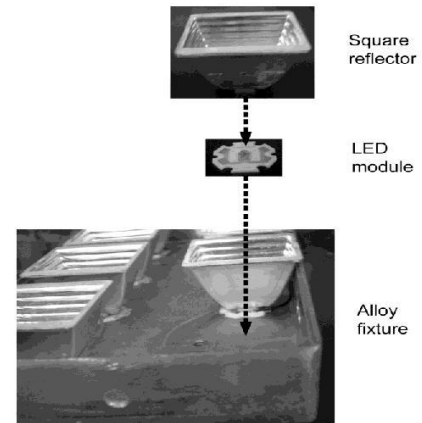


Figure 3. Flow diagram to indicate how the LED panel was constructed: it was started with mounting the open-ended pyramidal reflector to the LED module and is then followed by fixing them into an alloy fixture.

provided that thermal resistance of LED die junction-slug, $R_{\Theta_j} = 12^{\circ}\text{C/W}$; thermal resistance of PCB with ceramic substrate, $R_{\Theta_{\text{pcb}}} = 0.12^{\circ}\text{C/W}$; thermal resistance of silicone adhesive with 0.2 mm thickness, $R_{\Theta_{\text{ads}}} = 0.4^{\circ}\text{C/W}$; thermal resistance of alloy fixture, $R_{\Theta_f} = 0.8^{\circ}\text{C/W}$; where solder has extremely low thermal resistance less than 0.001°C/W and has been ignored in the calculation (Bai et al., 2004).

Temperature at outer surface of the alloy fixture was measured as 53°C . By using the system thermal resistance model of Philips Lumileds AB05 (Philips Lumileds, 2006), the temperature of LED junction should be $53^{\circ}\text{C} + (12 + 0.12 + 0.4 + 0.8)^{\circ}\text{C/W} \times (3.51 \times 0.7) \text{ W} = 85.7^{\circ}\text{C}$, which was quite close to the calculated temperature value, and it is still well below the maximum operating temperature of 135°C . In fact, these values are based on the maximum forward voltage to provide safety margin for the operation of the LED panel.

LED driver

The LED driver must deliver a DC output voltage greater than 28.1 V in order to forward bias all the Luxeon Rebel Red in the LED panel and is also capable of supplying constant current of up to 700 mA as shown in Figure 4. National semiconductor LM3404IC (2010) was used in the buck LED driver design due to its simplicity and capability to support a current up to 1.0 A, which was enough for the driving specification. Surface mounted device (SMD) resistors were chosen to sense and to feedback the output current for the purpose of regulating and delivering sufficient current to drive the LED circuit. In this design, two SMD resistors with the resistance of 0.68Ω each were connected in parallel to have a total resistance of 0.34Ω and total power rating of 0.25 W. Two resistors instead of one were used to increase the heat dissipation capacity when high current pass through them. A step down transformer was used to convert the AC voltage from 240 to 24 V and before it is supplied to the LED driver as shown in Figure 4. The overall efficiency of the LED driver is about 85%.

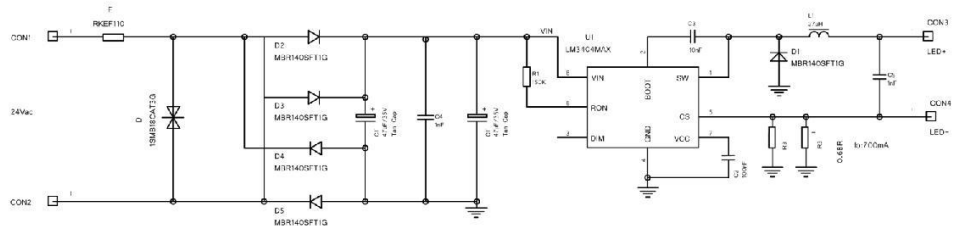


Figure 4. Circuit diagram to show a 24 V AC input LED driver that is capable of supplying constant output current of 700 mA and DC output voltage greater than 28.1 V in order to drive a maximum of eight Luxeon Rebel LEDs in series.

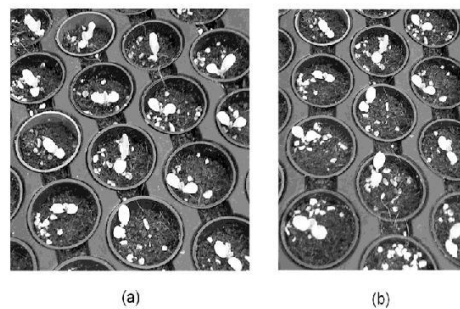


Figure 5. The Photos to show two pallets of germinated young *L. sativa* that were prepared as test specimen plants for cultivation under two different illumination conditions: (a) solar irradiance and (b) high power LED lighting system.

Experimental set-up

The young *L. sativa* plants were prepared in a pallet tray and the experiment only started after it appeared to have two pieces of leaves fully expanded and germinated from the seeds as shown in Figure 5a and b. Each pallet contained thirty three pots of germinated young *L. sativa*.

These experiments were carried out in a green house of lettuce farm at Kampung Raja, Cameron Highland in Malaysia with altitude of 1311 m, latitude of 4.57°N and longitude of 101.40°E which lies entirely in the equatorial region. In these experiments, there were two pallets of young *L. sativa* plants to be cultivated under two different illumination conditions for a comparison study: one pallet was placed inside a dark room equipped with high power LED lighting system and another pallet was placed outside the dark room to be exposed to normal solar irradiance. One pallet of young *L. sativa* was well aligned under the LED lamp that was hung at the height of 20 cm above the plants so that the light cone that irradiated from high power LED will just be sufficient to cover all the plants as shown in Figure 6. The ambient temperature was recorded ranging from 18 to 26°C during the testing period in which the lowest temperature happened in the midnight whilst the highest temperature happened in the sunny afternoon. The high power LED lighting system was powered up by a 24 V AC and the operating

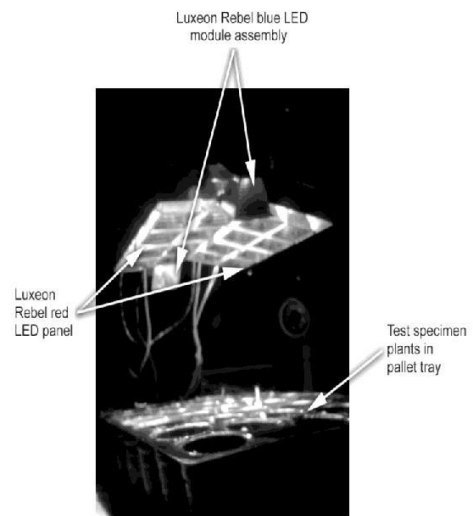


Figure 6. Picture to show the experimental setup in a dark room where the high power LED lighting system is placed at 20 cm above the test specimen plant where the high power LED lighting system was switched on for 16 h per day from 8 to 12 am throughout the whole experiment.

time was set from 8.00 to 12.00 am (or 16 h of photo-period) per day with the use of a timer. The young *L. sativa* plants cultivated in the dark room were watered twice daily, that is, in the morning and in the afternoon, with the same timing as those young *L. sativa* plants grown under the normal solar irradiance. It was continued for a period of 11 days in the first experiment and the same procedure was also repeated in the second experiment for a period of 8 days. The whole cultivation process had been monitored and recorded by CCD cameras for the purpose of tracing the development of *L. sativa*.

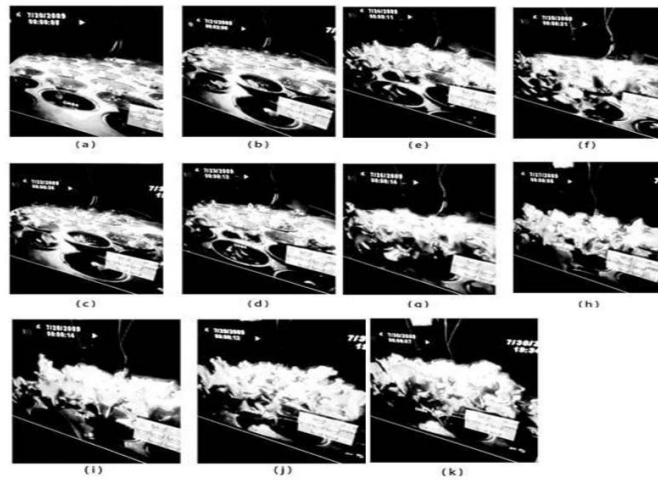


Figure 7. A series of photos taken with CCD video camera for 11 days starting from 20th to 30th July in experiment 1 to show the progress of plant growth under high power LED light system in the dark room: (a) Day 1, (b) Day 2, (c) Day 3, (d) Day 4, (e) Day 5, (f) Day 6, (g) Day 7, (h) Day 8, (i) Day 9, (j) Day 10 and (k) Day 11.

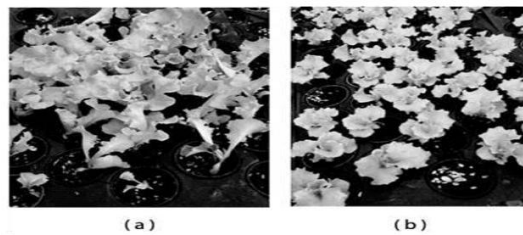


Figure 8. The Pictures to show the comparisons of final results for cultivating the *L. sativa* plants under the solar irradiance and high power LED lighting system in the experiments 1 and 2: (a) *L. sativa* plants cultivated under high power LED in experiment 1 and (b) *L. sativa* plants cultivated under solar irradiance in experiment 1

RESULTS AND DISCUSSION

To ensure the repeatability of the experimental result, two experiments were successfully conducted for different periods of growing time, that is, eleven days for experiment 1 and eight days for experiment 2. From the physical observation, the specimens of young *L. sativa* plants cultivated under high power LED lighting system

had shown faster growth rate than that of the specimens cultivated under normal solar irradiance. From the recorded video, Figure 7a to k shows the photos of specimen plants taken from day 1 to day 11 for the experiment 1. In the overall results as shown in Figure 8, the young *L. sativa* plants cultivated under high power LED lighting system have been observed to have larger leaf area and taller stem than those of the young *L. sativa*

Table 1. Measurement result of total leaf area index per plant, plant fresh weight and leaf width of the ten selected samples in Experiment 1.

Plant sample	Experiment 1 (11 days of plant)					
	Total leaf area index per plant (mm ²)		Plant fresh weight (g)		Leaf width (mm)	
	High power LED	Solar irradiance	High power LED	Solar irradiance	High power LED	Solar irradiance
S1	1515	502	3.0	0.8	36, 33, 28, 24, 10	22, 20, 19, 11, 6
S2	1479	487	2.8	0.7	34, 28, 26, 25, 10	22, 20, 18, 10, 5
S3	1423	485	2.5	0.7	30, 27, 26, 18, 9	22, 19, 18, 10, 6
S4	1202	463	1.7	0.6	29, 24, 16, 8, 8	21, 18, 17, 9, 5
S5	1487	445	2.7	0.6	32, 27, 27, 24, 10	19, 17, 15, 8, 5
S6	1265	435	1.8	0.6	29, 24, 18, 10, 9	18, 16, 13, 8, 5
S7	1390	470	2.2	0.7	29, 27, 19, 17, 9	21, 20, 18, 9, 5
S8	1338	486	2.0	0.7	29, 25, 20, 14, 8	21, 20, 18, 10, 6
S9	1476	412	2.8	0.5	33, 30, 26, 24, 10	16, 14, 12, 8, 5
S10	1426	403	2.4	0.5	30, 28, 23, 18, 10	15, 14, 12, 7, 5
Average	1400.1	458.8	2.39	0.64	21.8	13.6
Max	1515	502	3.0	0.8	36	22
Min	1202	403	1.7	0.5	8	5

Table 2. Measurement result of total leaf area index per plant, plant fresh weight and leaf width of the ten selected samples in Experiment 2.

Plant sample	Experiment 2 (8 days of plant)					
	Total leaf area index per plant (mm ²)		Plant fresh weight (g)		Leaf width (mm)	
	High power LED	Solar irradiance	High power LED	Solar irradiance	High power LED	Solar irradiance
S1	294	386	0.3	0.4	17, 4, 4	18, 16, 7, 6
S2	908	341	1.2	0.4	28, 24, 7, 6	16, 12, 4, 4
S3	587	335	0.8	0.4	24, 20, 5, 5	15, 14, 5, 4
S4	718	342	0.9	0.4	24, 24, 5, 5	16, 10, 6, 5
S5	667	330	0.8	0.3	23, 20, 6	14, 14, 4, 4
S6	868	359	1.1	0.4	28, 23, 5, 6	15, 14, 5, 4
S7	844	338	1.0	0.4	23, 25, 6, 6	16, 12, 5, 4
S8	550	343	0.6	0.4	18, 22, 5, 5	15, 14, 5, 5
S9	340	327	0.4	0.3	20, 14, 6	21, 7, 4
S10	479	316	0.5	0.3	10, 21, 5, 6	17, 6, 6
Average	625.5	341.7	0.76	0.37	13.7	9.7
Max	908	386	1.2	0.4	28	21
Min	294	316	0.3	0.3	4	4

plants cultivated under normal solar irradiance in the same period of time.

To compare the results of plant cultivation under the two different illumination conditions quantitatively, ten samples of specimen plants were selected from each pallet to perform a series of measurement in the last day of each experiment, such as leaf width, total leaf area index per plant and plant fresh weight. The measurement results were listed in Tables 1 and 2 for experiments 1 and 2, respectively. As a summary of experiment 1, most

of the specimen plants cultivated under high power LED lighting system grew up with four big leaves with average leaf width of 21.8 mm, average total leaf area index per plant of 1400.1 mm² and average plant fresh weight of 2.39 g as compared to plants cultivated under solar irradiance with average leaf width of 13.6 mm, average total leaf area index per plant of 458.8 mm² and average plant fresh weight of 0.64 g. As a summary of experiment 2, the specimen plants cultivated under high power LED lighting system grew up with two big leaves with average

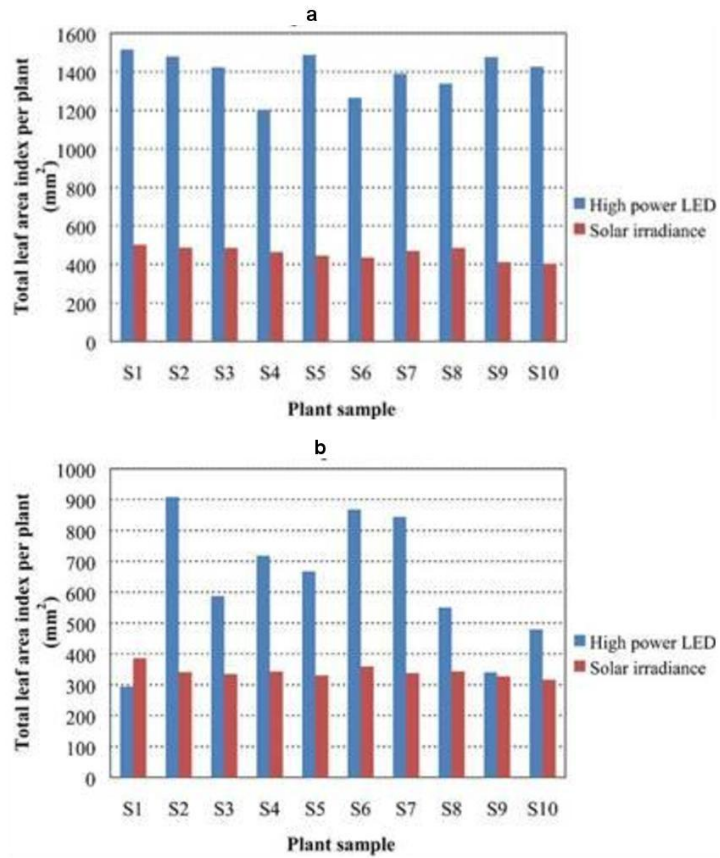


Figure 9. The Bar charts to show the total leaf area index per plant that were measured from 10 selected pots in the last day of the whole experiment for a comparison of *L. sativa* plants cultivated under solar irradiance and high power LED lighting system. (a) Experiment 1 and (b) Experiment 2.

leaf width of 13.7 mm, average total leaf area index per plant of 625.5 mm² and average plant fresh weight of 0.76 g whilst the specimen plants cultivated under solar irradiance grew up with average leaf width of 9.7 mm, average total leaf area index per plant of 341.7 mm² and average plant fresh weight of 0.37 g. For the comparison of the leaf size and plant fresh weight of the test specimen plants as shown in Figures 9 to 11, the *L. sativa* plants cultivated under high power LED lighting

system have shown a faster growth rate than that of plants cultivated under solar irradiance.

Conclusion

The high power LED lighting system that consists of the AlInGaP and InGaN LEDs has been successfully designed and constructed. The young *L. sativa* plants

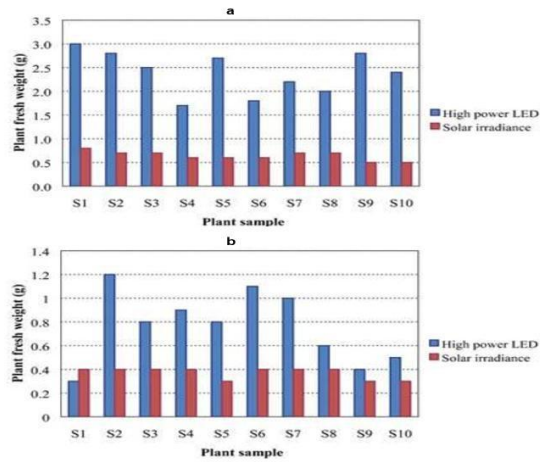


Figure 10. Bar charts to show the fresh weight that were measured from 10 selected pots in the last day of the whole experiment for a comparison of *L. sativa* plants cultivated under solar irradiance and high power LED lighting system (a) Experiment 1 and (b) Experiment 2.

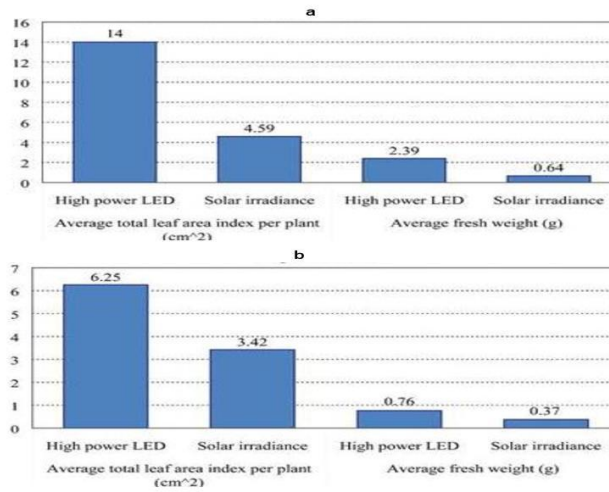


Figure 11. The Bar charts to show the average values of both total leaf area index per plant and fresh weight that were measured from 10 selected pots in the last day of the whole experiment for a comparison of *L. sativa* plants cultivated under solar irradiance and high power LED lighting system (a) Experiment 1 and (b) Experiment 2.

cultivated under the high power LED lighting system have higher growth rate when compared with plants cultivated under normal solar irradiance in terms of total leaf area index per plant, average fresh weight, etc.

ACKNOWLEDGEMENT

The authors would like to thank the Cameron Highland farmer, Mr. Hoo Chan Leang for his kind supply of young *L. sativa* and providing a suitable place to conduct this research. The authors are also grateful to Future Electronics for paying the publication fee.

REFERENCES

- Avago Technologies (2009). Precision Optical Performance AllGaP II LED Lamps. AV02-342EN: 6-7.
- Bai JG, Zhang ZZ, Lu GQ, Hasselman DPH (2004). Measurement of Solder/Copper Interfacial Thermal Resistance by the Flash Technique. *Int. J. Thermophys.*, 26: 1607.
- Diffraction Optics (2009). Product Specification. P3152. http://www.diffraction-optics.com/photo/675L_P3152.pdf.
- Dow Corning (2012). Information About Dow Corning® Brand Thermally Conductive Materials: 7.
- Goins GD, Yorio NC, Sanwo MM, Brown CS (1997). Photomorphogenesis, photosynthesis, and seed yield of wheat plants grown under red light-emitting diodes (LEDs) with and without supplemental blue lighting. *J. Exp. Botany*, 48: 1407-1413.
- Hokuriku (Malaysia) Sdn Bhd (2009). Ceracon Product Specification. <http://www.digital-safety.sg/edc.pdf>.
- Jao RC, Fang W (2004). Effects of frequency and duty ratio on the growth of potato plantlets *in vitro* using light-emitting diodes. *HortSci.*, 39: 375-379.
- Matthijs HCP, Balke H, Van Hes UM, Kroon BMA, Mur LR, Binot RA (1996). Application of light emitting diodes in bioreactors: flashing light effects and energy economy in algal culture (*Chlorella pyrenoidosa*). *Biotechnol. Bioeng.*, 50: 98-107.
- National Semiconductor LM3404 (2010). 1.0A Constant Current Buck Regulator for Driving High Power LEDs, pp. 1-5.
- Nhut DT, Takamura NT, Watanabe H, Tanaka M (2000). Light emitting diodes (LEDs) as a radiation source for micropropagation of strawberry. *Transplant Production in the 21st century*, pp. 114-118.
- Okamoto K, Yanagi T, Kondo S (1997). Growth and morphogenesis of lettuce seedlings raised under different combination of red and blue light. *Acta Horticulturae*, 435: 149-157.
- Philips L (2006). Thermal Design Using Luxeon Power Light Source. Appl. Brief AB05: 2-3.
- Philips L (2011). Luxeon Rebel and Luxeon Rebl ES Color Portfolio. Technical Datasheet DS68, pp. 4-10.
- Photosynthesis Timeline (2008). http://www.photobiology.info/History_Timelines/Hist-Photosyn.html.
- Schuerger AC, Brown CS (2004). Spectral quality may be used to alter plant disease development in CELSS. *Adv. Space Res.*, 14: 395-398.
- Yeh N, Chung JP (2009). High-brightness LEDs-Energy efficient lighting sources and their potential in indoor cultivation. *Renew. Sustain. Energy Rev.*, 13: 2175-2180.